AXIALY CHIRAL N-(*O*-ARYL)-2-THIOXO-OXAZOLIDINE-4-ONE AND RHODANINE DERIVATIVES: ENANTIOMERIC SEPARATION AND DETERMINATION OF RACEMIZATION BARRIERS

by

Esra Mujde Yılmaz

B.S. in Chem., Marmara University, 1998

M.S. in Chem., Boğaziçi University, 2002

Submitted to the Institute for Graduate Studies in
Science and Engineering in partial fulfillment of
the requirements for the degree of
Doctor of Philosopy

Graduate Program in Chemistry

Boğaziçi University

2008

AXIALY CHIRAL N-(*O*-ARYL)-2-THIOXO-OXAZOLIDINE-4-ONE AND RHODANINE DERIVATIVES: ENANTIOMERIC SEPARATION AND DETERMINATION OF RACEMIZATION BARRIERS

APPROVED BY:

Prof. İlknur Doğan (Thesis Supervisor)	……..
Prof. Safiye Erdem	……
Prof. Belkıs Halfon	……
Prof. Selim Küsefoğlu	……
Prof. Hadi Özbal	……

DATE OF APPROVAL: …….

To my son Yavuz and my husband Mustafa Yılmaz

ACKNOWLEDGEMENTS

I would like to express in depth my sincere gratitude to my advisor Prof. İlknur Doğan for her inspiration, guidance and continue support throughout my graduate years. Her patience and confidence in me have made my Ph.D. study a smooth and enjoyable experience.

I would like also to thank the members of my advisory committee: Prof.Selim Küsefoğlu, Prof.Hadi Özbal, Prof.Belkıs Halfon and Prof. Safiye Erdem for their valuble advices, comments and suggestions.

I would also like to thank my labaratory partners Öznur Demir and Şule Erol for their help and friendship.

I wish to thank all my friends Dr. Funda Oğuz, Gökhan Çaylı, Elif Olgun, Sinan Şen, Cem Öztürk, Hatice Mutlu, Hikmet Karayel and Hüseyin Altın, Pınar Çakır and Selda Erkoç who helped me in different ways during this study.

I would like to thank to Ayla Türkekul and Burcu Selen Çağlayan for recording the NMR spectra.

I would like to thank to Hülya Metiner and Birgül Sönmez for help, advice and understanding in every aspect.

Finally, my deepest thanks are extended to my family for their love and support during my entire education, in particular, to my parents, Sedat and Zehra Yılmaz, my sister Aysel Yılmaz and my husband, Mustafa Yılmaz. Without them I couldn't overcome difficulties during the tough time.

This project has been supported by Boğaziçi University Scientific Research Fund with project numbers 08B506D and 07B503.

ABSTRACT

AXIALY CHIRAL N-(*O*-ARYL)-2-THIOXO-OXAZOLIDINE-4-ONE AND RHODANINE DERIVATIVES: ENANTIOMERIC SEPARATION AND DETERMINATION OF RACEMIZATION BARRIERS

In this study, sterically hindered 5,5-dimethyl-3-(*o*-aryl)-2-thioxo-4-oxazolidinones, 5,5-dimethyl-3-(*o*-aryl)-2-thioxo-4-thiazolidinones and 3-(*o*-aryl)-2-thioxo-4-thiazolidinones(rhodanines) have been synthesized as racemates by either the reaction of *o*-aryl isothiocyanates with α-hydroxyisobutyrate or by treatment of *o*-arylisothiocyanates with the correponding thioglycolic acid ethyl ester. The 5,5-dimethylrhodanines have been synthesized according to Modified Kaluza synthesis. Chirality of the compounds has been proven by the presence of diastereotopic methylene protons or methyl groups on C-5 of the heterocyclic ring detected by ^{1}H NMR or ^{13}C NMR spectroscopy.

The enantiomers of the synthesized compounds have been resolved or enriched micropreparetively on chiralpak AD-H column, packed with amylose tris-(3,5-dimethyl phenyl)carbamate.

The activation barriers for interconversion between the enantiomers have been determined by either temperature dependent NMR or by thermal racemization followed by enantioresolution on a chiral sorbent via HPLC.

The activation barriers to rotation around C-N bond showed a linear increase with the van der Waals radii of the *ortho*-halogen substitutents.

Absolute conformations have been determined by analysis of NMR spectra of N-naphthyl substituted derivatives of the series in the presence of the chiral auxiliary (S)-(+)-1-(9-antryl)-2,2,2-trifluoro ethanol ((S)-TFAE). Plausible diastereomeric association models between the enantiomers of the compounds 3-(α-naphthyl)-2-thioxo-4-

thiazolidinone and 3-(α-naphthyl)-2,4-thiazolidinedione and the chiral auxiliary (S)-TFAE have been proposed.

Enantiodifferentiation of 3-aryl-2-thioxo-4-oxazolidinones by NMR was also studied by using a dirhodium tetracarboxylate complex as the chiral auxiliary. Determination of relative conformations of the series have also been attempted by applying the dirhodium method to the enantiomerically enriched samples, however this could not be achieved.

ÖZET

AKSİYEL KİRAL N-(O-ARİL)-2-TİOKSO-OKSAZOLİDİN-4-ON VE RODANİN TÜREVLERİ: ENANTİOMERİK AYRIŞMA VE RASEMİZASYON BARİYERLERİNİN BELİRLENMESİ

Bu çalışmada sterik engelli 5,5-dimetil-3-(o-aril)-2-tiokso-4-oksazolidinon, 5,5-dimetil-3-(o-aril)-2-tiokso-4-tiazolidinon(rodanin) ve 3-(o-aril)-2-tiokso-4-tiazolidinon(rodanin) türevleri rasemik olarak arilisotiosiyanatların 2-hidroksiisobütratlarla ya da arilisotiosiyanatların tioglikolikasit etilesterle olan reaksiyonlarından sentezlenmişlerdir. 5,5-dimetil-rodaninler modifiye Kaluza metoduna göre sentezlenmişlerdir. Bileşiklerin kiraliteleri, heterosiklik halkanın C-5 posizyonundaki metil ve metilen protonlarının varlığında ^{1}H ve ^{13}NMR spektroskopisi ile ispatlanmıştır.

Sentezlenen bileşiklerin enantiomerleri amiloz tris-(3,5-dimetil aril) karbamet dolgu maddeli kiralpak AD-H kolon üzerinde ayrılmış ve mikroskalada toplanmıştır.

Enantiomerler arasındaki dönüşümün aktivasyon bariyerleri, sıcaklık bağımlı NMR ya da termal rasemizasyonla, HPLC ile kiral faz üzerinde enantiomerlerine ayrılma işleminin akabinde belirlenmiştir.

C-N bağı etrafındaki dönme için aktivasyon bariyeri o-halojen sübstitütentlerinin van der Waals çapları ile doğrusal bir artış göstermiştir.

Kiral okzalari, (S)-(+)-1-(9-antril)-2,2,2-trifloro etanol ((S)-TFAE) varlığında, N-naftil sübstitüentli serilerin türevlerinin NMR spektralarının analizi ile kesin konformasyonlar belirlenmiştir. 3-(alfa-naftil)-2-tiokso-4-tiazolidinon ve 3-(alfa-naftil)-2,4-tiazolidindion bileşiklerinin enantiomerleri ve kiral okzalari (S)-TFAE arasındaki muhtemel diasteomerik asosiasyon modelleri önerildi.

Kiral okzalari olan dirodyum tetrakarboksilat kompleksi kullanılarak 3-aril-2-tiokso-4-okzalidinonların NMR ile enantiomerlerinin ayrışımı üzerinde çalışıldı. Enantiomerlerince zenginleştirilmiş örneklere dirodyum metodunun uygulanmasıyla serilerdeki bağıl konformasyonların tayinine çalışılmış, ancak başarılı olunamamıştır.

TABLE OF CONTENTS

LIST OF FIGURES

LIST OF TABLES

LIST OF SYMBOL/ABBREVIATIONS

A_m	Amount of the compound in the mobile phase
A_s	Amount of the compound in the stationary phase
C_m	Concentration of the compound in the mobile phase
C_s	Concentration of the compound in the stationary phase
F	Flow rate
H	Planck's constant
Hz	Hertz
K	Equilibrium constant
k'	Capacity factor
k_b	Boltzman constant
k_f	Rate constant for forward reaction
k_r	Rate constant for reverse reaction
s	Second
T	Temperature
t_R	Retention time
V_0	Dead volume
V_n	Net retention volume
V_R	Retention volume
α	Separation factor
δ	Chemical shift
$\Delta G^{\#}$	Free energy of activation
$CDCl_3$	Deuterated chloroform
CSP	Chiral stationary phase
DMSO-d_6	Hexadeuterated dimethylsulfoxide
HPLC	High pressure liquid chromatography

1. INTRODUCTION

Non-biaryl axially chiral compounds have been receiving considerable attention [1-7] due to their interesting stereochemistries and also due to their potential uses as catalysts and ligands for asymmetric syntheses [8]. Thus, the synthesis of such atropisomeric compounds with high enantiomeric stability, their chiral separations and determination of their barriers to enantiomerization are of importance in chiral chemistry.

Heterocyclic compounds are very widely distrubuted in nature and are essential to life. An expanding number of drugs, agrochemicals, food additives and flavoring reagents are heterocylic compounds.

Some classes of N-aryl heterocycles have been studied in the past with reference to their stereostructures which are analogous to the well known case of biaryls. Among those heterocycles, two particular classes are especially attractive, 2-thioxo-4-oxazolidinones and 2-thioxo-4-thiazolidinones (rhodanines).

Oxazolidinones have been shown to fungicidal activity. Especially, 2-thioxo-4-oxazolidinones have been used as agricultural fungicides [9-12].

Rhodanines are used as vulcanizing agents and intermediates in the synthesis of dyes. The absorption spectra of rhodanines have been studied in connection with interesting photosensibilizing and physiological properties of some 4-thiazolidinone derivatives [13].

Rhodanines in recent years have been shown to have various pharmaceutical activities. Among the most well known pharmaceutical activities of rhodanines are their use as antidiabetic agents [14-17] especially in the treatment of non-insulin dependent diabet mellitus [18] and as non-peptide inhibitors of an enzyme (cathepsin-D and aspartyl protease) that has been implicated in many disease states including Alzheimer disease [19]. They have also been shown to have some antiviral and antibacterial activities [20].

Another interesting aspect of the chemistry of rhodanines is their donor ability toward metal ions, which makes them suitable as ligands in coordination compounds. It has been reported that rhodanines and their derivatives are used as highly sensitive reagents for the elements of the Pt group and selective reagents for Pb and Hg.

The research on the restricted rotation in N-heterocyclic compounds started after 1931, when Adams and coworkers reported on the resolution of N-phenyl pyrroles and N-N'-dipyrryls (Figure1.1), which are heterocyclic analogs of biaryls [21-23].

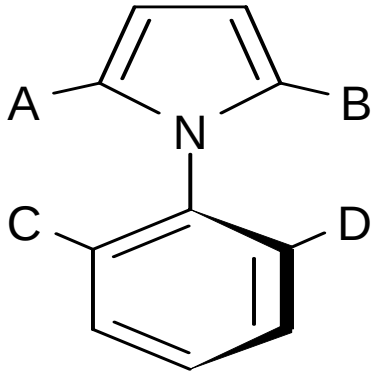

Figure 1.1. The general structure of N-phenylpyroles

The barriers to rotation about the aryl C-N bonds were determined by DNMR in 3-aryl-2-benzyl-4-(3H)-quinazolinones by Colebrook *et al*. They reported high barriers to rotation around C-N bond in aryl substituted heterocyclic compounds due to the presence of steric interaction between bulky ortho substitutent on the aryl group and the heterocyclic moiety [24-25].

In 1978 , Kashima *et al.* investigated the optical resolution of 1-aryl-4,6-dimethyl-2(H)- pyrimidinones and corresponding thiones. Enantiomeric separation via D-Camphor-10-Sulphonic acid and the polarimetric determination of the barrriers to racemization were done [26].

In 1989, Mannschreck et al. studied the sterically hindered N-aryl pyrroles. In this study diastereomeric association complexes of racemic pyrroles were studied by ^{1}H NMR spectroscopy in terms of chemical shifts and splittings induced by the optically active

auxiliary compound. The barriers were determined by variable temperature ^{1}H NMR spectroscopy. They obseved that the shift difference decreased with increasing temperature [27].

In 1992, Doğan *et al*. synthesized sterically hindered N-(*o*-tolyl) and N-(*o*-chlorophenyl) substituted 2-thioxo-4-oxazolidinones and thiazolidinones (Figure 1.2) which formed enantiomers by partial rotation around the C-N bond. Chirality of the synthesized compounds was proven by ^{1}H NMR or ^{13}C NMR . In the presence of (S)-(+)-1-(9-anthryl)-2,2,2-trifluoroethanol as a chiral auxiliary the enantiomers showed 1H NMR shift differences for otherwise isochronous nuclei [28].

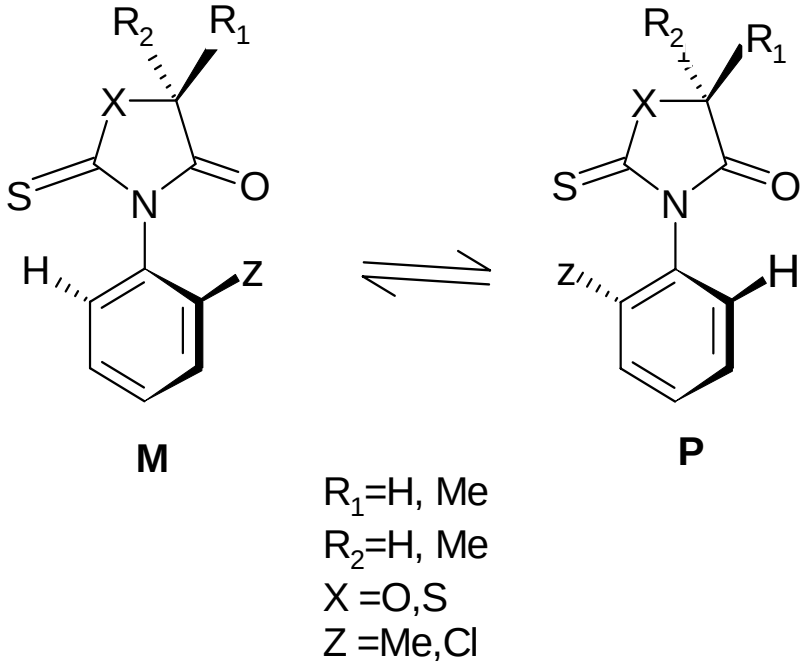

Figure 1.2. The structure of N-(*o*-aryl) and N-(*o*- aryl)- 2- thioxo-4-oxazolidinones and thiazolidinones

In 1993, Doğan and Mannschreck published a paper reporting on the enantiomers of N-aryl-2-thioxo-4-oxazolidinones and N-arylrhodanines where for the first time analytical separation and semi-preparative enrichment of enantiomers have been achieved by liquid chromatography on triacetyl and tribenzoylcellulose. The barriers to rotation about C-N

bond were determined by thermal racemization subsequent to chromatographic semipreparative enrichment of enantiomers [29].

In 2003, Oguz and Doğan presented a paper reporting on the determination of energy barriers and racemization mechanisms for thermaly interconvertible barbituric and thiobarbituric acid enantiomers. The enantiomers of 5,5-dimethyl-1-(*o*-aryl)barbituric and 2-thiobarbituric acid derivatives (Figure 1.3) have been separated by micropreparative liquid chromatography. The activation barriers have been detemined upon thermal racemization of separated enantiomers [30].

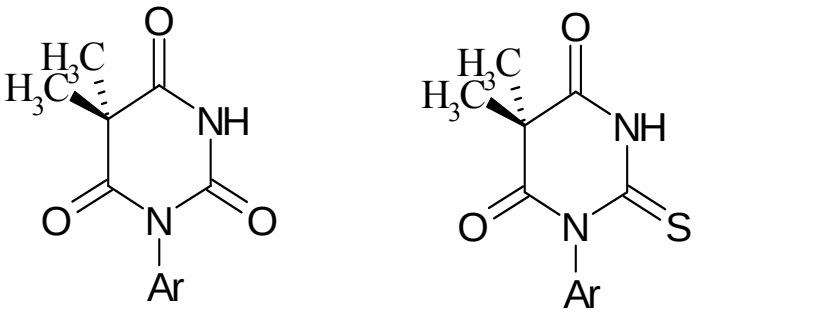

Ar= *o*-tolyl

Ar= *o*- tolyl
o- fluorophenyl
o- methoxyphenyl
o- chlorophenyl
α- naphthyl

Figure 1.3. The structure of 5,5-dimethyl-1-(*o*-aryl)barbituric and 2-thiobarbituric acid derivatives.

In 2005, Roussel *et al*. studied on the synthesis of some N-(*o*-aryl)-4-alkyl-thiazolin-2-thiones and thiazoline-2-ones in which amino, alkoxy or hydroxy groups were situated at the *ortho* position of the aryl group (Figure 1.4). They reported the chiral HPLC resolutions of the atropisomers and the determination of the barrier to rotation [31].

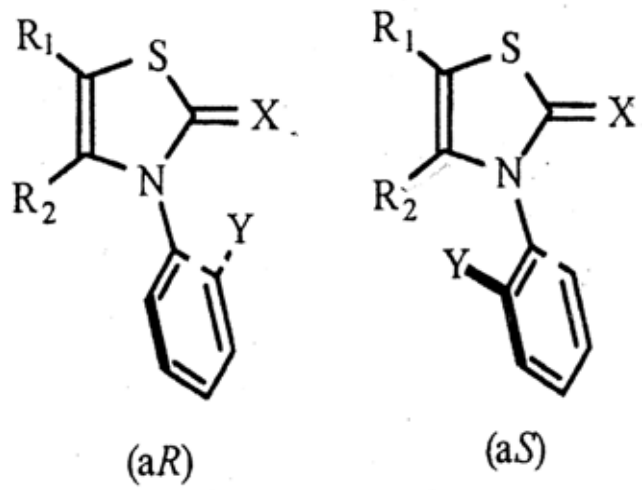

X= O, S

R_1= H, CH_3, COOR

R_2= CH_3, t-Bu

Y= OH, OCH_3, NH_2, NCS

Figure 1.4. The general structure for the thiazoline atropisomers

In this study, axially chiral 5,5-dimethyl-3-(*o*-aryl) rhodanine, 3-(*o*-aryl) rhodanine and 5,5-dimethyl-3-(*o*-aryl)-2-thioxo-4-oxazolidinone derivatives have been synthesized as racemates and the energy barriers to enantiomerization have been determined by either dynamic ^{1}H NMR or by following the thermal equilibration of the separated enantiomers using chiral HPLC. The compounds that have been synthesized are shown in Figure 1.5.

In these molecules the internal rotation around C-N bond is hindered due to the presence of the exocyclic thiocarbonyl group and carbonyl group of the heterocyclic ring and Z substitutent *ortho* position of the aryl ring. As a result, the ground state of the molecules is not planar. The *o*-aryl substitution (Z) as well as causing hindered rotation also brings dissymmetry to the molecule. Therefore, the C_{aryl}-N_{sp2} bond of the molecules is a chiral axis. Thus molecules are expected to be chiral and exist as a racemic mixture of the enantiomers M and P.

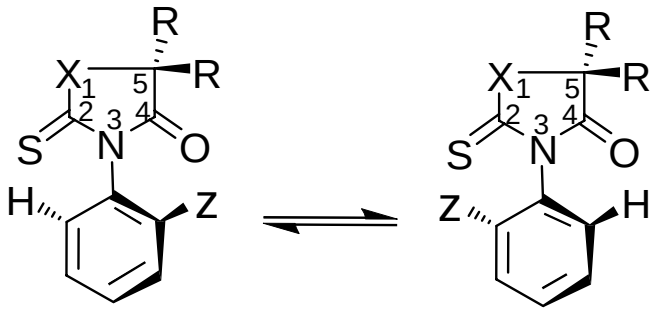

(±) -1 R= CH_3; X= O Z= F

(±) -2 R= CH_3; X= O Z= Cl

(±) -3 R= CH_3; X= O Z= Br

(±) -4 R= CH_3; X= O Z= I

(±) -5 R= CH_3; X= O Z= CH_3

(±) -6 R= CH_3; X= S Z= F

(±) -7 R= CH_3; X= S Z= Cl

(±) -8 R= CH_3; X= S Z= Br

(±) -9 R= CH_3; X= S Z= I

(±) -10 R= CH_3; X= S Z= CH_3

(±) -11 R= H; X= S Z= F

(±) -12 R= H; X= S Z= Cl

(±) -13 R= H; X= S Z= Br

(±) -14 R= H; X= S Z= I

(±) -15 R= H; X= S Z= CH_3

Figure 1.5. The structure of axially chiral 5,5-dimethyl-3-(o-aryl) rhodanine, 3-(o-aryl) rhodanine and 5,5-dimethyl-3-(o-aryl)-2-thioxo-4-oxazolidinone

2. THEORY

2.1. Chirality

Chirality is a fundamental property of many three-dimensional objects. An object is chiral if it can not be superimposed on its mirror image. A chiral molecule and its non-superimposable mirror image, which is also a chiral molecule, are described as "enantiomers" of each other. Enantiomers have identical chemical and physical properties in the absence of an external chiral influence. That is, they have identical melting points, identical boiling points, identical solubilities in the same solvent, identical infrared and nuclear magnetic resonance spectra. Also each enantiomer undergoes chemical reactions at the same rate as long as the other reagent (and the solvent) is not chiral. However, in the case in which the other reagent is chiral, the two enantiomers react at different rates. Enantiomers rotate the plane polarized light into different directions. This is called as optical activity.

Diastereomers are basically stereoisomers that are not enantiomers of each other and exhibit different physical and chemical properties.

There are four main types of chirality. These are central chirality, axial chirality, planar chirality, and helical chirality.

Central chirality is imposed on a molecule when it has an atom having a molecular geometry of a tetrahedron, the corners of which are occupied by four different groups. Such an atom is called a 'stereocenter' and the most common example is a carbon atom having four different groups attached to it. Besides carbon, tetrahedral nitrogen, sulfur and phosphorus would be a stereocenter.

Planar chirality is possible in a molecule when the groups about a hypothetical plane are arranged in an asymmetric fashion.

A helical molecule can adopt either a right- or left-handed twist giving rise to helical chirality.

Ortho substituted biphenyls and their analogues are commonly encountered molecules that display axial chirality. The chirality observed for these compounds arises from the fact that rotation around the bond joining the aromatic units is restricted (Figure 2.1).

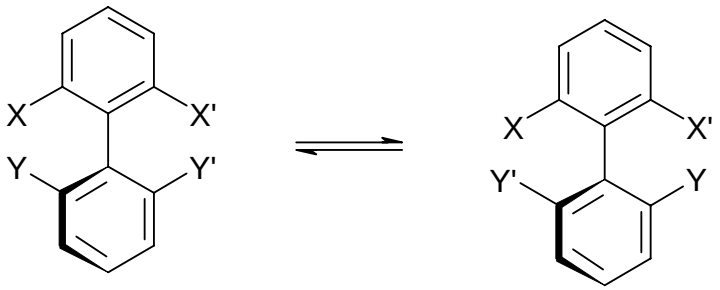

Figure 2.1. Enantiomeric chiral biphenyls

The substitutents at the *ortho* positions restrict free rotation of the phenyl rings and prevent the rings from lying in the same plane. The result is that the rings remain orthogonal (or nearly orthogonal) to each other. When the substitutents on either side of this inter-ring bond are different, as in Figure 2.1, then the structure is able to exist in two enantiomeric forms. Such stereoisomers, resulting from restricted rotation about single bonds which interconvert with a half-life of more than 1000 s at a given temperature are called atropisomers [32]. Therefore interconvertible enantiomers with a barrier to rotation greater than 100 kJ/mol are atrpisomeric at room temperature.

2.2. Axial Chirality in 5,5-Dimethyl-3-(*o*-aryl)-2-thioxo-4-oxazolidinones, 5,5-Dimethyl-3-(*o*-aryl)-2-thioxo-4-thiazolidinones and 3-(*o*-aryl)-2-thioxo-4-thiazolidinones

The studied compounds in this project are heterocyclic analogues of biphenyls and form rotational isomers due to the hindered rotation around the C-N single bond. The hindered rotation caused by the steric interactions between the *ortho* substitutent on the aryl and the exocyclic oxygen or the sulfur of the heterocyclic moiety. The aryl ring in the

ground state of the molecule is expected to be orthogonal to the ring. On the other hand, transition state structures, T_1 or T_2, during the conversion of one rotamer to the other one are expected to be planar. As a result, the *ortho* substitutent on the aryl ring brings disymmetry to the molecule leading to the chirality of the ground state conformations and thus to the existence of enantiomers M and P (Figure 2.2).

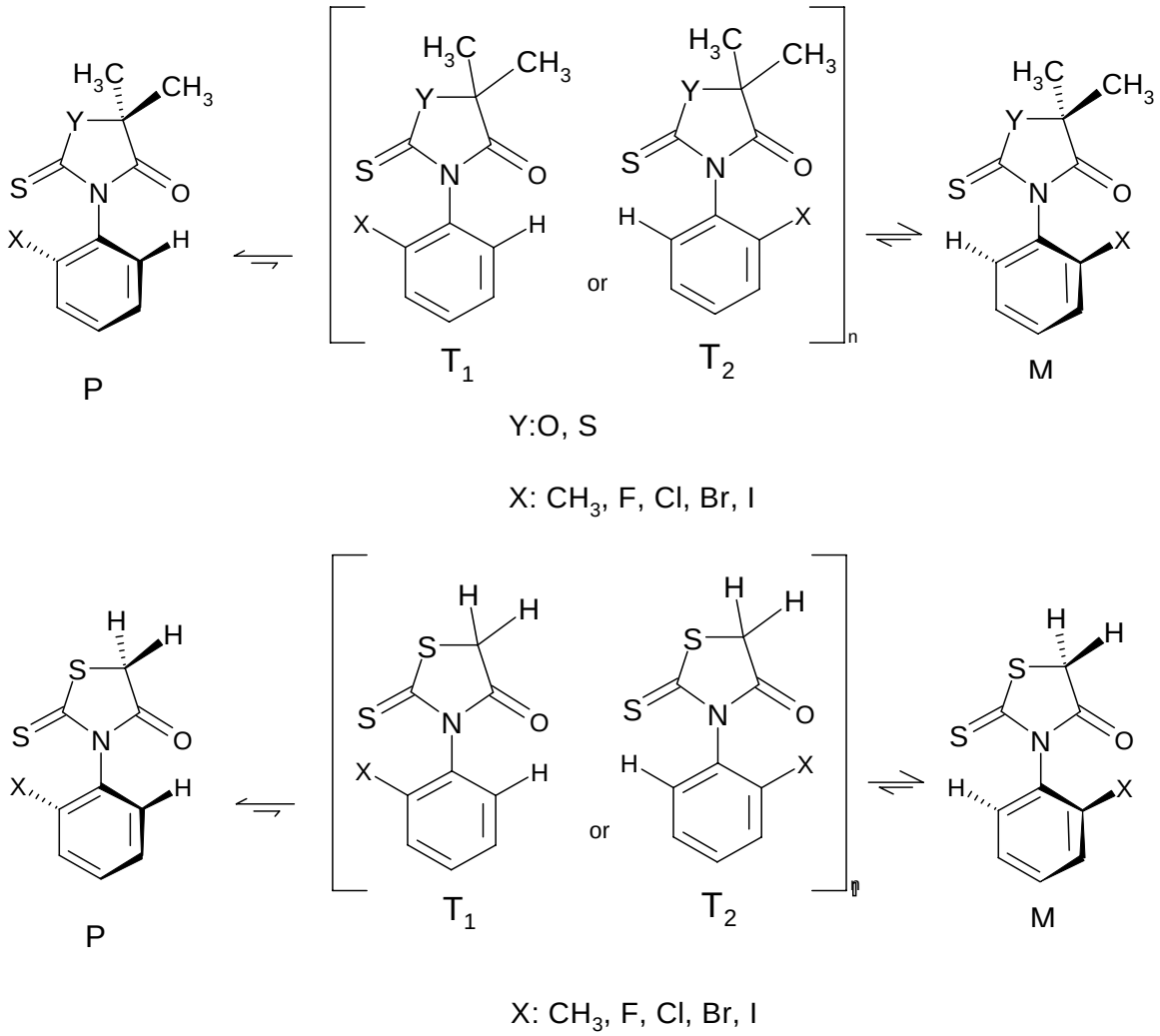

Figure 2.2. Rotational Isomers of 5,5-Dimethyl-3-(*o*-aryl)-2-thioxo-4-thiazolidinones, 5,5-dimetyl-3-(*o*-aryl)-2-thioxo-4-oxazolidinones, and 3-(*o*-aryl)-)-2-thioxo-4-thiazolidinones derivatives

2.3. Nomenclature

The chirality of axial chiral molecules can be defined in terms of their helicities M and P in the Cahn-Ingold-Prelog system [33]. In this system, first an axis is drawn through the single bond around which conformation is defined and the smallest torsion angle formed between the carbon atoms bearing the groups of the highest priority is used to define helix. A resulting clockwise rotation is denoted as “P” (plus) and the counter clockwise rotation is denoted as “M” (minus) (Figure 2.3). Generally, M and P helix nomenclature correspond to aR and aS chiral axis nomenclature.

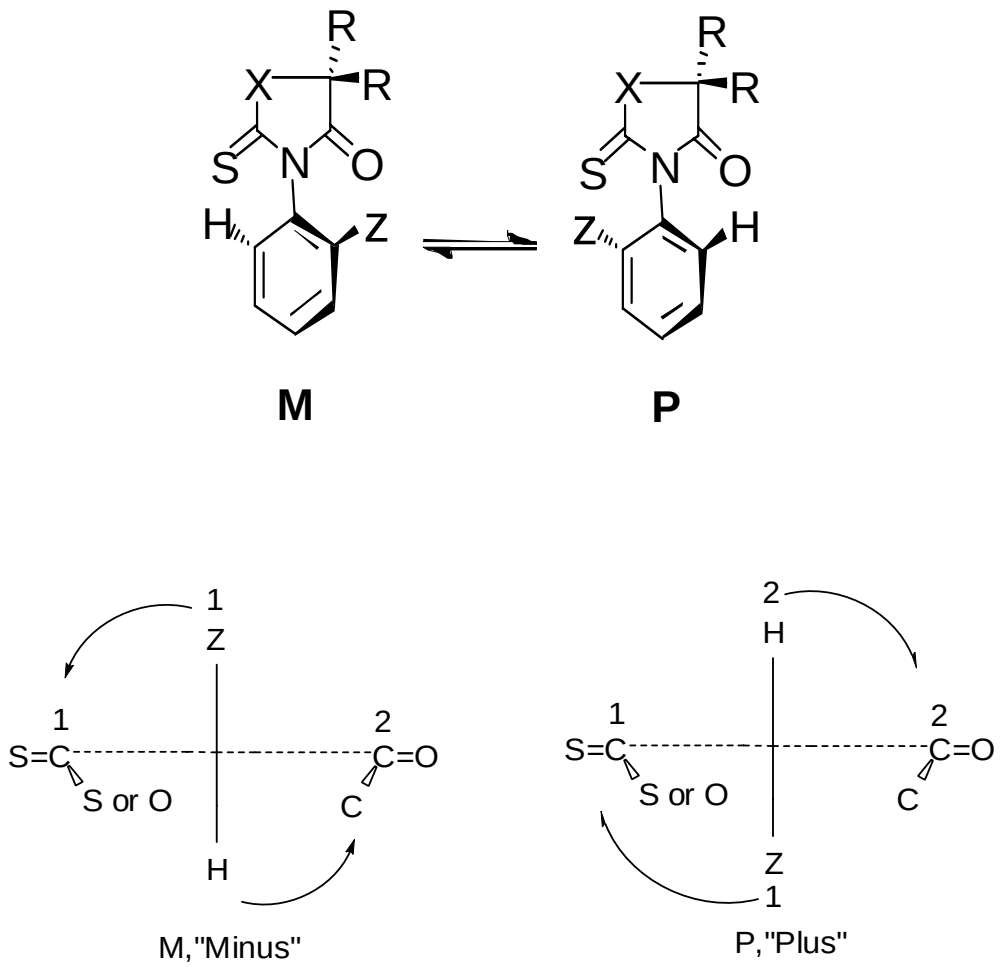

Figure 2.3. Descriptors for the axially chiral studied compounds

2.4. Chromatographic Separation of Stereoisomers

2.4.1. A Review of HPLC Tecnique and Basic Cromatography Theory

The concept of chromatography relies basically on the distribution of a compound between two phases, one of which (the mobile phase) is moving with respect to other (the stationary phase). The stationary phase is either a solid, porous, surface active material in small particle form or a thin film of liquid coated on a solid support or column wall. The mobile phase is a liquid or a gas. The various modes of chromatograph depend on the respective nature of the two phases. The essential part of a chromatograhic system is the column which contains the stationary phase over which the mobile phase flows and the where the separation of the mixture into the individiual components takes place. The sample is introduced onto the column by an injection device and the separated components are monitored by a suitable detection system and recorded as Gaussian curves. The signals are known as peaks.

In the tecnique called liquid chromatography, the stationary phase has a solid nature and the mobile phase is liquid. There are different modes for liquid chromatography, one of which is the high performance liquid chromatography (HPLC). In HPLC, the chromatographic process is carried out in such a way that the liquid mobile phase is forced through a thin column under high pressure. The components that are strongly retained by the stationary phase move slowly with the flow of the mobile phase. Those that are weakly held by the stationary phase travel rapidly. This difference in retentions of components plays a key role for separation in HPLC, as well as in other chromatographic tecniques.

In theoretical terms, the retention of a compound on a column can be expressed by its retention time (t_R), retention volume ($V_R = t_R F$, where F is the flow rate) or the capacity ratio (k'), which is directly related to its equilibrium distribution constant (K) in the stationary mobile phase system.

The capacity ratio is defined by:

$$k'=A_s/A_m \quad (2.1)$$

Where A_S and A_m denote the amount of the compound in the stationary and the mobile phase, respectively. Let V_S and V_m be the volumes of the respective phases; then

$$k'=CsVs/C_mV_m=KV_S/V_m \quad (2.2)$$

V_m is commonly writen as V_0 and represents the dead volume in the column,which does not contribute to the separation. Consequently, the net retention volume, V_n, can be written as $V_n=V_R-V_0$, since $K=V_n/V_s$, combination with equation (2.2) gives:

$$k'=(V_R-V_0)/V_0 \quad (2.3)$$

This expression permits the determination of the capacity factor from the chromatogram. The chromatographic separation of two components (1 and 2) depends on the separation factor (α) of a column. It can be written as $k_2'/k_1'=K_2/K_1=\alpha$. From Equation (2.3), α can be formulated as:

$$\alpha= (V_{R2}-V_0)/(V_{R1}-V_0) \quad (2.4)$$

Thus the separation factor is simply the ratio of the net retention volumes of the two components. If the dead volume V_0, has been determined, the separation factor is easly calculated from Equation (2.4) [34].

2.5. Separation of Enantiomers by Using Chiral Phases

Chirality of a molecule was first reported in 1815 by the French physicist Jean-Baptiste Biot. He found that quartz rotated the plane of polarized light [35]. However, the first chiral separation, which laid the foundation for stereochemistry, was reported in 1848 by Louis Pasteur [36]. Because of the hemihedral faces on the crystals of racemic sodium ammonium tartrate, he was able to separate the mirror image crystals of the isomers by the

use of a magnifying glass and tweezers. Characterization of the physicalproperties of individual enantiomers, (in which the only difference lies in the opposite rotation of a plane polarized light) led Pasteur to postulate that the enantiomers have different three-dimensional arrangements and on the macroscopic and microscopic levels they are mirror-images of each other. Furthermore, he advanced the field by studying the influence of one chiral compound upon another and introduced the technique of resolution via diastereoisomer formation. This separation of enantiomers by diastereomer formation is the basis of many modern chromatographic separations.

It is interesting to note that Pasteur's discovery of spontaneous enantiomeric resolution applies only to rare cases in which each isomer crystallizes separately and in a recognizable morphologic form. For more than a century, spontaneous resolution, as well as diastereomeric separation and differential enzymatic reactivity were the only methods employed for enantiomeric separations. In all of these techniques the separation and characterization of enantiomers require a chiral environment.

Enantiomers can be separated by chromatography, provided that the system used is dissymmetric. This can be achieved by various means.

- The mobile phase is chiral, the stationary phase non-chiral.
- The liquid stationary phase is chiral, the mobile phase non-chiral.
- The solid stationary phase is chiral, the mobile phase non-chiral

In the latter method , enantiomers can be resolved by the formation of diastereomeric complexes between the chiral stationary phase (CSP) and chiral molecule that is bound to the stationary phase.

The separation of enantiomeric compounds on CSP is due to the differences in energy between temporary diastereomeric complexes formed between the solute isomers and the CSP, the larger the difference, the greater the separation. The observed retention and efficiency of a CSP is the total of all the interactions between the solutes and the CSP, including achiral inteactions. To completely resolve a mixture of two components, they

must differ in the free energy of interaction with stationary phase by as little as 0.025 kJ/mol, which corresponds to the column selectivity value of α=1.01.

There are so many HPLC-CSPs available to the chromatographer. Some of these CSPs are polysaccaharide phases, ligand-exchange phases and protein bonded phases. Polysaccaharide derivatives, particularly carbamate derivatives, such as cellulose carbamate and amylose carbamate, exhibit high chiral recognition and can separate a broad range of racemic compounds into optical isomers.

In this study, amylose tris-(3,5-dimethyl)phenylcarbamate (Figure 2.4) was used as chiral stationary phase. Although the mechanism of chiral recognition by carbamate has not been clarified, it is believed that the chiral attractive interaction results from the urethane linkages. Some chiral space like a concave or a ravine existing on the chiral stationary phase may also enable chiral separations.

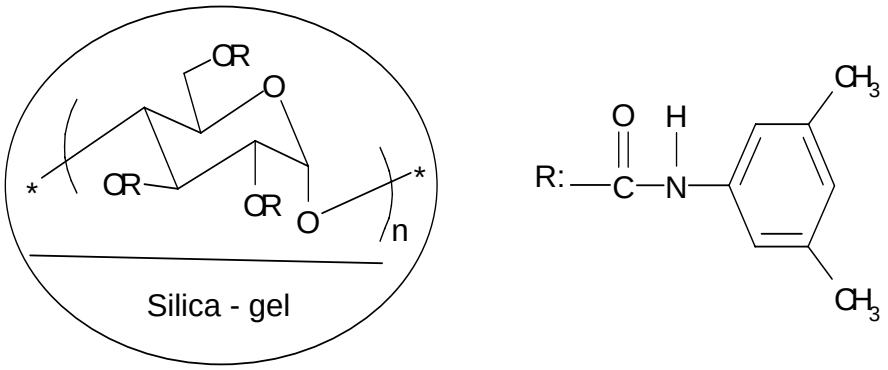

Figure 2.4. Amylose tris(3,5-dimethylphenyl) carbamate coated on a 10μm silica-gel substrate(Chiralcel AD-H)

2.6. Determination of Kinetic and Thermodynamic Constants of the Internal Rotation

5,5-Dimethyl-3-(*o*-aryl)-rhodanines and 5,5-Dimethyl-3-(*o*-aryl)-2-thioxo-4-oxazolidinone derivatives, and 3-(*o*-aryl)-rhodanine derivatives were obtained as racemic mixtures. If one of the enantiomers is separated from the other one or enriched, it thermally interconverts to the other one with time through rotation around C-N bond and finally

reaches equilibrium. The process follows a reversible first-order kinetics, the theory of which is given below:

The reversible reaction M $\rightleftharpoons$ P is first order in both the forward (f) and the reverse direction (r), so that $r_f = k_f [M]$ and $r_r = k_r [P]$. If $(d[M]/dt)_f$ denotes the rate of change of [M] due to forward reaction, then $-(d[M]/dt)_f = r_f = k_f[M]$. The rate of formation of [M] by reverse reaction is $(d[M]/dt)_r = r_r = k_f[P]$. Then,

$$(d[M]/dt) = -k_f[M]+k_r[P] \tag{2.8}$$

We have $\Delta[P]=-\Delta[M]$, so $[P]-[P]_0=-([M]-[M]_0)$. Substitution of $[P]=[P]_0+[M]_o-[M]$ into Equation (2.8) gives

$$d[M]/dt=k_r[P]_0+k_r[M]_0-(k_f+k_r)[M] \tag{2.9}$$

At equilibrium, the rates of the forward and reverse reactions become equal, the concentration of each species being constant, thus d[M]/dt is 0. Let $[M]_{eq}$ be the equilibrium concentration of M. Setting d[M]/dt=0 and $[M]=[M]_{eq}$ in Equation (2.9), we get

$$k_r[P]_0+k_r[M]_0= (k_f+k_r)[M]_{eq} \tag{2.10}$$

The use of Equation (2.10) in Equation (2.9) gives $d[M]/dt= (k_f+k_r) ([M]_{eq}-[M])$. Using the identity $\int(x + s)^{-1}dx= \ln(x + s)$ to integrate this equation, we get,

$$\ln ([M]-[M]_{eq}/[M]_0-[M]_{eq})= -(k_f+k_r)t \tag{2.11}$$

Since $k_f=k_r$ for the racemization of enantiomers, Equation (2.11) could be written as Equation (2.12) for the racemization of enantiomers

$$\ln ([M]-[M]_{eq}/[M]_0-[M]_{eq})=-2kt \tag{2.12}$$

By using Equation (2.12), a plot of ln ([M]-$[M]_{eq}$/$[M]_0$-$[M]_{eq}$) versus time gives a straight line, the slope being equal to -2k. Having determined k, the free energy of activation can be calculated using the Eyring Equation (2.13),

$$\Delta G^{\#}=RTln(k_b.T/k.h) \quad (2.13)$$

where R=8.3143 J/mol.K, T=temperatue(Kelvin) at which the interconversion takes place, k_b(Boltzmann constant)=$1.3805.10^{-23}$J/K, h (Planck constant)=$6.6256.10^{-34}$J.s, k=the rate constant for the racemization reaction.

2.7. Determination of Activation Barriers for Hindered Rotation by Dynamic NMR Spectroscopy

Dynamic NMR spectroscopy is a tool for analyzing the exchange behavior of certain nuclei, varying with the temperature. In this tecnique, two groups of chemically equivalent nuclei, which are differently shielded in NMR spectroscopy due to the difference in their magnetic environment, become indistinguishable by increasing temperature. The temperature, at which the groups become equivalent, is called coalescence temperature, T_c.

At room temperature, diastereotopic methyl protons on C-5 give two singlets with chemical shifts, δA and δB. If the energy is increased by heating , then the rotation around $C_{(Aryl)}$-$N_{(sp2)}$ bond becomes faster, so that two singlet peaks broaden and at coalescence temperature they coalesce into one broad band and become indistinguishable. If the temperature is increased more, this broad band becomes a narrow peak of double intensity with the average shift (δA + δB)/2.

For the coalescence temperature, T_c , the rate constant k_c is given by:

$$k_c =2.22\Delta\upsilon \quad (2.5)$$

Δυ: the separation in Hz between the two signals in the absence of interconversion. This is only valid when the conditions below are provided.

- The dynamic process occuring is first-order kinetically,

- The two singlets have equal intensities,
- The diastereotopic nuclei are not coupled to each other.

After estimation of the rate of rotational interconversion, k_c, it is substituted into the Eyring equation, which expresses the exponential decrease of k_c with the free molar activation energy, $\Delta G^{\#}$, as :

$$k_c=(k_b.T_c/ h).e^{\Delta G\# / R.T} \quad (2.6)$$

R: the gas constant

k_b: the boltzman constant

h: the planck's constant

Following substitution of fundamental constants, they give equation for the molar activation energy, $\Delta G^{\#}$, for the first order interconversion process.

$$\Delta G^{\#} = 19.1\ T_c.[10.32+\log (T_c / k_c)].10^{-3}\ \text{Kj/mol} \quad (2.7)$$

2.8. Enantiodifferentiation by Nuclear Magnetic Resonance Spectroscopy in the Presence of an Optically Active Auxiliary

NMR spectroscopy can not normally be used directly for discriminating enantiomers in solution. The NMR signals for enantiomers are isochronic under achiral conditions. So, nuclei which are enantiotopic are equally screened by environments in achiral solvents and they exhibit the same NMR chemical shifts. However, NMR tecniques can be used for the determination of enantiomer compositions when diastereomeric interactions are introduced to the system.

In chiral solvents, enantiomeric nuclei will reside in different (diastereomeric) environments and, in principle, will have different chemical shifts. That is, a chiral environment might dissimilarly pertub the properties of enantiomeric molecules, alter the stereochemical course of reactions. This principle has been embodied in many forms in the

practical applications of selectively preparing, separating and determining the absolute configuration and enantiomeric purity of optical isomers.

In the presence of an optically active auxiliary compound, the enantiomers are expected to give different NMR spectra, if the auxiliary compound is able to make diastereomeric association complexes with the enantiomers. If a solute contains sites capable of spesific bonding with the auxiliary, then assosciation complexes can be formed between the auxiliary and the solute, by bonding of a type which is associated with a specific geometry. As a result, the various portions of the solute molecules will bear different spatial relationships with respect to the complexed auxiliary molecules. They will therefore, in principle experience different magnetic environments associated with any long range effects due to the auxiliary molecules. Diamagnetic anisotropy and dipole-dipole interactions would enhance the long range effects, thus magnify the chemical shift differences of diastereomeric nuclei in the association complex.

2.9. Chiral solvating agents (CSA)

The CSA and the solute have the common feature of functionality, which permits their interaction. Both are in general hydrogen bond donors or acceptors. The CSAs are optically pure compounds. Solute refers to the substance which may be racemic, enantiomerically enriched, or even a single enantiomer, and CSA to the substance whose chirality influences solute spectral behaviour. Occasionally, for a given pair of compounds, these roles may be interchangeable. In nearly every case the CSA contains a group of high diamagnetic anisotropy near its asymmetric center, a feature that is advantageous in translating the different average spatial environments of solute nuclei into different magnetic environments measurableby the NMR method.

The CSA makes complexes with the enantiomers of the racemic mixture. The differences in magnetic environment of the nuclei are generated by diastereomeric complexes that form and dissociate rapidly on the NMR time scale (Equation (2.8) where (P)-A and (M)-A stand for the enantiomers of the substrate and (S)-X stands for a chiral auxiliary (CAS)). The NMR shifts observed are thus average shifts of the complexed

(right-hand side of the equations 2.8 and 2.9) and uncomplexed (left-hand side of the equations) species.

$$(P)\text{-}A+(S)\text{-}X \overset{K_{PS}}{\rightleftharpoons} (P)\text{-}A.(S)\text{-}X \qquad (2.8)$$

$$(M)\text{-}A+(S)\text{-}X \overset{K_{MS}}{\rightleftharpoons} (M)\text{-}A.(S)\text{-}X \qquad (2.9)$$

There are two reasons why the equlibria in Equation 2.8 and 2.9 taking place in the presence of CSA lead to differently shifted signals:

(a) *Intrinsic:* (P)-A.(S)-X and (M)-A.(S)-X are diasteomers and therefore have, at least in principle, different chemical shifts. (P)-A and (M)-A, being enantiomers, have the same shift, so the existence of rapid equilibrium diminishes the obseved shift differences (by averaging) but does not obliterate it.

(b) *Differential stability of diasteomeric solvates*: $K_{PS} \neq K_{MS}$, since the species on the right hand side of the two equations are diasteomers, and hence may be unequally stable (the species on the left hand side, in contrast, have the equal stability). Thus, complexing may not be same for the two enantiomers; other things being equal, the more complexed enantiomer is likely to present the larger chemical shift change by the CSA [37].

When these equilibria are fast on the NMR time scale a single average species is observed for each of the two systems. Besides, the solute enantiomers might themselves associate, forming a different type of diasteomeric complex. The various possible complexes may have nonidentical spectra or formation constants. The spectral consequences of solute-solute interactions contribute to the time-averaged nonequivalence pool. Solute-solute association is second (or higher order) in solute concentration, whereas

solute-CSA association is first order in solute concentration of each solute enantiomer, even if K_{PS} and K_{MS} are equal. In general, the effects of solute-solute interactions are minimal and can be ignored, especially when an excess of a strongly complexing CSA is employed. Hence, the overall nonequivalence that is observed is a function of the differences between the spectra of the diastereomeric complexes and the uncomplexed enantiomers, and of their relative populations (hence the component concentrations and equilibrium constants K_{PS} and K_{MS}).

2.10. Enantiodifferentiation by Nuclear Magnetic Resonance Spectroscopy by Applying Dirhodium Method

Enantiodifferentiation by NMR spectroscopy has a long standing tradition in NMR spectroscopy. However, NMR is an achiral technique so that the presence of an enantiopure auxiliary is mandatory in order to convert enantiotopic nuclei of the substrate molecules into diastereotopic ones. Already in1966, Pirkle introduced enantiopure "Chiral Solvating Agents" (CSA) which form association complexes with chiral alcohols and amines [38]. This method, however, is effective only if the CSAs possess aromatic moieties for secondary binding with other aromatic groups within the substrates. This concept has been refined and is still the focus of research [39].

In the 1970s, "Chiral Lanthanide Shift Reagents" (CLSR) were shown to be particularly useful in enantiodifferentiation of alcohol, amines and various carbonyl and carboxyl derivatives [40] because Ln^{3+} complexes form adducts which are thermodynamically more stable than solvation complexes. Recently, the development in the field of chiral solvation reagents has been reviewed [41]. However, most of these methods involve hard Lewis acid auxiliaries (alcohols, amines, carboxylic acids and so forth) so that their use is more or less restricted to hard Lewis base substrates.

In principle, the dirhodium method resembles the CLSR experiment. Free ligand and Rh* (Figure 2.5) molecules form an equilibrium with 1 : 1- and 2 : 1-adducts (Figure 2.6).

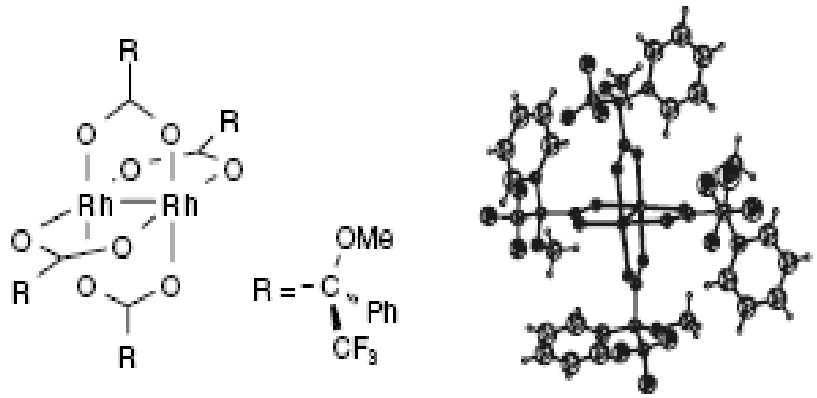

Figure 2.5. Structure of Rh*

Whether or not adducts of higher stoichiometry exist in solution is not yet clear and requires further investigation but there are some indications for their existence. In most cases, reaction rates are so high that only averaged NMR signals can be observed the position of which depend on the thermodynamics and the stoichiometry of the equilibria. It is often possible to go through coalescence effects by sample temperature decrease so that the individual species of free components and adducts can be observed separately. Since the dirhodium method has been designed primarily for enantiodifferentiation of chiral substrates (ligands), the appearance of time-averaged signals is a favorite situation because it is better, i.e. easier to evaluate.

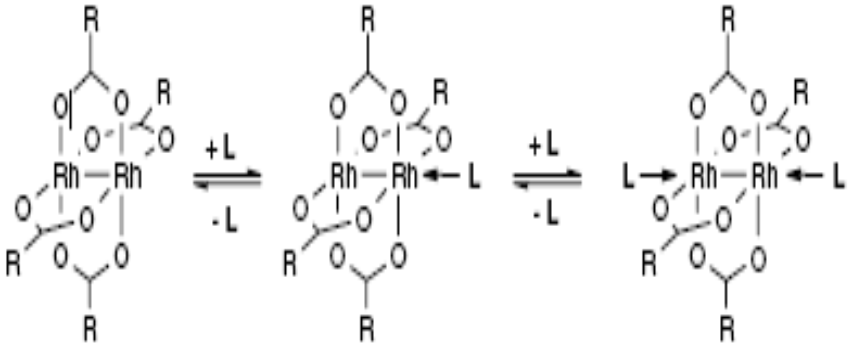

Figure 2.6. Equilibria of a dirhodium complex with ligand molecules (**L**) forming 1 : 1-adducts (center) and 2 : 1-adducts (right)

Two important parameters can be extracted from such enantiodifferentiation experiments:

(a) *The complexation shift* Δδ: This is the chemical shift of the averaged signal compared with the corresponding one of the pure ligand. In general, such Δδ-values are positive (deshielding), small or even close to zero for ^{1}H. Only if the ^{1}H nucleus in question is close to the complexation site, a deshielding of a few tenths of a ppm may be observed. This is a great advantage of the dirhodium method because individual NMR signals appearing in the spectra of the free ligand and the mixture can easily be recognized. It is not necessary to record a series of spectra with increasing proportions of Rh* (as required in the CLSR method) in order to identify the signals which may have exchanged sequences.

On the other hand, negative (shielding) Δδ-values are indicative of a larger distance between the respective nucleus and the binding site because shielding can be interpreted as influence of ring-current effects of the phenyl groups in the Mosher acid residues at the periphery of the dirhodium complex.

(b) *The diastereomeric dispersion effect Δυ*: The second parameter, which is decisive for enantiodifferentiation, is the diastereomeric dispersion effect *Δυ*. It has been mentioned above that enantiotopic nuclei become diastereotopic in the adducts. Hence, the signals of a given nucleus in the ligand are split into two anisochronous signals, and the chemical shift difference is the dispersion *Δυ*. The relative signal areas (integrated signals) represent the ratio of the enantiomers. Here, the precision of *Δυ* -values is restricted to integers which are within the range of experimental reproducibility.

If it is known which of the enantiomers is the major constituent in a non-racemic mixture, it is possible to define signs of dispersion effects by comparing the individual shifts, for example:

$$\Delta\upsilon = \upsilon(R) - \upsilon(S)$$

It is reasonable to assume that the major part of diastereomeric interactions between Rh* and the chiral ligand molecules involves the magnetic anisotropy of the phenyl rings in the Mosher acid residues.

The use of Rh* in the dirhodium method has several advantages beyond the small or moderate complexation shifts already mentioned. In contrast to CLSR, it is diamagnetic so that no line broadening due to paramagnetism is to be expected. Moreover, it is stable, not air-sensitive and nonhygroscopic so that it is easy to prepare samples for NMR measurements.

It should be stated that the dirhodium method can not yet be extended into a direct method for determining absolute configuration because that would require a rigorous conformational analysis of the adduct(s) and, even more, a quantitative prediction of chemical shift influences exerted from each group. Unfortunately, the adduct systems have such an enormous conformational flexibility that it is hard to believe that all this can be simulated with sufficient precision.

On the other hand, the dirhodium method offers an indirect way: once the absolute configuration of one member of a compound family is known, and signs of dispersion effects are uniform, the absolute configuration of the other members follows with high probability. In other words, this is an example of a correlation method for assigning absolute configurations, a methodology which has been very successful in the history of stereochemistry.

3. ORGANIC SYNTHESIS

3.1. Synthesis of 5,5-Dimethyl-3-(o-Aryl)-2-thioxo-4-oxazolidinones

3.1.1. General Procedure

The 5,5-dimethyl-3-(*o*-aryl)-2-thioxo-4-oxazolidinones were synthesized by the reaction of the corresponding arylisothiocyanates with α-hydroxyisobutrayte (Figure 3.1).

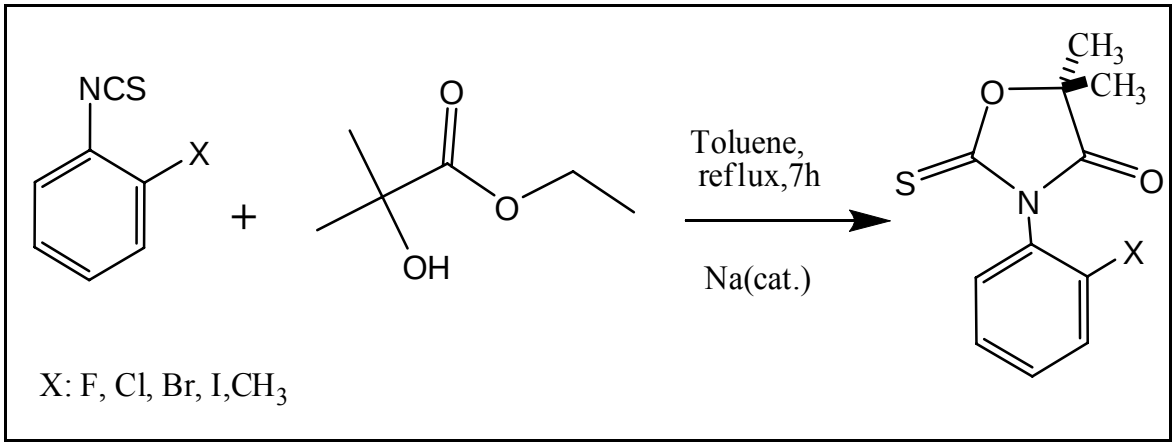

Figure 3.1. Synthesis of 5,5-Dimethyl-3-(*o*-Aryl)-2-thioxo-4-oxazolidinone

In a 100 ml round bottom flask, fitted with a reflux condenser and magnetic stirrer. The appropriate arylisothiocyanate was mixed with α-hydroxyisobutrayte in the presence of metallic sodium in toluene. The reaction mixture was refluxed for 7 hours. Toluene was distilled out and the remaining crude product was purified by recrystallization from ethanol. Starting material data, yield, melting point, ^{1}H NMR, ^{13}C NMR, UV-Vis, IR(KBr) and elemental analysis data for the compounds (±)-1-5 are given in Table 3.1, 3.2, 3.3, 3.4, 3.5, 3.6 and 3.7.

3.1.1.1. 5,5-Dimethyl-3-(*o-fluoro*phenyl)-2-thioxo-4-oxazolidinone, (±)-1. The compound was synthesized according to the general procedure. 5,5-Dimethyl-3-(*o-fluoro*phenyl)-2-thioxo-4-oxazolidinone was obtained as white crystals.

3.1.1.2. 5,5-Dimethyl-3-(*o-chloro*phenyl)-2-thioxo-4-oxazolidinone, (±)-2. The compound was synthesized according to the general procedure. After recrystallizations from ethanol, 5,5-Dimethyl-3-(*o-chloro*phenyl)-2-thioxo-4-oxazolidinone was obtained as white crystals.

3.1.1.3. 5,5-Dimethyl-3-(*o-bromo*phenyl)-2-thioxo-4-oxazolidinone, (±)-3. The compound was synthesized according to the general procedure. 5,5-Dimethyl-3-(*o-bromo*phenyl)-2-thioxo-4-oxazolidinone was obtained as white crystals.

3.1.1.4. 5,5-Dimethyl-3-(*o-iodo*phenyl)-2-thioxo-4-oxazolidinone, (±)-4. The compound was synthesized according to the general procedure. 5,5-Dimethyl-3-(*o-iodo*phenyl)-2-thioxo-4-oxazolidinone was obtained as white crystals.

3.1.1.5. 5,5-Dimethyl-3-(*o-tolyl*)-2-thioxo-4-oxazolidinone, (±)-5. The compound was synthesized according to the general procedure. 5,5-Dimethyl-3-(*o-tolyl*)-2-thioxo-4-oxazolidinone was obtained as white crystals.

Table 3.1. Starting materials used in synthesis of the compounds (±) -1-5

Starting material	Compound (±) -1	Compound (±) -2	Compound (±) -3	Compound (±) -4	Compound (±) -5
o-Fluoro phenylisothiocyanate	5 g (0.033 mol)	-	-	-	-
o-Chloro phenylisothiocyanate	-	6.78 g (0.040 mol)	-	-	-
o-Bromo phenylisothiocyanate	-	-	2.17 g (0.01 mol)	-	-
o-Iodo phenylisothiocyanate	-	-	-	5.0 g (0.019 mol)	-
*o-Tolyl*isothiocyanate	-	-	-	-	4.47 g (0.03 mol)
α-Hydroxyisobutrayte	4.31 g (0.033 mol)	5.28 g (0.040 mol)	1.32 g (0.01 mol)	2.5 g (0.019 mol)	3.96 g (0.03 mol)
Metallic sodium	0.075 g (0.0033 mol)	0.092 g (0.0040 mol)	0.023 g (0.001 mol)	0.043 g (0.0019 mol)	0.069 g (0.003 mol)

Table 3.2. Yield and melting point for the compounds (±) -1-5

Compound No	Yield (g,%)	Melting Point (ºC)
(±) -1	1.00 g (12.7 %)	82.84
(±) -2	3.05 g (29.8 %)	90
(±) -3	0.97 g (32.3 %)	112
(±) -4	3.10 g (47.0 %)	152 - 154
(±) -5	3.00 g (42.5 %)	90

Table 3.3. 400 MHz ^{1}H NMR spectral data for the compounds (±) -1-5

Compound No	Solvent	Diastereotopic methyl protons at C-5	Aromatic protons	*o-Methyl*phenyl protons
(±) -1	Toluene-d_8	1.16, 1.14 (s)	7.20 – 6.60 (m)	-
(±) -2	$CDCl_3$	1.75, 1.77 (s)	7.62 – 7.26 (m)	-
(±) -3	$CDCl_3$	1.79, 1.76 (s)	7.76 – 7.30 (m)	-
(±) -4	$CDCl_3$	1.82, 1.75 (s)	8.20 – 7.20 (m)	-
(±) -5	$CDCl_3$	1.75 (s, 6H)	7.37 – 7.16 (m)	2.19 (s)

Table 3.4. 100 MHz ^{13}C NMR spectral data for the compounds (±) -1-5

Compound No	(±) -1	(±) -2	(±) -3	(±) -4	(±) -5
Solvent	$CDCl_3$	$CDCl_3$	$CDCl_3$	$CDCl_3$	$CDCl_3$
o-Methyl carbon	-	-	-	-	17.30
Diastereotopic methyl carbons	25.3, 22.3	24.1, 23.4	25.1, 23.2	24.1, 23.7	23.9-23.4
Carbonyl carbon of the heterocyclic ring	173.6	174.9	175.8	174.6	175.4
C-5 carbon of the heterocyclic ring	87.5	87.4	88.0	87.6	86.7
Thiocarbonyl carbon of the heterocyclic ring	188.0	187.8	188.0	187.4	188.3
Aromatic carbons	128.3-158.2	132.2 – 128.3	136.2 – 123.3	140.4 – 98.2	131.3 – 128.3

Table 3.5. UV-Vis data for the compounds (±) -1-5

Compound No	UV – Vis data (EtOH) λ_{max}, (log ε_{msx})
(±) -1	206 nm, (4.07); 272 nm, (3.86); 336 nm, (1.71)
(±) -2	206 nm, (4.07); 272 nm, (3.86); 336 nm, (1.71)
(±) -3	206 nm, (3.86); 272 nm, (3.62); 335 nm, (1.68)
(±) -4	206 nm, (3.93); 272 nm, (3.69); 334 nm, (1.53)
(±) -5	206 nm, (3.84); 272 nm, (3.69); 337 nm, (1.67)

Table 3.6. IR (KBr) data for the compounds (±) -1-5

Compound No	C=O stretching ($\bar{\upsilon}_{-N-C=O}$) cm^{-1}	–N-C stretching ($\bar{\upsilon}_{-N-C=S}$) cm^{-1}	C=S stretching ($\bar{\upsilon}_{-C=S}$) cm^{-1}	C=S stretching ($\bar{\upsilon}_{-N-C=S}$) cm^{-1}
(±) -1	1775	1345	1269	1092
(±) -2	1774	1351	1258	1114
(±) -3	1785	1340	1269	1148
(±) -4	1764	1339	1259	1146
(±) -5	1775	1339	1221	1146

Table 3.7. Elemental analysis data for the compounds (±) -1-5

Compound No	Calculated data for C,H,N,S	Found data for C,H,N,S
(±) -1	$C_{11}H_{10}O_2NSF$ C, 55.22; H, 4.21; N, 5.85; S, 13.40	$C_{11}H_{10}O_2NSF$ C, 55.06; H, 4.25; N, 5.77; S, 13.66
(±) -2	$C_{11}H_{10}O_2NSCl$ C, 51.66; H, 3.94; N, 5.48; S, 12.54	$C_{11}H_{10}O_2NSCl$ C, 51.61; H, 3.95; N, 5.51; S, 12.89
(±) -3	$C_{11}H_{10}O_2NSBr$ C, 44.01; H, 3.36; N, 4.67; S, 10.68	$C_{11}H_{10}O_2NSBr$ C, 44.35; H, 3.45; N, 4.77; S, 10.50.
(±) -4	$C_{11}H_{10}O_2NSI$ C, 38.05; H, 2.90; N, 4.03; S, 9.24	$C_{11}H_{10}O_2NSI$ C, 38.27; H, 2.99; N, 4.01; S, 9.53
(±) -5	$C_{12}H_{13}O_2NS$ C, 61.28; H, 5.53; N, 5.96; S, 13.61	$C_{12}H_{13}O_2NS$ C, 61.24; H, 5.47; N, 6.00; S, 13.68

3.2. Synthesis of 5,5-Dimethyl-3-(o-Aryl)-2-thioxo-4-thiazolidinones

3.2.1. General procedure for the preperation of 5,5-Dimethyl-3-(o-Aryl)-2-thioxo-4-thiazolidinones

The 5,5-dimethyl-3-(*o*-aryl)-2-thioxo-4-thiazolidinones were synthesized according to the Modified Kaluza Synthesis (Figure 3.2). The following is the generalized procedure used for the preparation of the compounds (±)-6-9. At the first part of the procedure, the amine was dissolved in the minimum amount of benzene and treated with carbon disulfide and triethylamine (as a base). The solution was cooled to 0 ºC. After complete precipitation of the triethylammonium dithiocarbamate salt, the solution was filtered. The solid was washed with anhydrous ether and air dried for about 15 minutes. At the second part of the procedure, the salt was dissolved in chloroform, treated with triethylamine, and cooled again to 0 ºC. To this solution was added α-bromoisobutryic acid ethyl ester dropwise over a 20 minutes period with hand stirring. The resulting solution was stirred at 0 ºC for 2 hours and then heated at 50 ºC for 4 hours. Then, the chloroform solution was washed with 3M HCl and twice with water and dried over calcium chloride. The chloroform was evaporated in vacuo and the crude product was recrystallized from ethanol. Starting material data, yield, melting point, ^{1}H NMR, ^{13}C NMR, UV-Vis, IR(KBr) and elemental analysis data for the compounds (±)-6-10 are given in Table 3.8, 3.9, 3.10, 3.11, 3.12, 3.13 and 3.14.

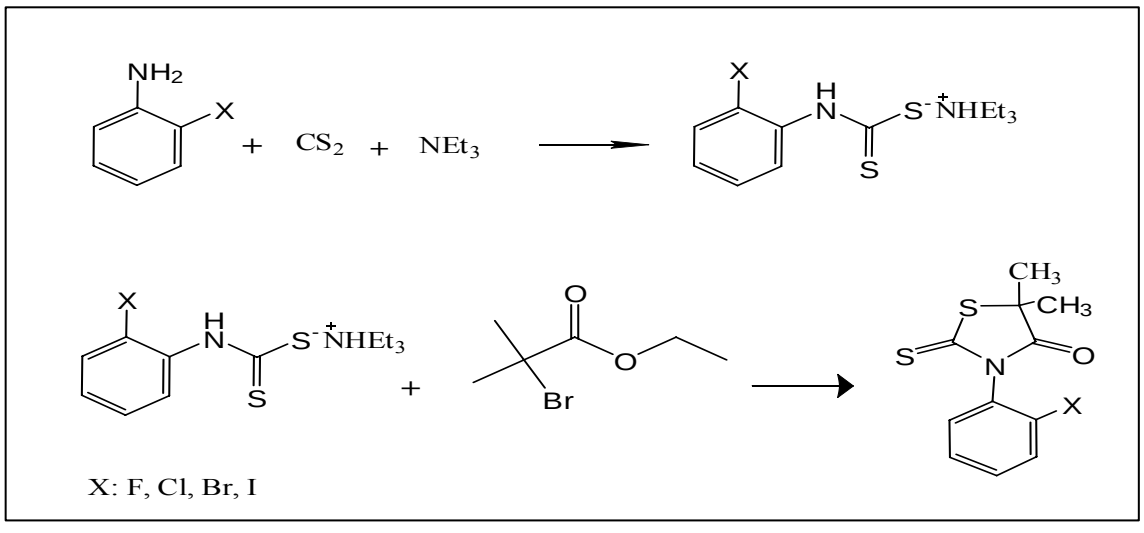

Figure 3.2. Synthesis of 5,5-dimethyl-3-(*o*-aryl)-2-thioxo-4-thiazolidinones

3.2.1.1. 5,5-Dimethyl-3-(*o-fluoro*phenyl)-2-thioxo-4-thiazolidinone, (±)-6. The compound was synthesized according to the general procedure. 5,5-Dimethyl-3-(*o-fluoro*phenyl-2-thioxo-4-thiazolidinone was obtained as yellow crystals.

3.2.1.2. 5,5-Dimethyl-3-(*o-chloro*phenyl)-2-thioxo-4-thiazolidinone, (±)-7. The compound was synthesized according to the general procedure. 5,5-Dimethyl-3-(*o-chloro*phenyl-2-thioxo-4-thiazolidinone was obtained as yellow crystals.

3.2.1.3. 5,5-Dimethyl-3-(*o-bromo*phenyl)-2-thioxo-4-thiazolidinone, (±)-8. The compound was synthesized according to the general procedure. 5,5-Dimethyl-3-(*o-bromo*phenyl-2-thioxo-4-thiazolidinone was obtained as yellow crystals.

3.2.1.4. 5,5-Dimethyl-3-(*o-iodo*phenyl)-2-thioxo-4-thiazolidinone, (±)-9. The compound was synthesized according to the general procedure. 5,5-Dimethyl-3-(*o-iodo*phenyl-2-thioxo-4-thiazolidinone was obtained as yellow crystals.

3.2.1.5. 5,5-Dimethyl-3-(*o-toyl*)-2-thioxo-4-thiazolidinone, (±)-10. The compound had been synthesized by Doğan *et al.* [33], for the first time. During the present study, it was used for the purpose of determination of its activativation barrier.

Table 3.8. Starting materials used in synthesis of the compounds (±) -6-9

Starting material	Compound (±) -6	Compound (±) -7	Compound (±) -8	Compound (±) -9
*o-Fluoro*aniline	14.55 g (0.15 mol)	-	-	-
*o-Chloro*aniline	-	12.75 g (0.1 mol)	-	-
*o-Bromo*aniline	-	-	34.4 g (0.2 mol)	-
*o-Iodo*aniline	-	-	-	10.95 g (0.05 mol)
Carbon disulfide	9.9 ml (0.15 mol)	7.6 ml (0.1 mol)	13.2 ml (0.2 mol)	3.8 ml (0.05 mol)

Table 3.8. Starting materials used in synthesis of the compounds (±) -6-9 (continued)

Starting material	Compound (±) -6	Compound (±) -7	Compound (±) -8	Compound (±) -9
Triethylamine for 1st part	21 ml (0.15 mol)	14 ml (0.1 mol)	28 ml (0.2 mol)	7 ml (0.05 mol)
Triethylamine for 2nd part	9.66 ml (0.069 mol)	3.85 ml (0.027 mol)	17.22 ml (0.123 mol)	3 ml (0.021 mol)
*o-Fluoro*phenyl dithiocarbamate	19.87 g (0.069 mol)	-	-	-
*o-Chloro*phenyl dithiocarbamate	-	8.22 g (0.027 mol)	-	-
*o-Bromo*phenyl dithiocarbamate	-	-	42.87 g (0.123 mol)	-
*o-Iodo*phenyl dithiocarbamate	-	-	-	8.48 g (0.021 mol)
α-Bromoisobutyric acid ethyl ester	13.4 g (0.069 mol)	5.27 g (0.027 mol)	23.9 g (0.123 mol)	4.1 g (0.021 mol)

Table 3.9. Yield and melting point for the compounds (±) -6-10

Compound No	Yield (g,%)	Melting Point (ºC)
(±) -6	1.87 g (25.5 %)	72 - 76
(±) -7	2.00 g (11.4 %)	72 - 74
(±) -8	11.00 g (25.6 %)	98 - 100
(±) -9	1.00 g (13.9 %)	130

Table 3.10. 400 MHz ^{1}H NMR spectral data for the compounds (±) -6-10

Compound No	Solvent	Diastereotopic methyl protons at C-5	Aromatic protons	*o-Methyl*phenyl protons
(±) -6	DMSO-d_6	1.76, 1.72 (s)	7.59 – 7.34 (m)	-
(±) -7	DMSO-d_6	1.76, 1.74 (s)	7.68 – 7.49 (m)	-
(±) -8	$CDCl_3$	1.85, 1.80 (s)	7.74 – 7.25 (m)	-
(±) -9	$CDCl_3$	1.79, 1.76 (s)	7.98 – 7.23 (m)	-
(±) -10	DMSO-d_6	1.73, 1.74 (s)	7.44 – 7.33 (m)	2.01 (s)

Table 3.11. 100 MHz ^{13}C NMR spectral data for the compounds (±) -6-10

Compound No	(±) -6	(±) -7	(±) -8	(±) -9	(±) -10
Solvent	Benzene-d_6	$CDCl_3$	$CDCl_3$	DMSO-d_6	Benzene-d_6
o-Methyl carbon	-	-	-	-	17.0
Diastereotopic methyl carbons	25.9, 24.8	28.3, 26.9	28.3, 27.0	28.0, 26.0	26.4, 27.2
Carbonyl carbon of the heterocyclic ring	177.3	178.8	178.7	179.0	178.8
C-5 carbon of the heterocyclic ring	54.1	56.1	56.2	57.0	55.1
Thiocarbonyl carbon of the heterocyclic ring	197.0	198.4	198.4	200.2	198.4
Aromatic carbons	158.1 – 123.3	133.3 – 128.1	134.8 – 123.0	140.0 – 100.0	127.1 – 136.3

Table 3.12. UV-Vis data for the compounds (±) -6-10

Compound No	UV – Vis data (EtOH) λ_{max}, (log ε_{msx})
(±) -6	300 nm, (4.28); 205 nm, (4.07); 398 nm, (1.66)
(±) -7	294 nm, (4.14); 205 nm, (3.83); 336 nm, (1.71)
(±) -8	295 nm, (4.16); 205 nm, (3.92)
(±) -9	295 nm, (4.04); 205 nm, (3.88)
(±) -10	257 nm, (4.09); 207 nm, (4.18)

Table 3.13. IR (KBr) data for the compounds (±) -6-10

Compound No	C=O stretching ($\bar{\upsilon}_{-N-C=O}$) cm^{-1}	–N-C stretching ($\bar{\upsilon}_{-N-C=S}$) cm^{-1}	C=S stretching ($\bar{\upsilon}_{-C=S}$) cm^{-1}	C=S stretching ($\bar{\upsilon}_{-N-C=S}$) cm^{-1}	–C-S stretching ($\bar{\upsilon}_{-N-C=S}$) cm^{-1}
(±) -6	1747	1343	1247	1139	1042
(±) -7	1725	1344	1263	1150	1037
(±) -8	1729	1346	1245	1154	1042
(±) -9	1734	1340	1246	1138	1046
(±) -10	1740	1341	1261	1143	1048

Table 3.14. Elemental analysis data for the compounds (±) -6-10

Compound No	Calculated data for C,H,N,S	Found data for C,H,N,S
(±) -6	$C_{11}H_{10}ONS_2F$ C, 51.74; H, 3.94; N, 5.48; S, 25.12	$C_{11}H_{10}ONS_2F$ C, 52.12; H, 3.91; N, 5.41; S, 25.09
(±) -7	$C_{11}H_{10}ONS_2Cl$ C, 48.61; H, 3.71; N, 5.15; S, 23.59	$C_{11}H_{10}ONS_2Cl$ C, 48.56; H, 3.69; N, 5.31; S, 23.26
(±) -8	$C_{11}H_{10}ONS_2Br$ C, 41.78; H, 3.18; N, 4.43; S, 20.28	$C_{11}H_{10}ONS_2Br$ C, 41.86; H, 3.19; N, 4.43; S, 20.67
(±) -9	$C_{11}H_{10}ONS_2I$ C, 36.37; H, 2.77; N, 3.85; S, 17.65	$C_{11}H_{10}ONS_2I$ C, 36.54; H, 2.65; N, 3.78; S, 17.87
(±) -10	$C_{12}H_{13}ONS_2$ C, 57.34; H, 5.21; N, 5.57; S, 25.50	$C_{12}H_{13}ONS_2$ C, 57.01; H, 5.15; N, 5.65; S, 25.82

3.3. Synthesis of 3-(o-Aryl)-2-thioxo-4-thiazolidinones

3.3.1. General procedure for preparation of 3-(o-Aryl)-2-thioxo-4-thiazolidinones

The 3-(*o*-aryl)-2-thioxo-4-thiazolidinones the compounds (±)-11-15, were synthesized by the reaction of corresponding aryl isothiocyanates with thioglycolic acid ethyl ester in the presence of sodium metal in toluene (Figure 3.3).

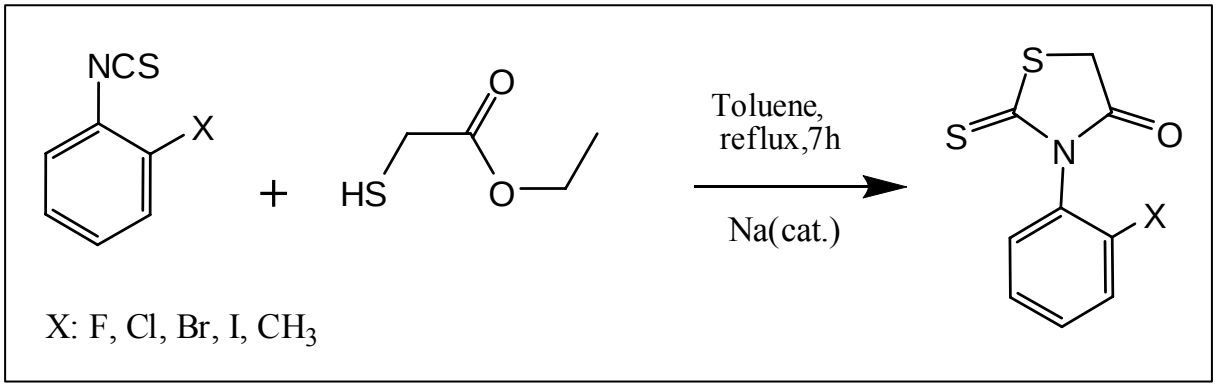

Figure 3.3. Synthesis of 3-(*o*-aryl)-2-thioxo-4-thiazolidinones

The reaction was carried out in toluene which allows dissolution of aryl isothiocyanates. In a 100 ml round bottom flask, aryl isothiocyanate was mixed with

thioglycolic acid ethyl ester in the presence of the small pieces of sodium metal in toluene. The reaction was refluxed for 7 hours. The compound formed at the end of the this period, after distillation of toluene was purified by recrystallization from ethanol. Starting material data, yield, melting point, ^{1}H NMR, ^{13}C NMR, UV-Vis, IR(KBr) and elemental analysis data for the compounds (±)-11-15 are given in Table 3.15, 3.16, 3.17, 3.18, 3.19, 3.20 and 3.21.

3.3.1.1. 3-(*o-flouro*phenyl)-2-thioxo-4-thiazolidinone, (±)-11. The compound was synthesized according to the general procedure. After recrystallizations from ethanol, 3N-(*o-fluoro*phenyl)-2-thioxo-4-thiazolidinone was obtained as yellow crystals and identified by its ^{1}H NMR and ^{13}C NMR spectrum.

3.3.1.2. 3-(*o-chloro*phenyl)-2-thioxo-4-thiazolidinone, (±)-12. The compound was synthesized according to the general procedure. 3N-(*o-chloro*phenyl)-2-thioxo-4-thiazolidinone was obtained as yellow crystals and identified by its ^{1}H NMR and ^{13}C NMR spectrum.

3.3.1.3. 3-(*o-bromo*phenyl)-2-thioxo-4-thiazolidinone, (±)-13. The compound was synthesized according to the general procedure. 3N-(*o-bromo*phenyl)-2-thioxo-4-thiazolidinone was obtained as yellow crystals and identified by its ^{1}H NMR and ^{13}C NMR spectrum.

3.3.1.4. 3-(*o-iodo*phenyl)-2-thioxo-4-thiazolidinone, (±)-14. The compound was synthesized according to the general procedure. 3N-(*o-iodo*phenyl)-2-thioxo-4-thiazolidinone was obtained as red crystals and identified by its ^{1}H NMR and ^{13}C NMR spectrum.

3.3.1.5. 3-(*o-tolyl*)-2-thioxo-4-thiazolidinone, (±)-15. The compound was synthesized according to the general procedure. 3N-(*o-tolyl*)-2-thioxo-4-thiazolidinone was obtained as orange crystals and identified by its ^{1}H NMR and ^{13}C NMR spectrum.

Table 3.15. Starting materials used in synthesis of the compounds (±) -11-15

Starting material	Compound (±) -11	Compound (±) -12	Compound (±) -13	Compound (±) -14	Compound (±) -15
o-Fluoro phenylisothiocyanate	3.06 g (0.02 mol)	-	-	-	-
o-Chloro phenylisothiocyanate	-	3.38 g (0.02 mol)	-	-	-
o-Bromo phenylisothiocyanate	-	-	4.28 g (0.02 mol)	-	-
o-Iodo phenylisothiocyanate	-	-	-	5.22 g (0.02 mol)	-
*o-Tolyl*isothiocyanate	-	-	-	-	2.9 g (0.02 mol)
Thioglycolic ethyl ester	2.4 g (0.02 mol)	2.4 g (0.02 mol)	2.4 g (0.02 mol)	2.4 g (0.02 mol)	2.4 g (0.02 mol)
Metallic sodium	0.046 g (0.002 mol)	0.046 g (0.002 mol)	0.046 g (0.002 mol)	0.046 g (0.002 mol)	0.046 g (0.002 mol)

Table 3.16. Yield and melting point for the compounds (±) -11-15

Compound No	Yield (g,%)	Melting Point (ºC)
(±) -11	1.7 g (40.0 %)	103 – 104
(±) -12	2.0 g (41.1 %)	112 – 113
(±) -13	1.7 g (29.8 %)	142 – 146
(±) -14	3.45 g (54 %)	158 – 160
(±) -15	1.5 g (33.6 %)	110

Table 3.17. 400 MHz ^{1}H NMR spectral data for the compounds (±) -11-15

Compound No	Solvent	Diastereotopic methylene protons at C-5	Aromatic protons	*o-Methyl*phenyl protons
(±) -11	Toluene-d_8	2.82, 2.79 (AB quartet, 1H each, J_{AB}=18.33 Hz)	7.20 – 7.09 (m)	-
(±) -12	$CDCl_3$	4.25, 4.19 (AB quartet, 1H each, J_{AB}=17.94 Hz)	7.40 – 7.15 (m)	-
(±) -13	$CDCl_3$	4.27, 4.21 (AB quartet, 1H each, J_{AB}=18.33 Hz)	7.76 – 7.22 (m)	-
(±) -14	$CDCl_3$	4.26, 4.19 (AB quartet, 1H each, J_{AB}=18.33 Hz)	8.1 – 7.6 (m)	-
(±) -15	$CDCl_3$	4.20, 4.18 (AB quartet, 1H each, J_{AB}=18.33 Hz)	7.43 – 7.06 (m)	2.13 (s)

Table 3.18. 100 MHz ^{13}C NMR spectral data for the compounds (±) -11-15

Compound No	(±) -11	(±) -12	(±) -13	(±) -14	(±) -15
Solvent	$CDCl_3$	$CDCl_3$	Benzene-d_6	$CDCl_3$	$CDCl_3$
o-Methyl carbon	-	-	-	-	17.4
Carbonyl carbon of the heterocyclic ring	173.6	172.6	171.9	172.6	173.10
C-5 carbon of the heterocyclic ring	37.0	36.6	35.6	36.9	36.40
Thiocarbonyl carbon of the heterocyclic ring	200.08	198.08	199.5	197.7	200.5
Aromatic carbons	160.20 – 117.36	133.03 – 128.27	135.8 – 128.5	140.3 – 98.5	134.0 – 128.5

Table 3.19. UV-Vis data for the compounds (±) -11-15

Compound No	UV – Vis data (EtOH) λ_{max}, (log ε_{msx})
(±) -11	300 nm, (4.11)
(±) -12	300 nm, (4.14)
(±) -13	301 nm, (4.06)
(±) -14	296 nm, (4.17)
(±) -15	301 nm, (4.09)

Table 3.20. IR (KBr) data for the compounds (±) -11-15

Compound No	C=O stretching ($\bar{\upsilon}_{-N-C=O}$) cm^{-1}	–N-C stretching ($\bar{\upsilon}_{-N-C=S}$) cm^{-1}	C=S stretching ($\bar{\upsilon}_{-C=S}$) cm^{-1}	C=S stretching ($\bar{\upsilon}_{-N-C=S}$) cm^{-1}	–C-S stretching ($\bar{\upsilon}_{-N-C=S}$) cm^{-1}
(±) -11	1727	1344	1238	1166	1055
(±) -12	1731	1350	1250	1100	1050
(±) -13	1730	1346	1230	1176	1033
(±) -14	1736	1340	1225	1159	1066
(±) -15	1736	1335	1242	1165	1044

Table 3.21. Elemental analysis data for the compounds (±) -11-15

Compound No	Calculated data for C,H,N,S	Found data for C,H,N,S
(±) -11	$C_9H_6ONS_2F$ C, 47.56; H, 2.66; N, 6.16; S, 28.21	$C_9H_6ONS_2F$ C, 47.71; H, 2.92; N, 6.44; S, 28.20
(±) -12	$C_9H_6ONS_2Cl$ C, 44.35; H, 2.48; N, 5.47; S, 26.31	$C_9H_6ONS_2Cl$ C, 44.40; H, 2.43; N, 5.71; S, 25.99
(±) -13	$C_9H_6ONS_2Br$ C, 37.51; H, 2.09; N, 4.86; S, 22.25	$C_9H_6ONS_2Br$ C, 37.53; H, 2.05; N, 4.83; S, 22.12
(±) -14	$C_9H_6ONS_2I$ C, 32.25; H, 1.80; N, 4.17; S, 19.13	$C_9H_6ONS_2I$ C, 32.49; H, 1.75; N, 4.14; S, 19.09
(±) -15	$C_{10}H_9ONS_2$ C, 53.78; H, 4.06; N, 6.27; S, 28.72	$C_{10}H_9ONS_2$ C, 53.77; H, 4.06; N, 6.49; S, 28.79

3.4. Apparatus

^{1}H NMR and ^{13}C NMR spectra were recorded on the Varian-Mercury VX-400 MHz-BB.

Melting points were recorded using a Bibby Stuart Scientific melting point apparatus.

The IR analyses were performed on a Perkin Elmer 1600 FTIR using KBr windows.

Liquid chromatography analyses were performed using analytical Chiralpak AD-H column (Daicel Ltd., partical size: 5µm, column size:250×4.6 mm) ,Semi-preperative Chiralpak AD-H column (Daicel Ltd., partical size: 5µm, column size:250×10 mm) and Chiralpak IB column (Daicel Ltd., partical size: 5µm, column size:250×4.6 mm), Lab Alliance Series III pump and Water Assoc. UV absorbance detector.

Elemental analysis were performed on Thermo Scientific FlashEA 1112 elemental analyzer.

3.5. List of Chemicals

Table 3.22. Reagents

Name	**Formula**	**Supplier**	**% Purity**
o-Fluorophenylisothiocynate	C_7H_4NSF	Aldrich	98
o-Chlorophenylisothiocynate	C_7H_4NSCl	Aldrich	98
o-Bromophenylisothiocynate	C_7H_4NSBr	Aldrich	98
o-Iodophenylisothiocynate	C_7H_4NSI	Aldrich	98
2-Methylphenylisothiocynate	C_8H_7NS	Aldrich	98
α-Hydroxyisobutyricacid ethyl ester	$C_6H_{12}O_2$	Merck	99
o-Fluroaniline	C_6H_6NF	Merck	98
o-Chloroaniline	C_6H_6NCl	Merck	98
o-Bromoaniline	C_6H_6NBr	Merck	98
o-Iodoaniline	C_6H_6NI	Merck	98
2-Methylaniline	C_7H_9N	Merck	98
Ethyl thioglycolate	$HSCH_2C00C_2H_5$	Merck	98
Triethylamine	$N(C_2H_5)_3$	Merck	98
Carbon Disulfide	CS_2	Fluka	99
Sodium metal	Na	Reidel-de haen	99.5
Toluene	C_7H_8	Merck	>99
Ethanol	C_2H_5OH	Merck	98.5
(S)-(+)-TFAE	$C_{16}H_{11}OF_3$	Aldrich	>98
Hexane for HPLC	C_6H_{14}	J.T.Baker	>99.9

Table 3.22. Reagents (continued)

Absolute Ethanol for HPLC	C_2H_50H	J.T.Baker	>99.9
2-Propanol for HPLC	C_3H_7OH	J.T.Baker	>99.9
α-Bromoisobutyricacid ethyl ester	$C_6H_{11}O_2Br$	Fluka	>99
α-Naphthyl isothiocyanate	$C_{11}H_7NS$	Aldrich	>98
α-Naphthyl isocyanate	$C_{11}H_7NO$	Aldrich	>98

4. RESULTS AND DISCUSSION

4.1. ^{1}H NMR Spectra of the compounds

For the 5,5-dimethyl-3-(*o*-aryl)-2-thioxo-4-oxazolidinones, compounds (±)-1-5, 5,5-dimethyl-3-(*o*-aryl)-2-thioxo-4-thiazolidinones, compounds (±)-6-10, and 3-(*o*-aryl)-2-thioxo-4-thiazolidinones, compounds (±)-11-15, the barrier to rotation around C-N single bond is expected to be so high that these molecules will be non-planar in their ground states. Hindered rotation around the C-N single bond in these compounds results in formation of enantiomers M and P which will show identical NMR spectra in an achiral solvent. However, methyl groups on C-5 in compounds (±)-1-10 (Figure 4.1) and methylene protons on C-5 in compounds (±)-11-15 (Figure 4.2) are diastreotopic. This means that the C-5 substitutents are magnetically non-equivalent, so, they can be differentiated by NMR spectroscopy. Methyl groups on C-5 in compounds (±)-1-10 in fact exhibited two distinct singlets for the 5-methyl protons due to the diastereotopicity of these groups. The ^{1}H NMR results for compounds (±)-1-10 are summarized in Table 4.1.

The ^{1}H NMR spectra of the compounds (±)-1-15 are shown in Figures 4.3 to 4.26. In compounds (±)-1 and (±)-5 only a singlet around 1.75 ppm was seen instead of two singlets in $CDCl_3$. To differentiate diastereotopic methyl protons for compounds (±)-1 and (±)-5, the spectra were also taken in toluene-d_8, since it is a better solvent to observe the shift differences due to the anisotropy effect of the benzene ring. This time, the signals of the 5-methyl protons were distingquishable, chemical shift differences between methyl groups being 0.02 ppm for the compoud (±)-1 and 0.01 ppm for the compound (±)-5.

In the compounds (±)-2, (±)-3 and (±)-4, the chemical shift differences between the methyl groups were 0.02 ppm, 0.03 ppm and 0.07 ppm, respectively in $CDCl_3$. The chemical shift differences between the diastreotopic groups can be expected to be affected by the anisotropic influence of the substitutent at the *ortho* positions as well as by the dihedral angles between the two rings, which will be determined largely by the size of the *ortho* aryl substitutents.

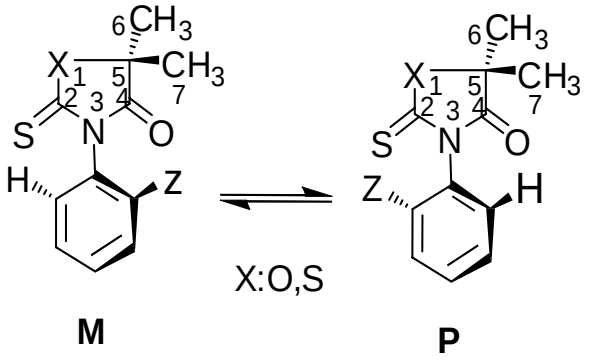

Figure 4.1. The general structure of the 5,5-dimethyl-3-(*o*-aryl)-2-thioxo-4-oxazolidinones and 5,5-dimethyl-3-(*o*-aryl)-2-thioxo-4-thiazolidinones

Table 4.1. 400 MHz ^{1}H NMR spectral data for the compounds (±)-1-10 in $CDCl_3$ at 30 ^{o}C

Compound No	X	Z	δ (ppm) of 5-CH_3	δ (ppm) of Aromatic Protons	δ (ppm) of o-CH_3
(±)-1	O	F	1.75[c] 1.14 and 1.16[a,b]	7.25-7.53 6.60-7.20	-
(±)-2	O	Cl	1.75 and 1.77[a]	7.26-7.62	-
(±)-3	O	Br	1.76 and 1.79[a]	7.3-7.76	-
(±)-4	O	I	1.75 and 1.82[a]	7.2-8.2	-
(±)-5	O	CH_3	1.75[c] 1.17 and 1.18[a,b]	7.16-7.37 6.89-7.09	2.19 1.98[b]
(±)-6	S	F	1.82[c] 1.72 and 1.76[a,d]	7.34-7.59	-
(±)-7	S	Cl	1.74 and 1.76[a,d] 1.80 and 1.84[a]	7.49-7.68 7.25-7.57	-
(±)-8	S	Br	1.75and 1.76[a,d] 1.80 and 1.85[a]	7.43-7.81 7.25-7.74	-
(±)-9	S	I	1.76 and 1.79[a,d] 1.81 and 1.89[a]	7.23-7.98	-
(±)-10	S	CH_3	1.73and 1.74[a,d] 1.80 and 1.81[a]	7.25-7.33 7.33-7.44	2.01 2.12

[a]: Diastereotopic methyl protons, [b]: Solvent is Toluene-d_8, [c] Only one singlet was observed, [d] Solvent is DMSO-d_6

The magnitude of the dihedral angle depends on the steric repulsion between the *ortho* substitutents and the carbonyl oxygen atom in the transition state. Since, *ortho* chloro, *ortho* bromo and *ortho* iodo substitutents possessed lone pair electrons that interacted with that of carbonyl oxygen in the transition state, the chemical shift differences were higher for *ortho* halogen substitutents than the *ortho* methyl substitutent. Also, a smaller chemical shift difference was observed for the *ortho* chloro substituted (±)-2 than *ortho* bromo and *ortho* iodo substituted (±)-3 and (±)-4 because of the smaller size of the chlorine atom.

The ^{1}H NMR spectra of the compounds (±)-6-10 are shown in Figures 4.10 to 4.19. For the compounds (±)-7 and (±)-8, where the *ortho* substitutents were chloro and bromo, the chemical shift differences were 0.04 ppm and 0.05 ppm, respectively. These values were larger compared with that of compounds (±)-2 and (±)-3, where *ortho* substitutents were also chloro and bromo. This difference can be explained by the difference in the bond lenghts of the O-C and S-C bonds of the corresponding rings. On the other hand, the chemical shift differences for (±)-4 and (±)-9, where the *ortho* substitutents was iodo, were the same as 0.07 ppm.

In $CDCl_3$ only one singlet was observed around 1.82 ppm for the *o*-fluoro compound (±)-6. On the other hand, the chemical shift differences changed between 0.04 to 0.08 ppm for the compounds (±)-7, (±)-8 and (±)-9 in $CDCl_3$. The highest chemical shift difference was observed for the compound (±)-9 (0.08 ppm), where the *ortho* substitutent was iodo. This result also confirms the effect of dihedral angle on the chemical shift differences of diastereotopic protons in spectra. Also a solvent effect was observed for these compounds. In DMSO-d_6 for instance (±)-6 diastereotopic methyl groups were differentiated with a shift difference of 0.04 ppm.

The ^{1}H NMR results for compounds (±)-11-15 are summarized in Table 4.3. For the 3-(*o*-aryl)-2-thioxo-4-thiazolidinones, the two methylene protons at C-5 are diastereotopic and gave the expected AB splittings in $CDCl_3$ (Table 4.2).

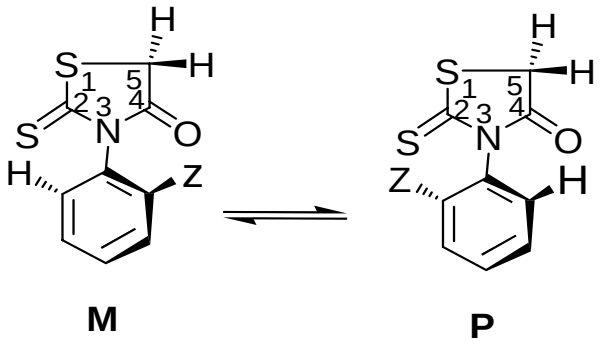

Figure 4.2. The general structure of the 3-(*o*-aryl)-2-thioxo-4-thiazolidinones

Table 4.2. 400 MHz ^{1}H NMR spectral data for the compounds (±)-11-15 in $CDCl_3$ at 30 ^{o}C

Compound No	Z	δ (ppm) of 5-CH_2	δ (ppm) of Aromatic Protons	δ (ppm) of o-CH_3
(±)-11	F	δ_A= 2.82, δ_B= 2.79 [a,b] δ_A= 4.27, δ_B= 4.16 [b]	7.09-7.20 7.25-7.50	-
(±)-12	Cl	δ_A= 4.25, δ_B= 4.19 [b]	7.15-7.40	-
(±)-13	Br	δ_A= 4.27, δ_B= 4.21 [b]	7.22-7.76	-
(±)-14	I	δ_A= 4.26, δ_B= 4.19 [b]	7.2-8.1	-
(±)-15	CH_3	δ_A= 4.54, δ_B= 4.40 [b,c] δ_A= 4.20, δ_B= 4.18 [b]	7.14-7.40 7.06-7.43	2.03 [c] 2.13

[a]: Solvent is Toluene-d_8, [b]: AB type splitting, [c] : Solvent is DMSO-d_6

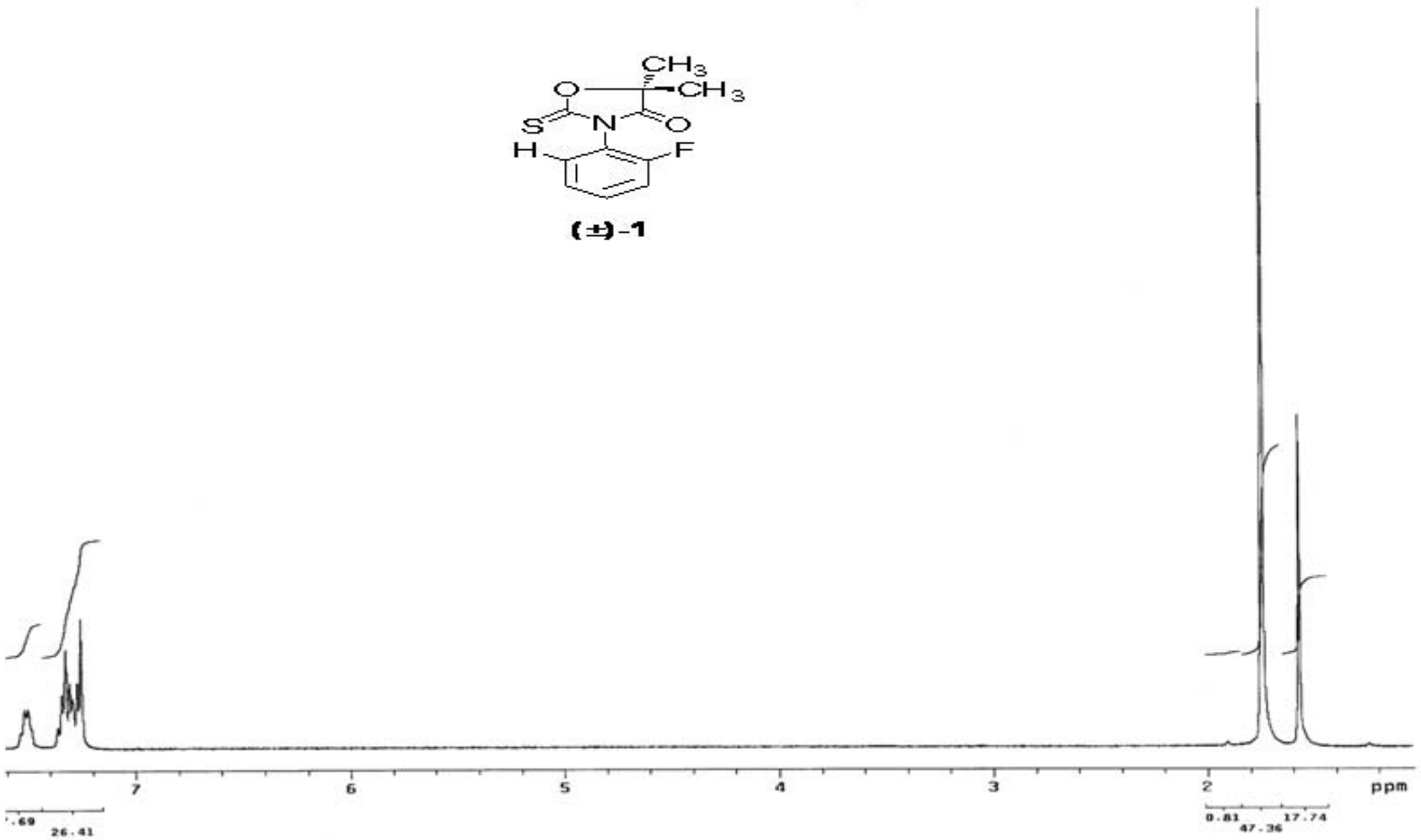

Figure 4.3. ^{1}H NMR spectrum of compound 1 in $CDCl_3$

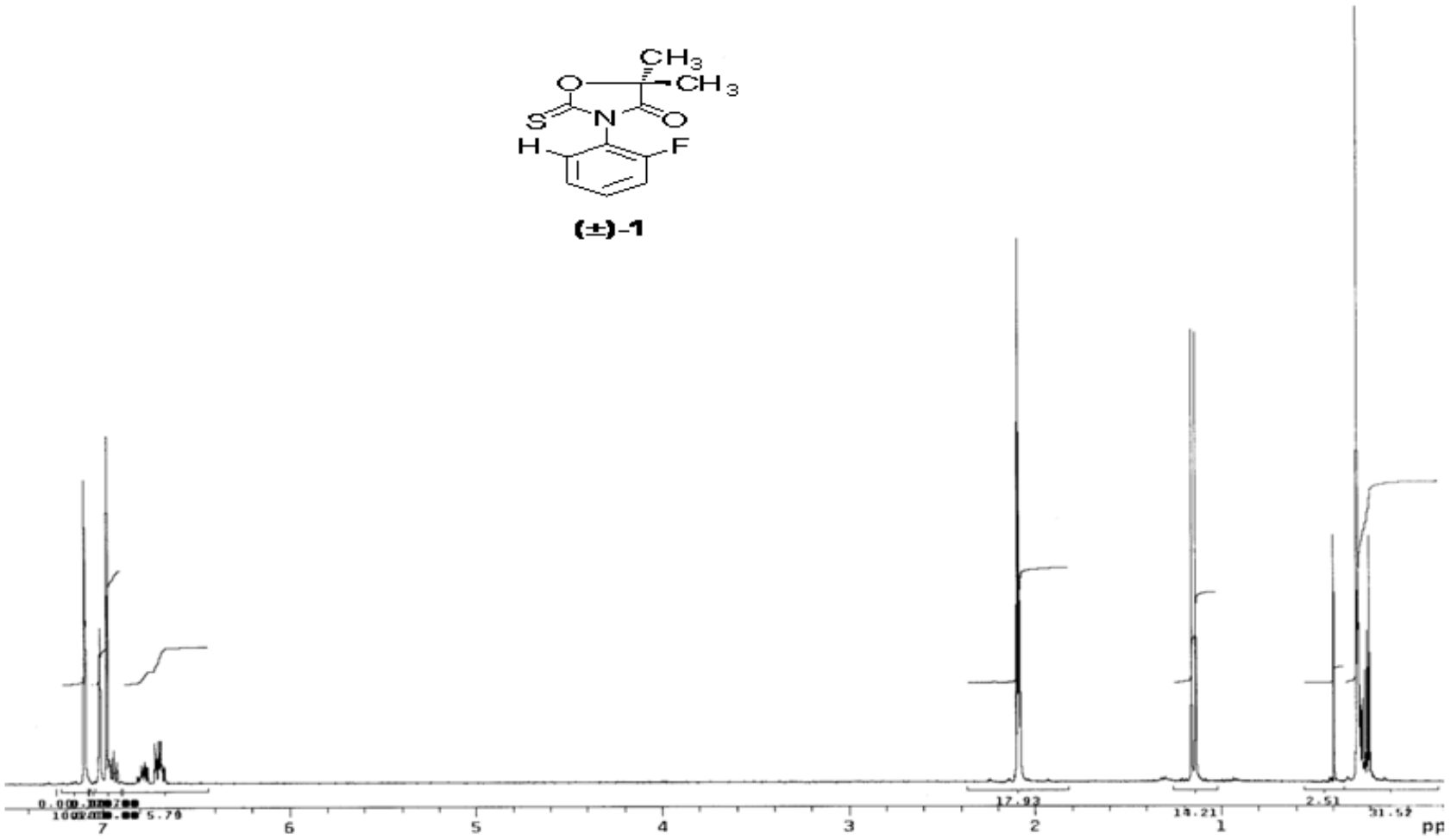

Figure 4.4. ^{1}H NMR spectrum of compound 1 in Toluene-d_8

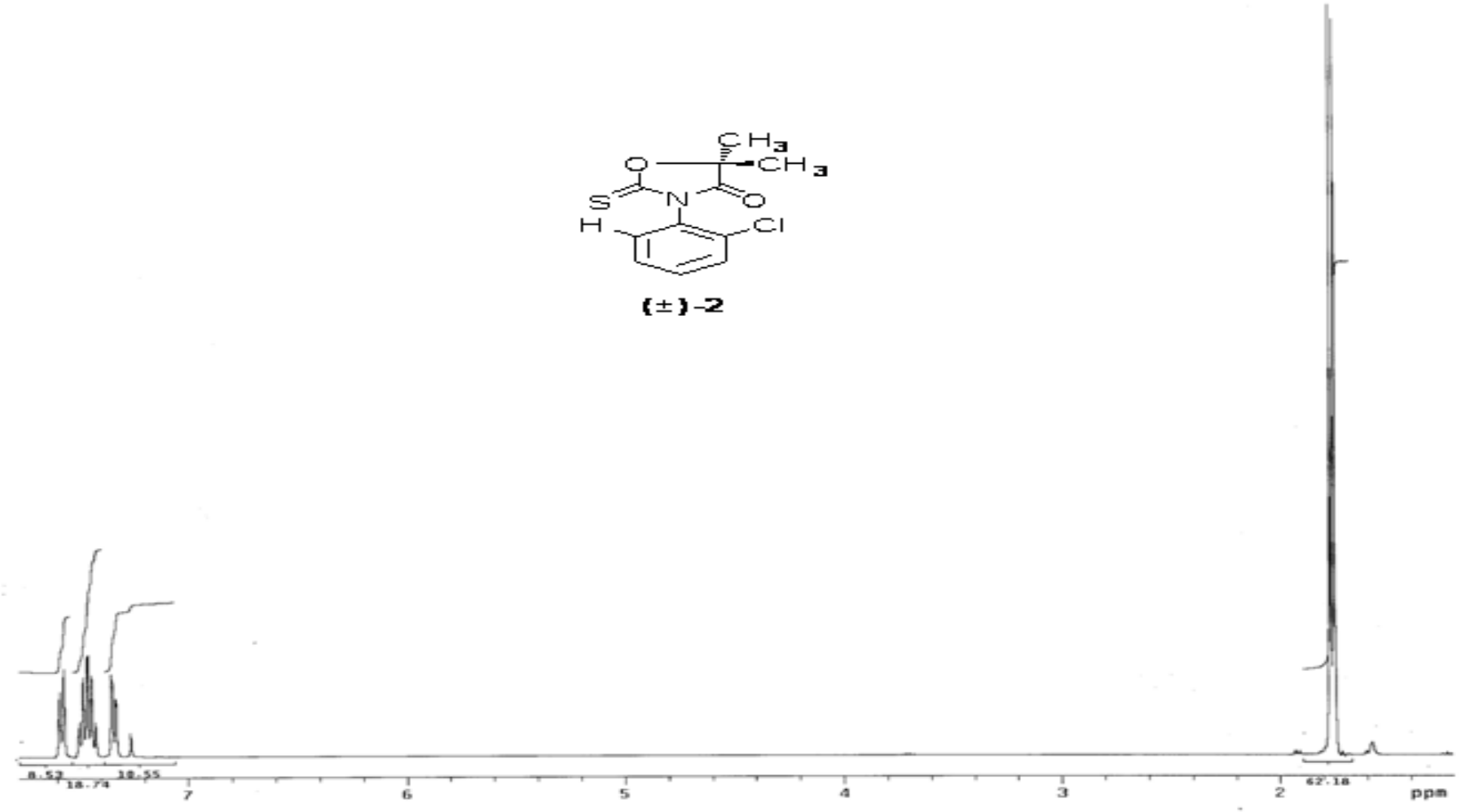

Figure 4.5. ^{1}H NMR spectrum of compound 2 in $CDCl_3$

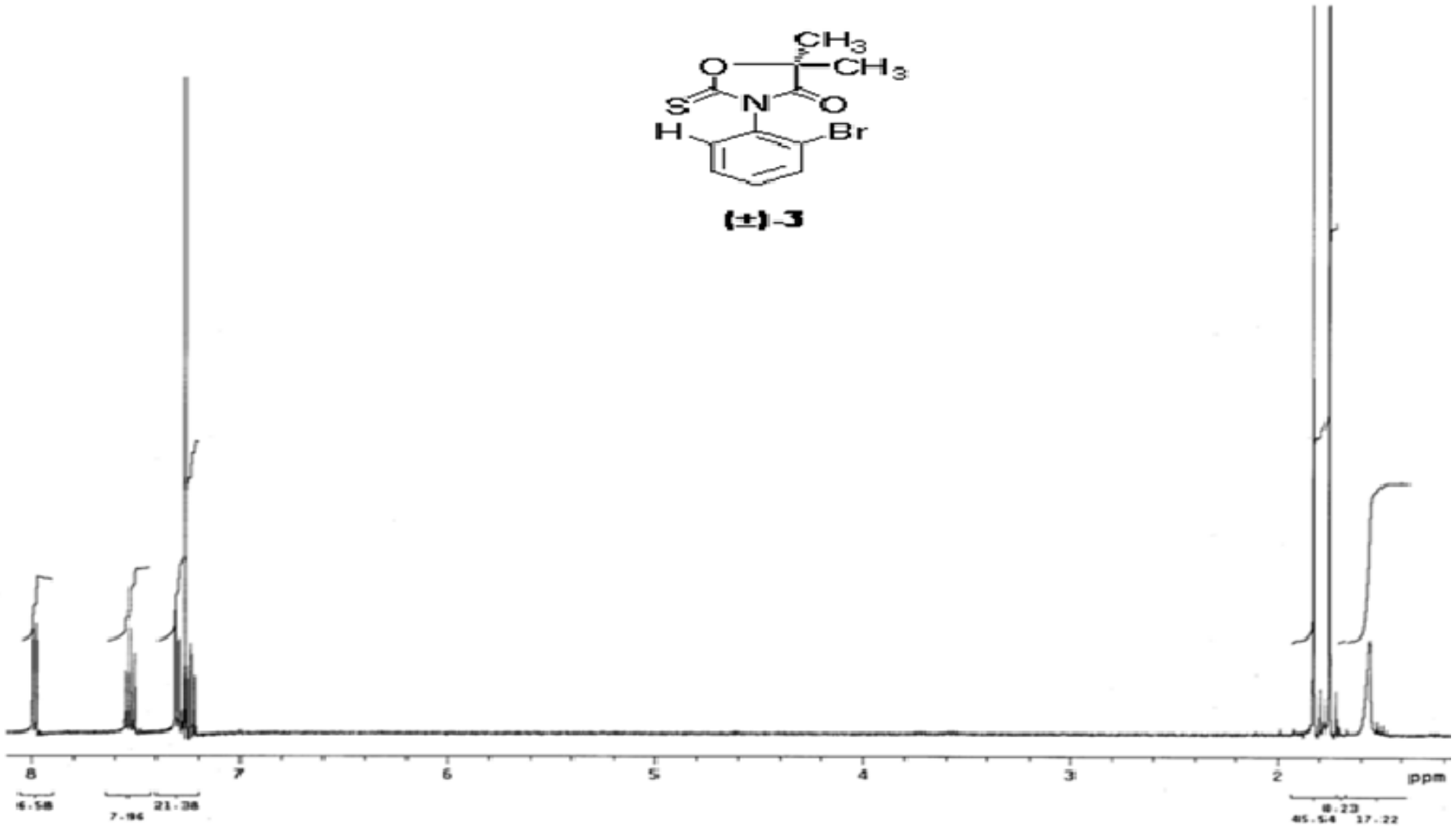

Figure 4.6. ^{1}H NMR spectrum of compound 3 in $CDCl_3$

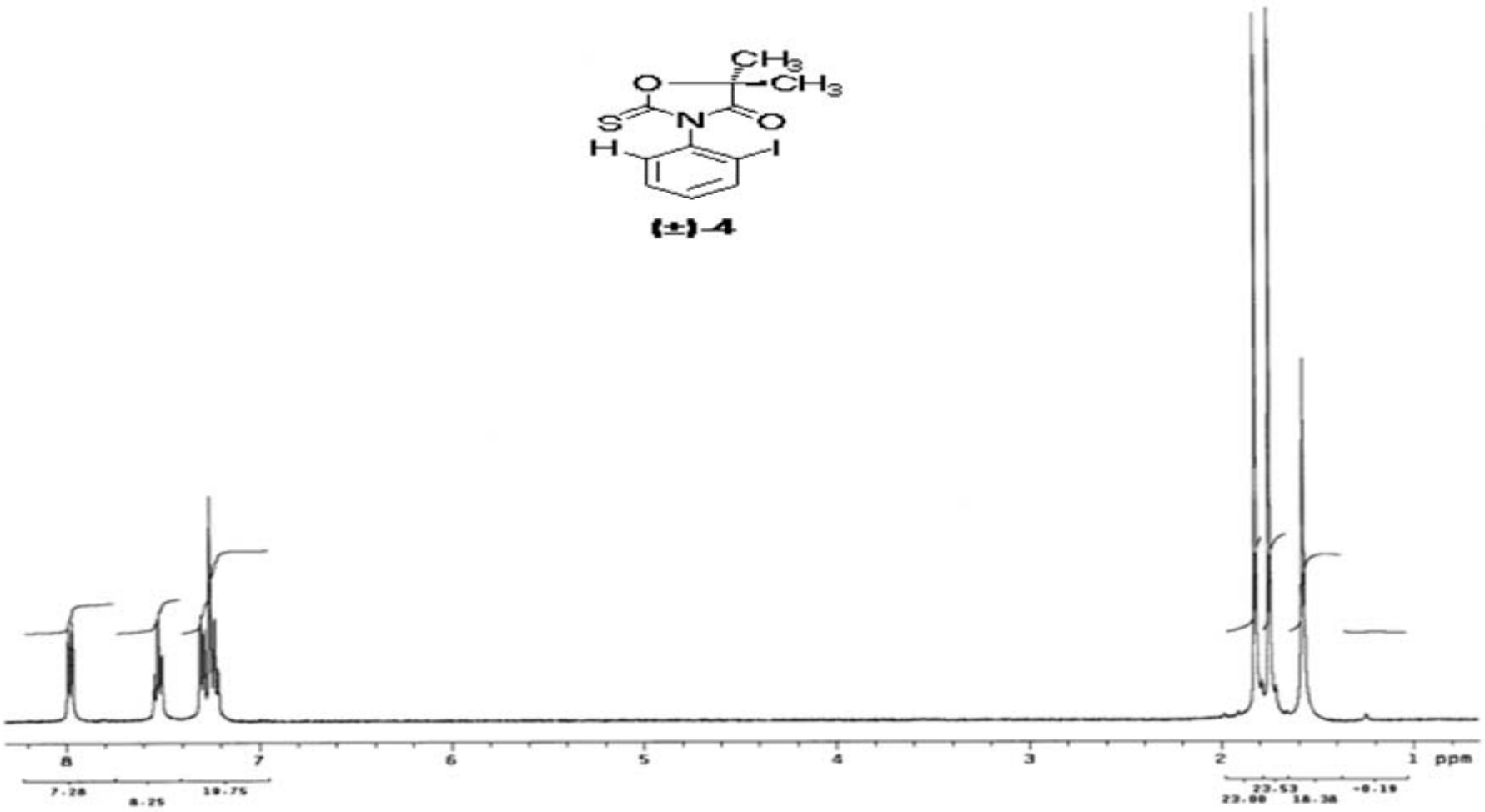

Figure 4.7. ^{1}H NMR spectrum of compound 4 in $CDCl_3$

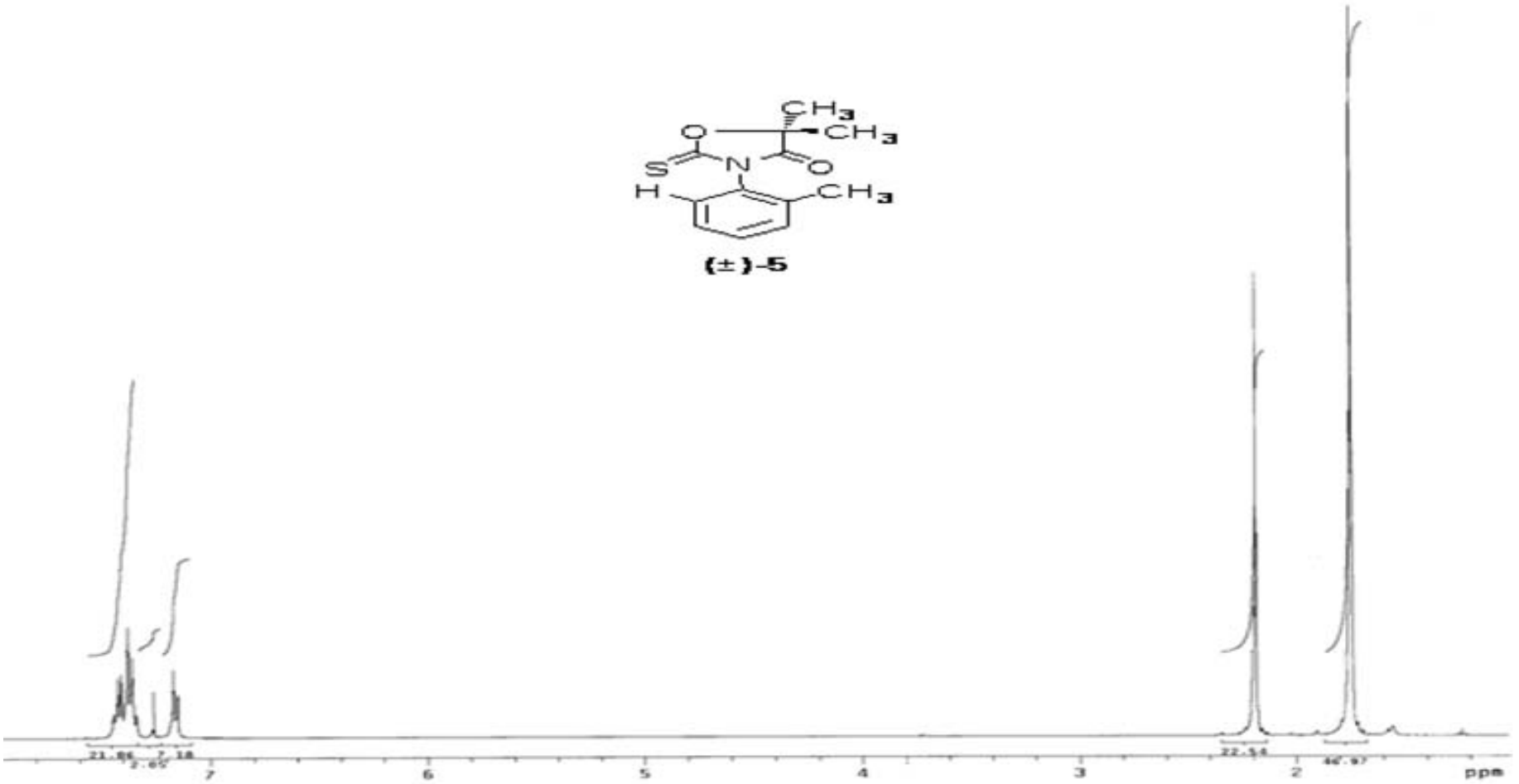

Figure 4.8. ^{1}H NMR spectrum of compound 5 in $CDCl_3$

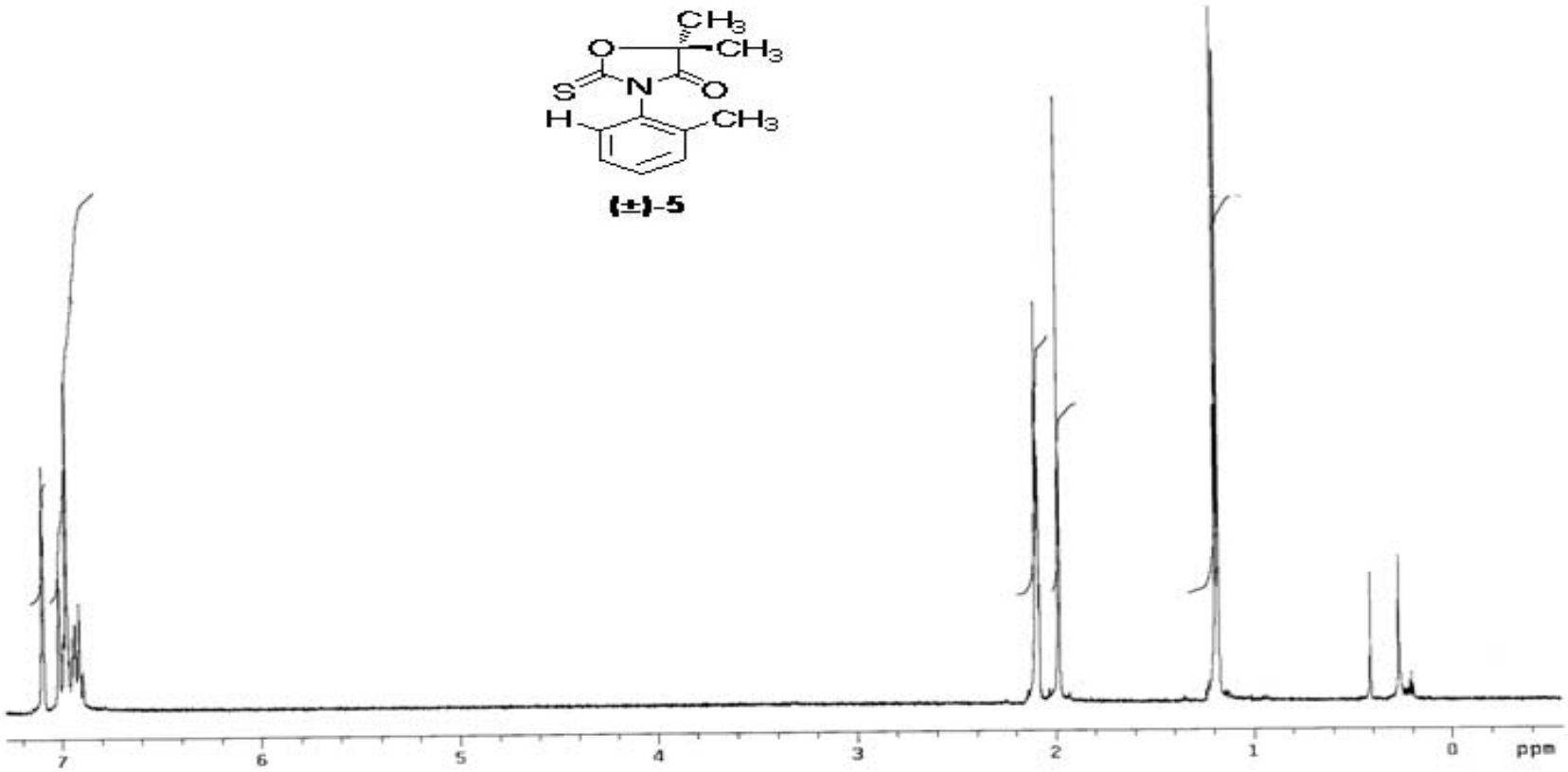

Figure 4.9. ^{1}H NMR spectrum of compound 5 in Toluene-d_8

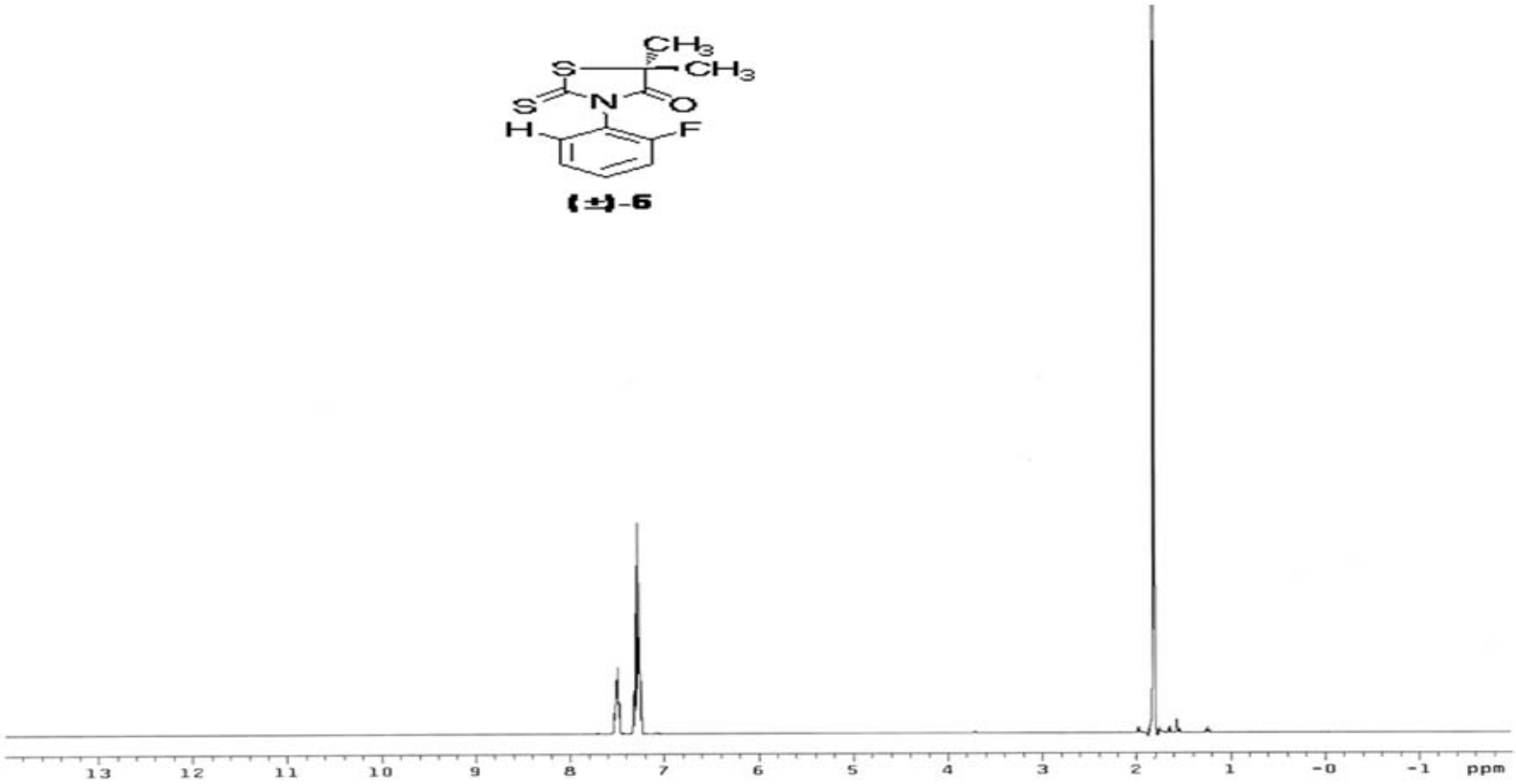

Figure 4.10. ^{1}H NMR spectrum of compound 6 in $CDCl_3$

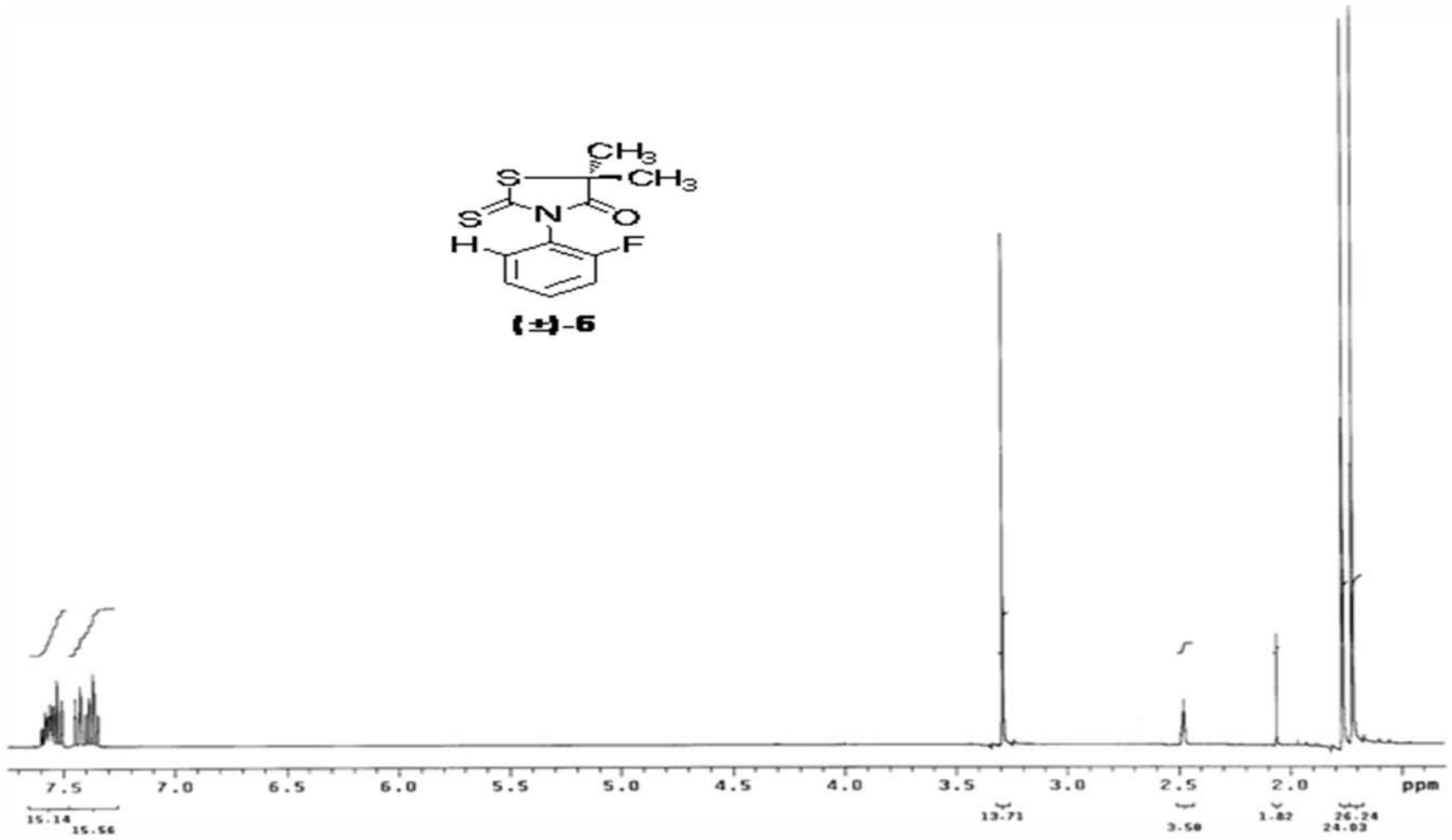

Figure 4.11. ^{1}H NMR spectrum of compound 6 in DMSO-d_6

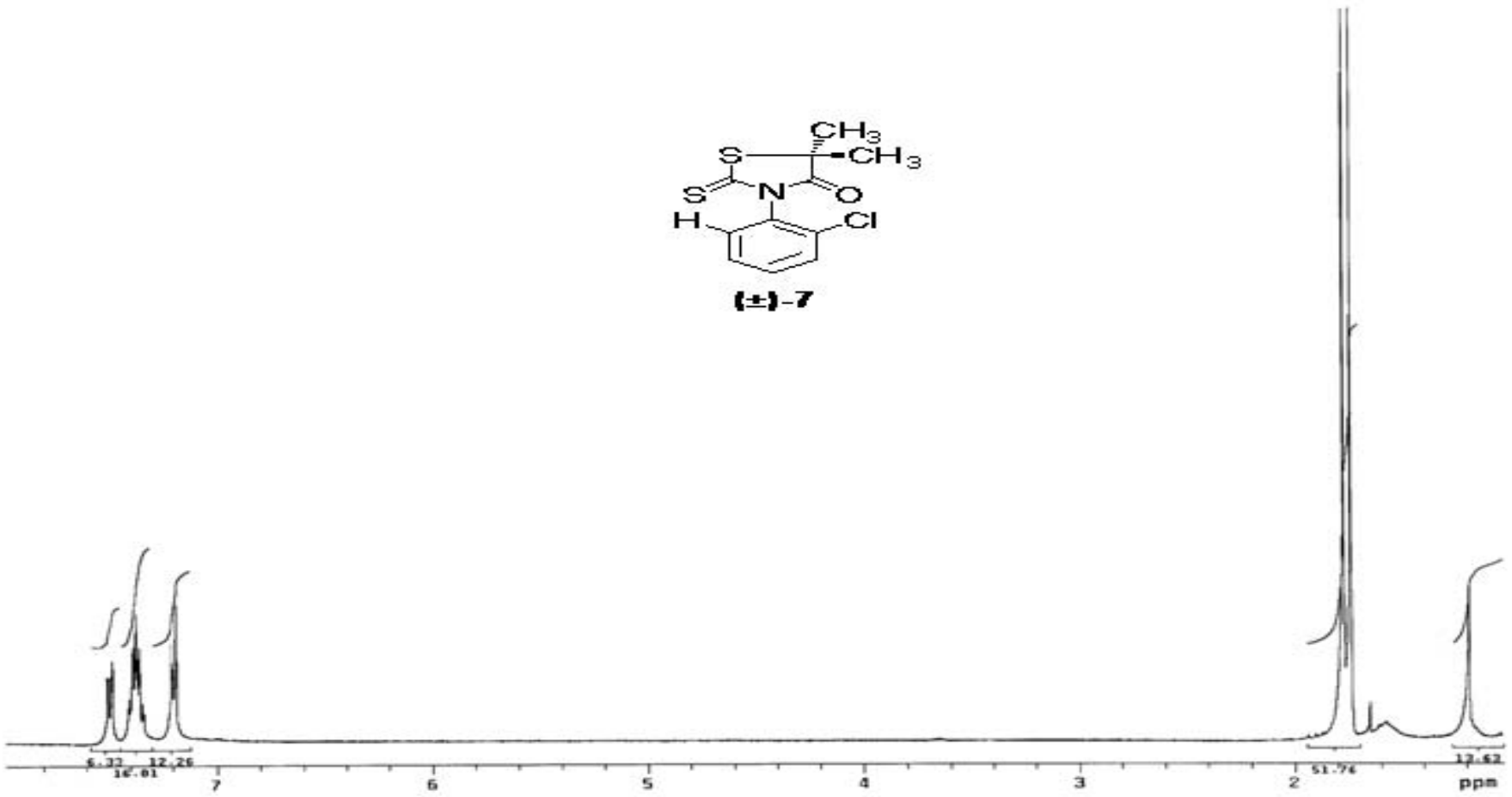

Figure 4.12 ^{1}H NMR spectrum of compound 7 in $CDCl_3$

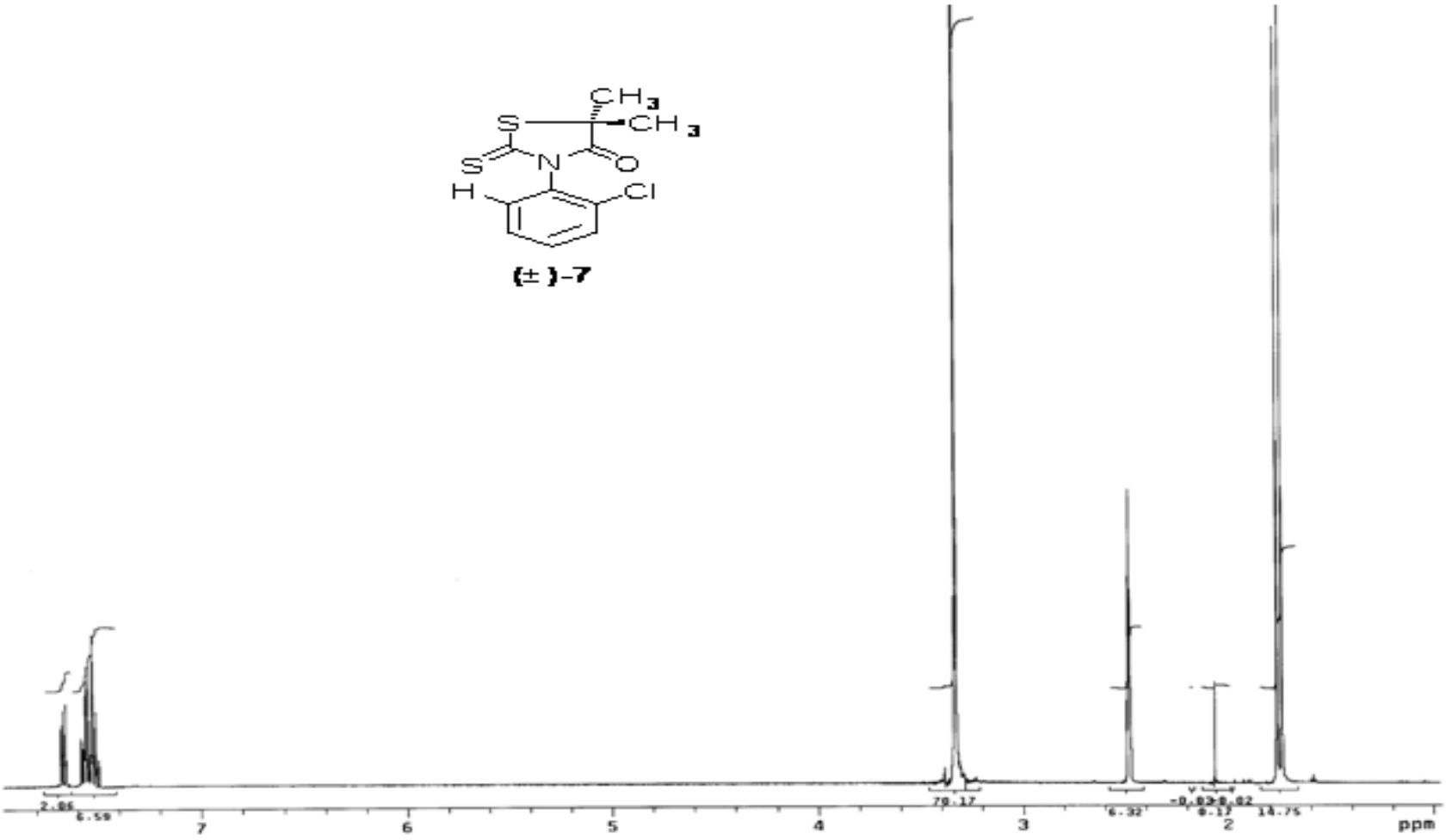

Figure 4.13. ^{1}H NMR spectrum of compound 7 in DMSO-d_6

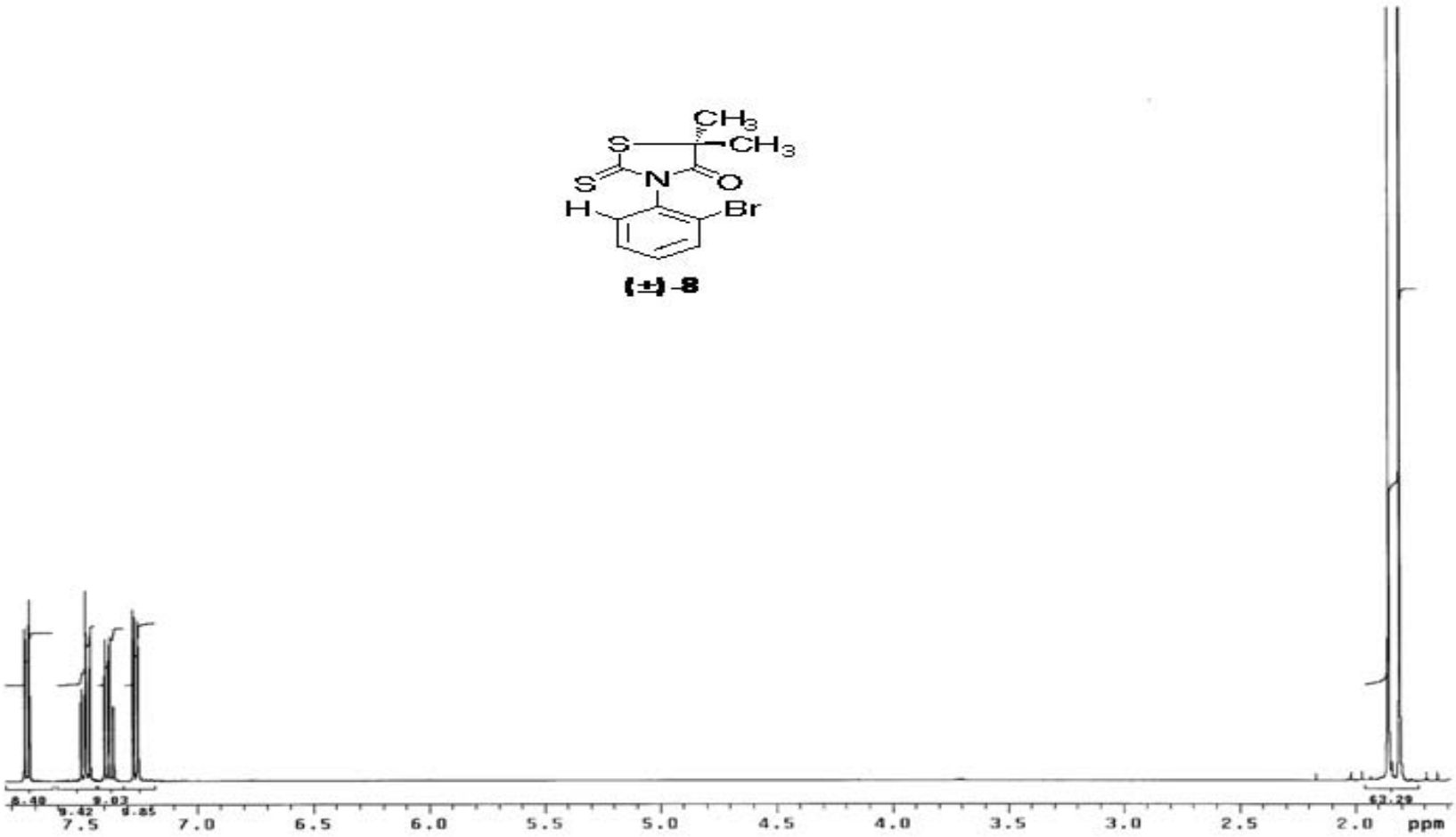

Figure 4.14. ^{1}H NMR spectrum of compound 8 in $CDCl_3$

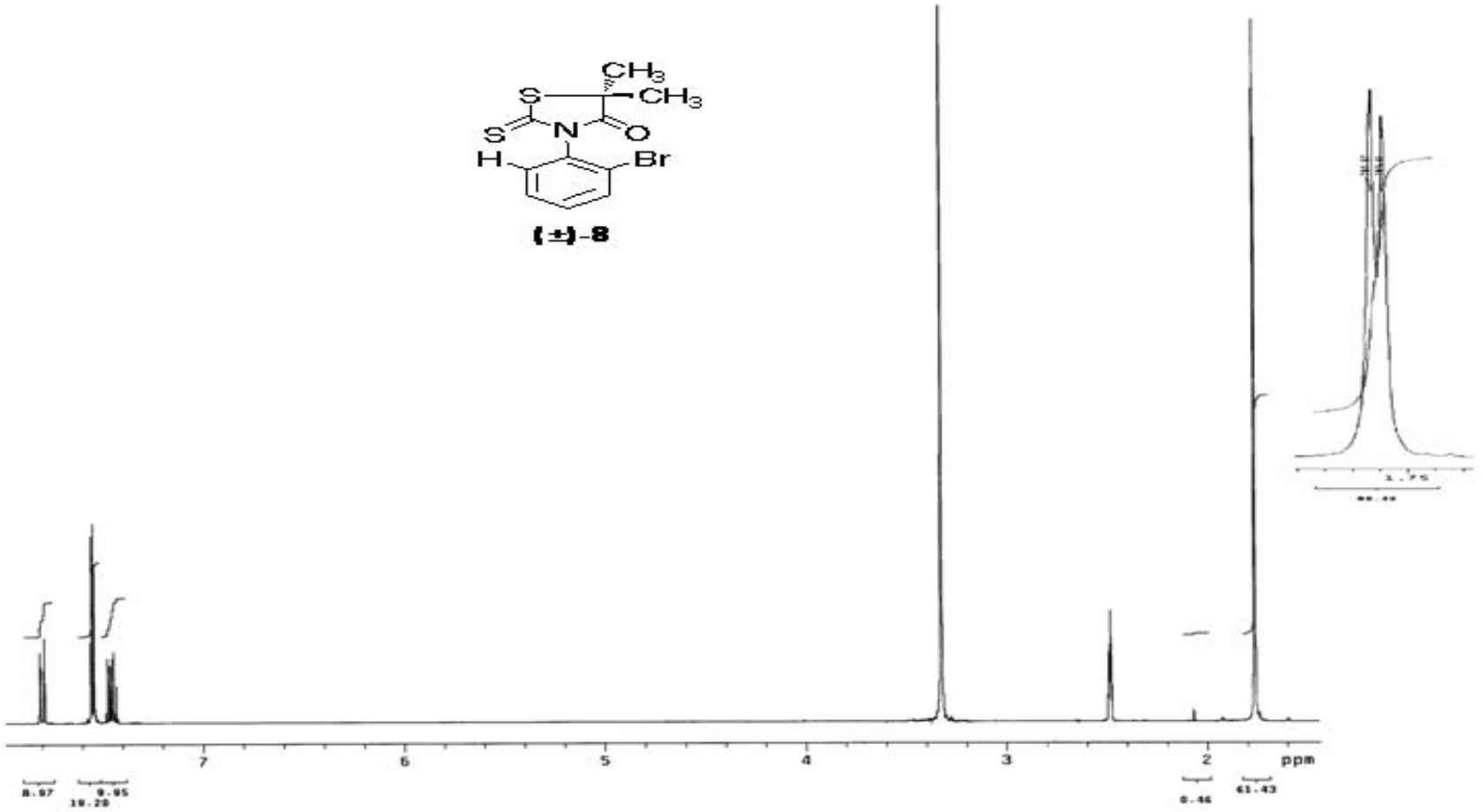

Figure 4.15. ^{1}H NMR spectrum of compound 8 in DMSO-d_6

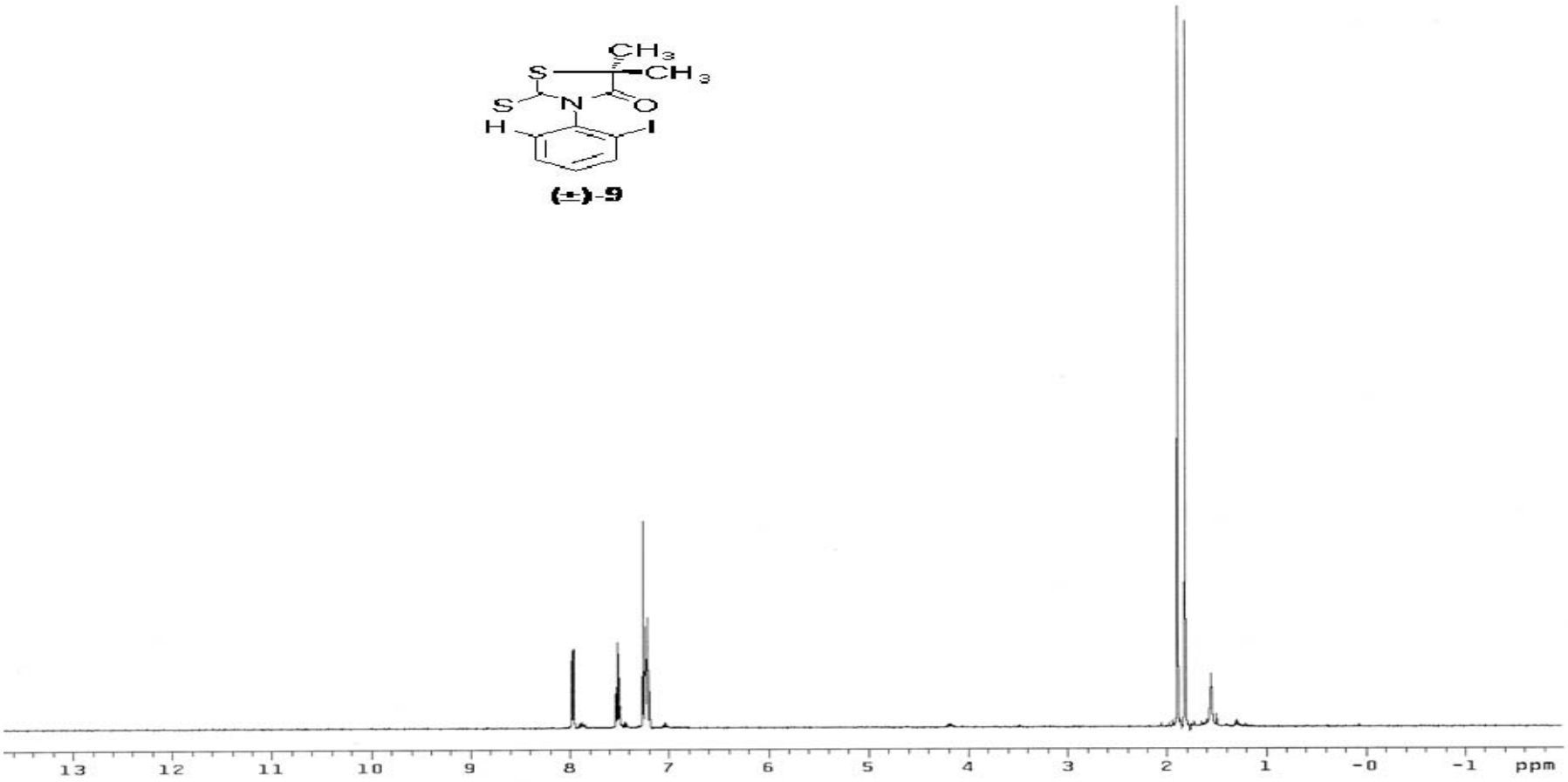

Figure 4.16. ^{1}H NMR spectrum of compound 9 in $CDCl_3$

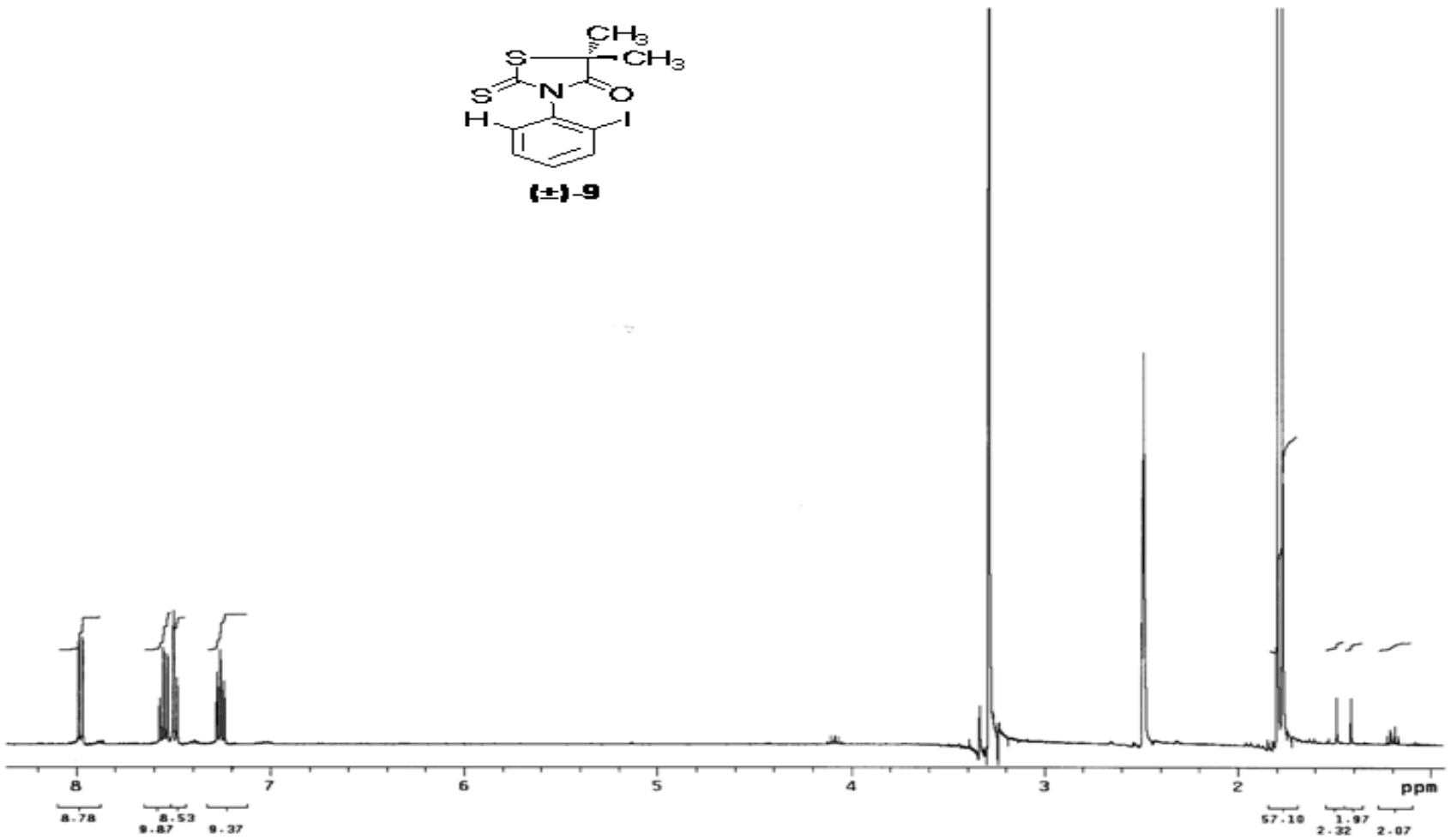

Figure 4.17. ^{1}H NMR spectrum of compound 9 in DMSO-d_6

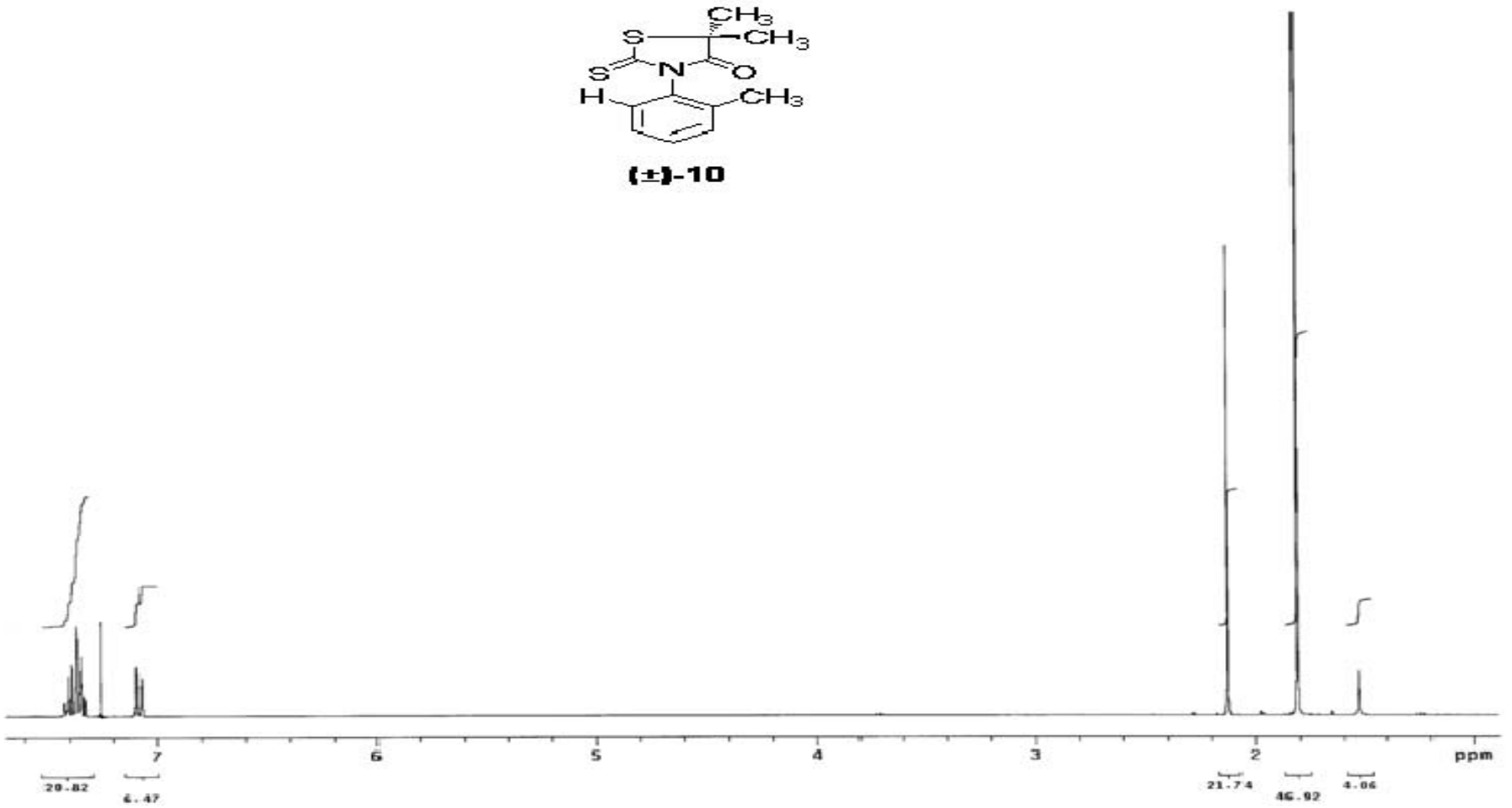

Figure 4.18. ^{1}H NMR spectrum of compound 10 in $CDCl_3$

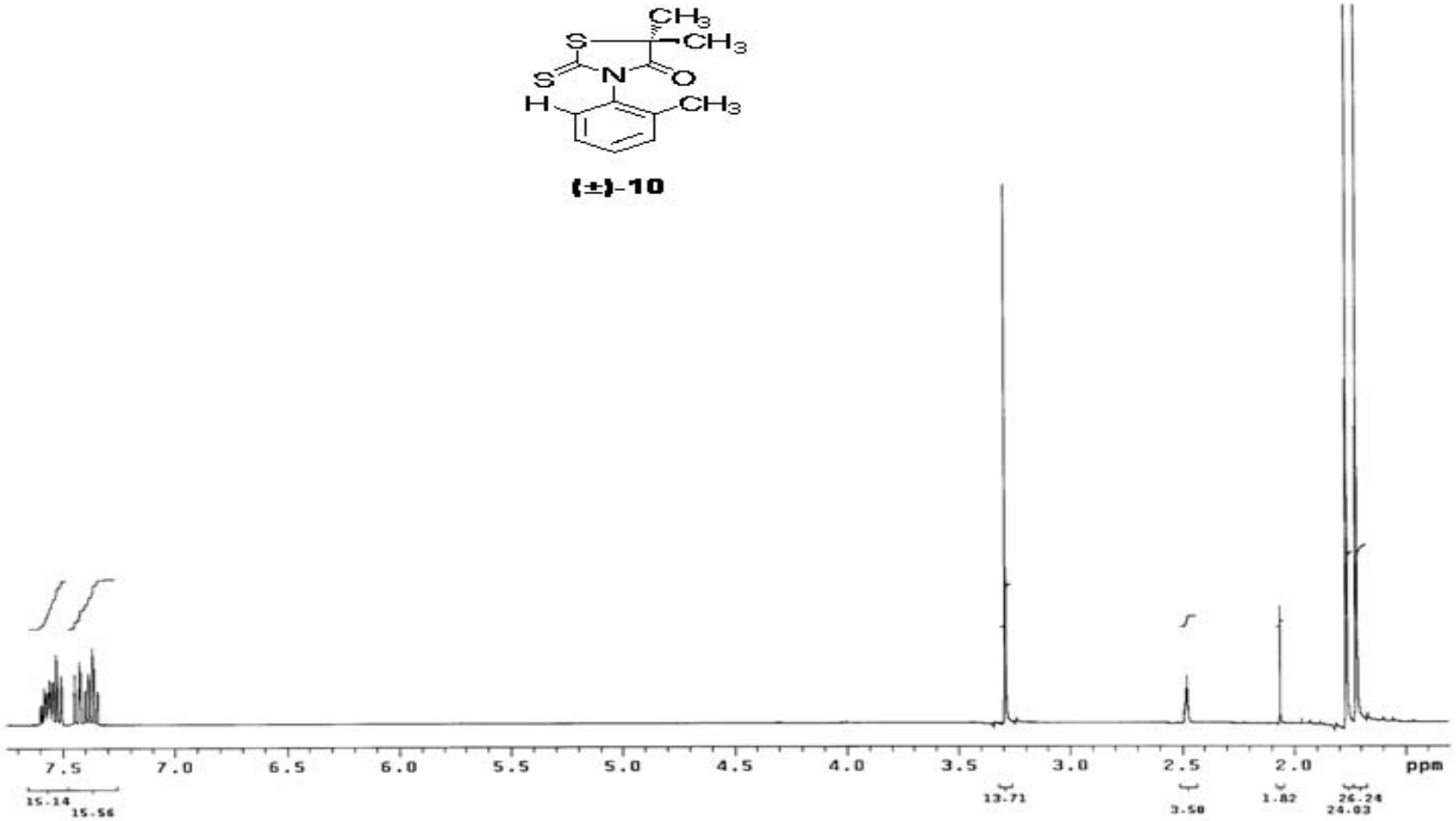

Figure 4.19. ^{1}H NMR spectrum of compound 10 in DMSO-d_6

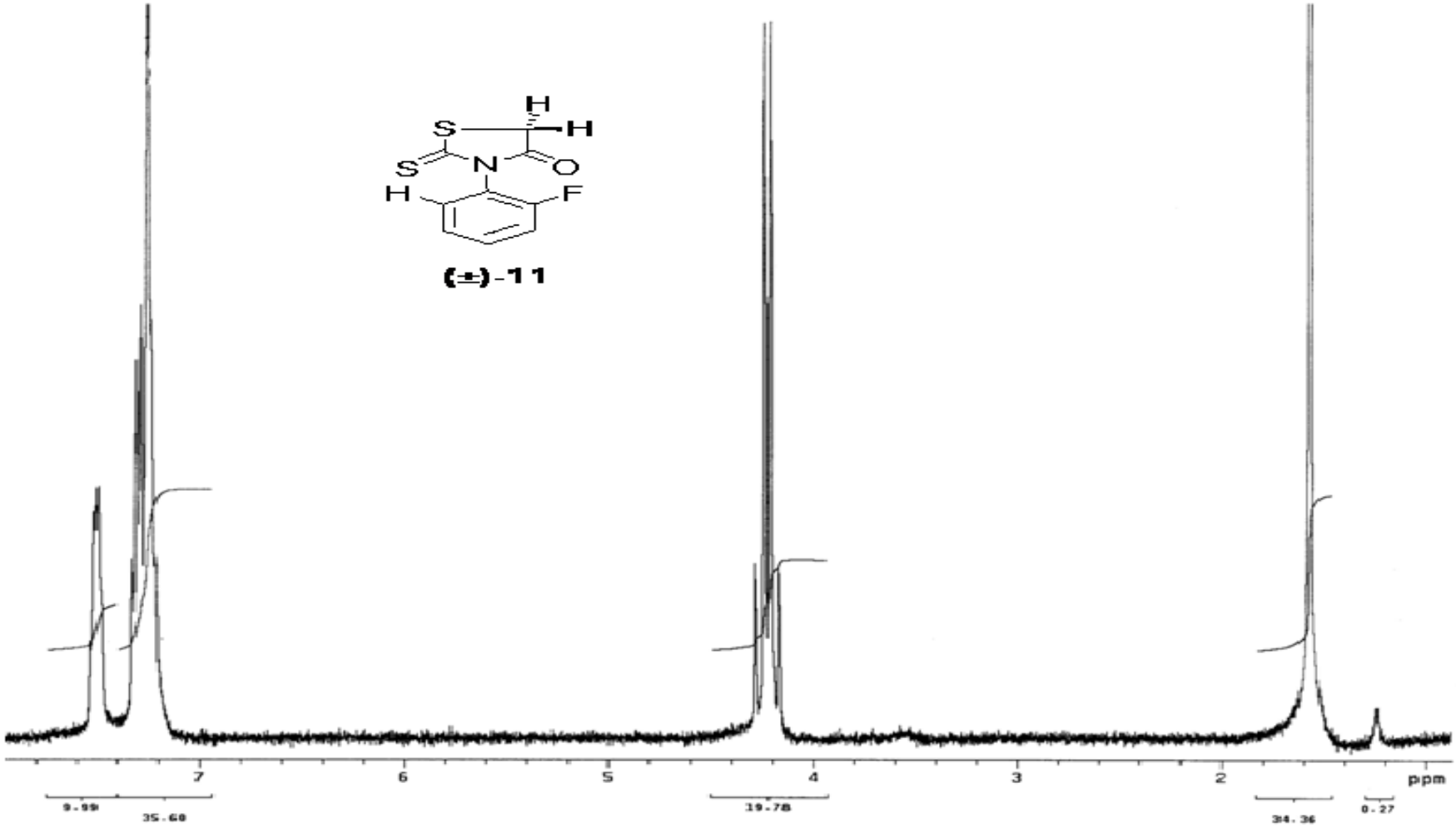

Figure 4.20. ^{1}H NMR spectrum of compound 11 in $CDCl_3$

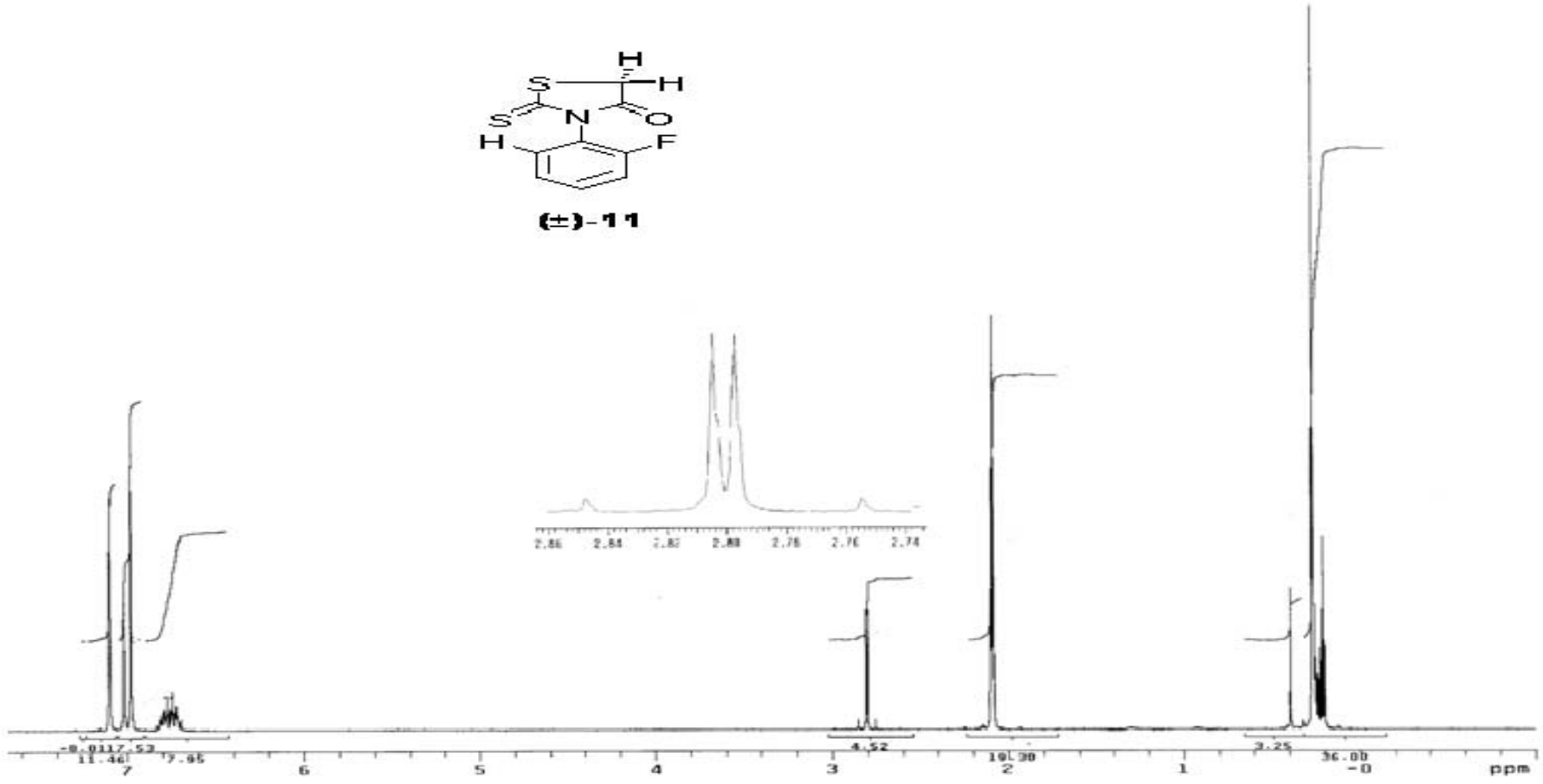

Figure 4.21. ^{1}H NMR spectrum of compound 11 in Toluen-d_8

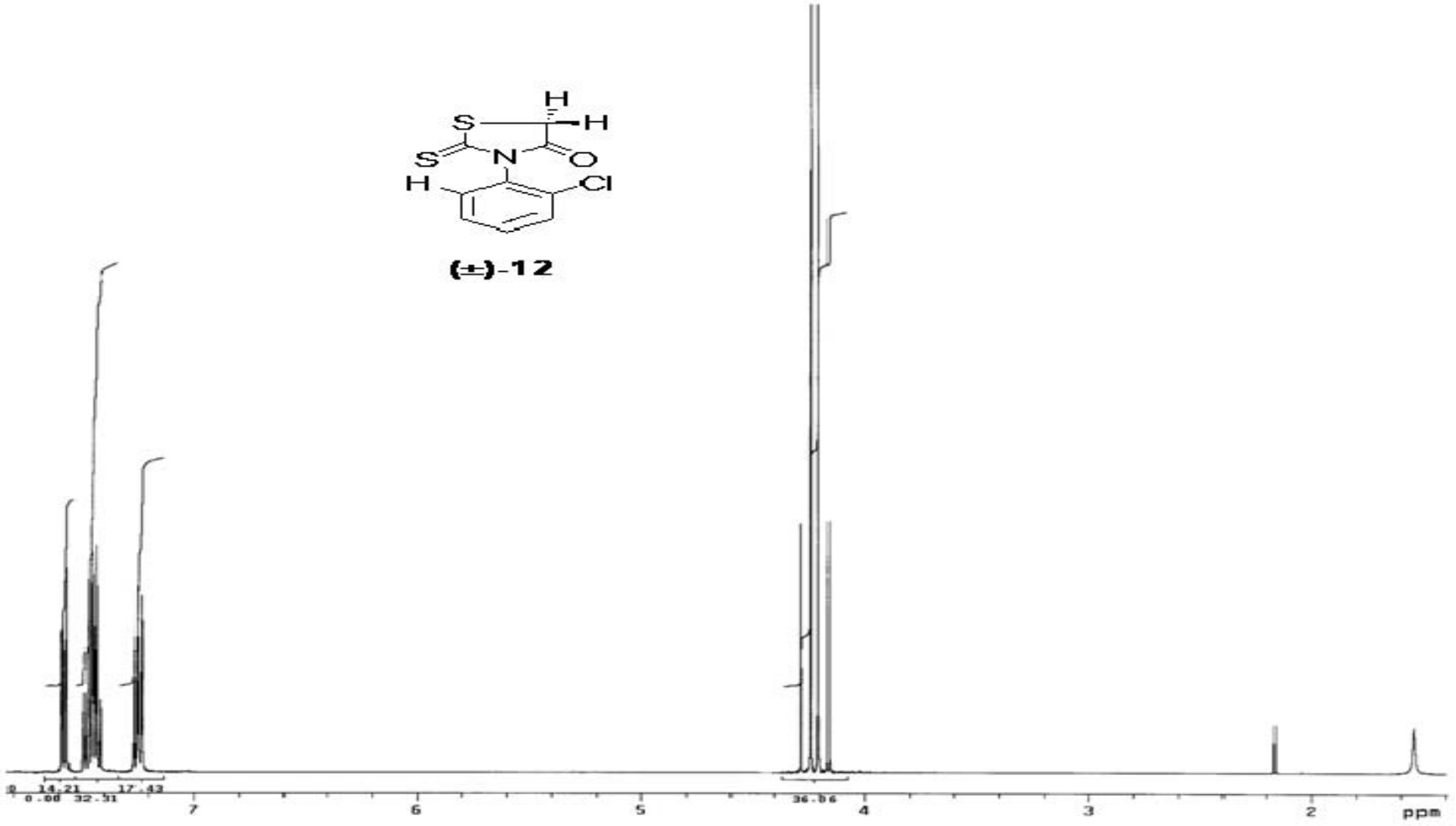

Figure 4.22. ^{1}H NMR spectrum of compound 12 in $CDCl_3$

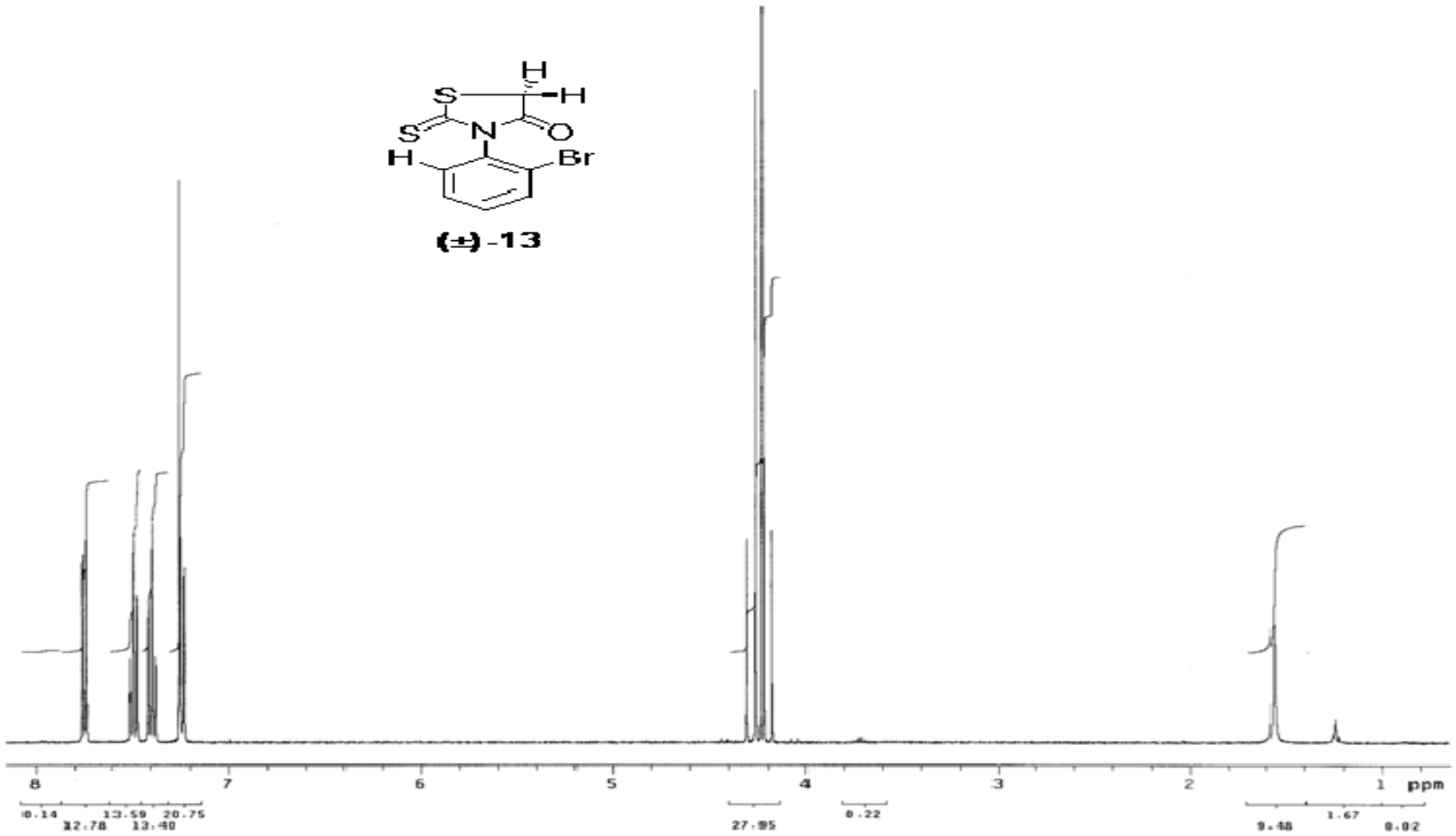

Figure 4.23. ^{1}H NMR spectrum of compound 13 in $CDCl_3$

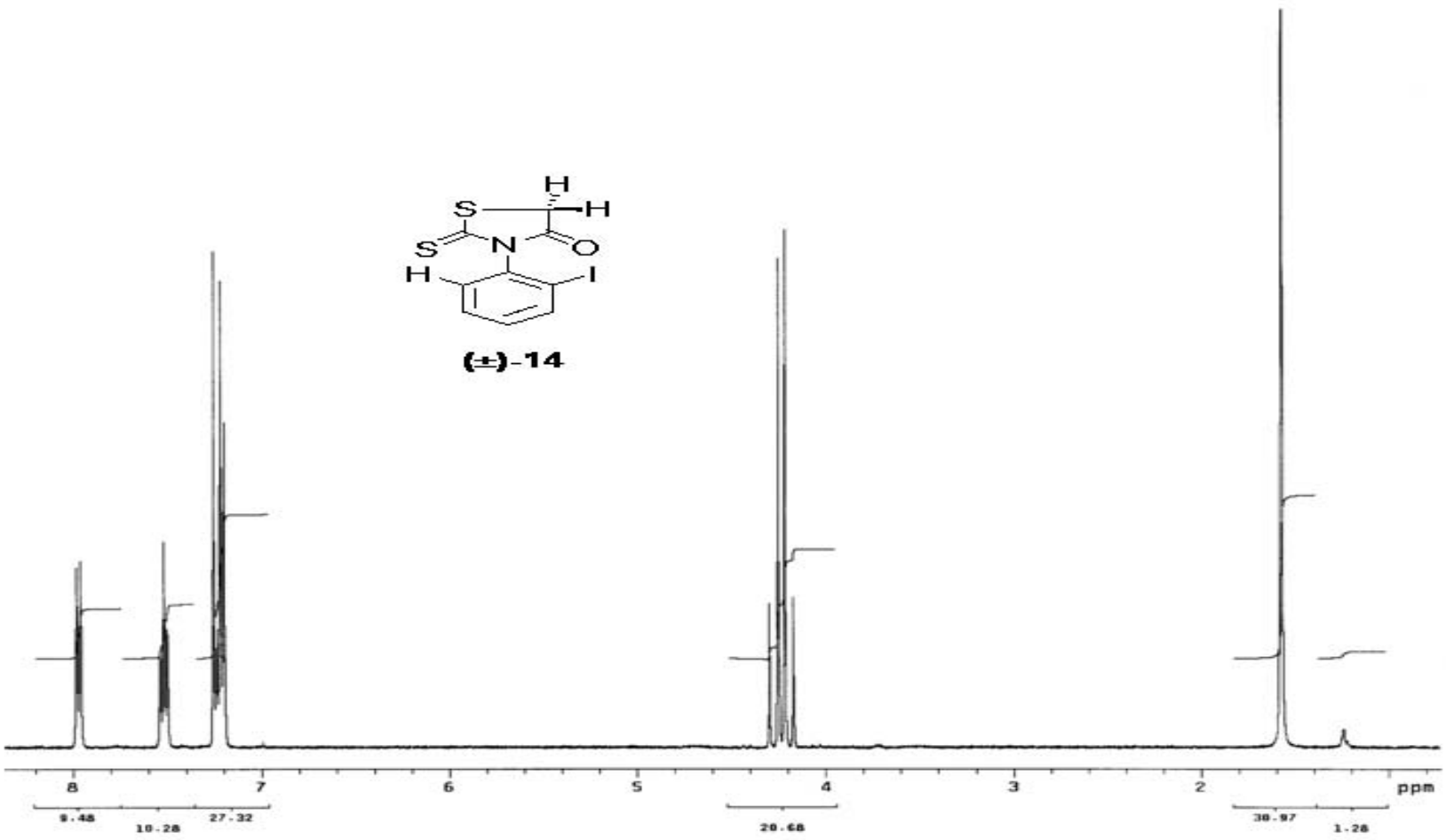

Figure 4.24. ^{1}H NMR spectrum of compound 14 in $CDCl_3$

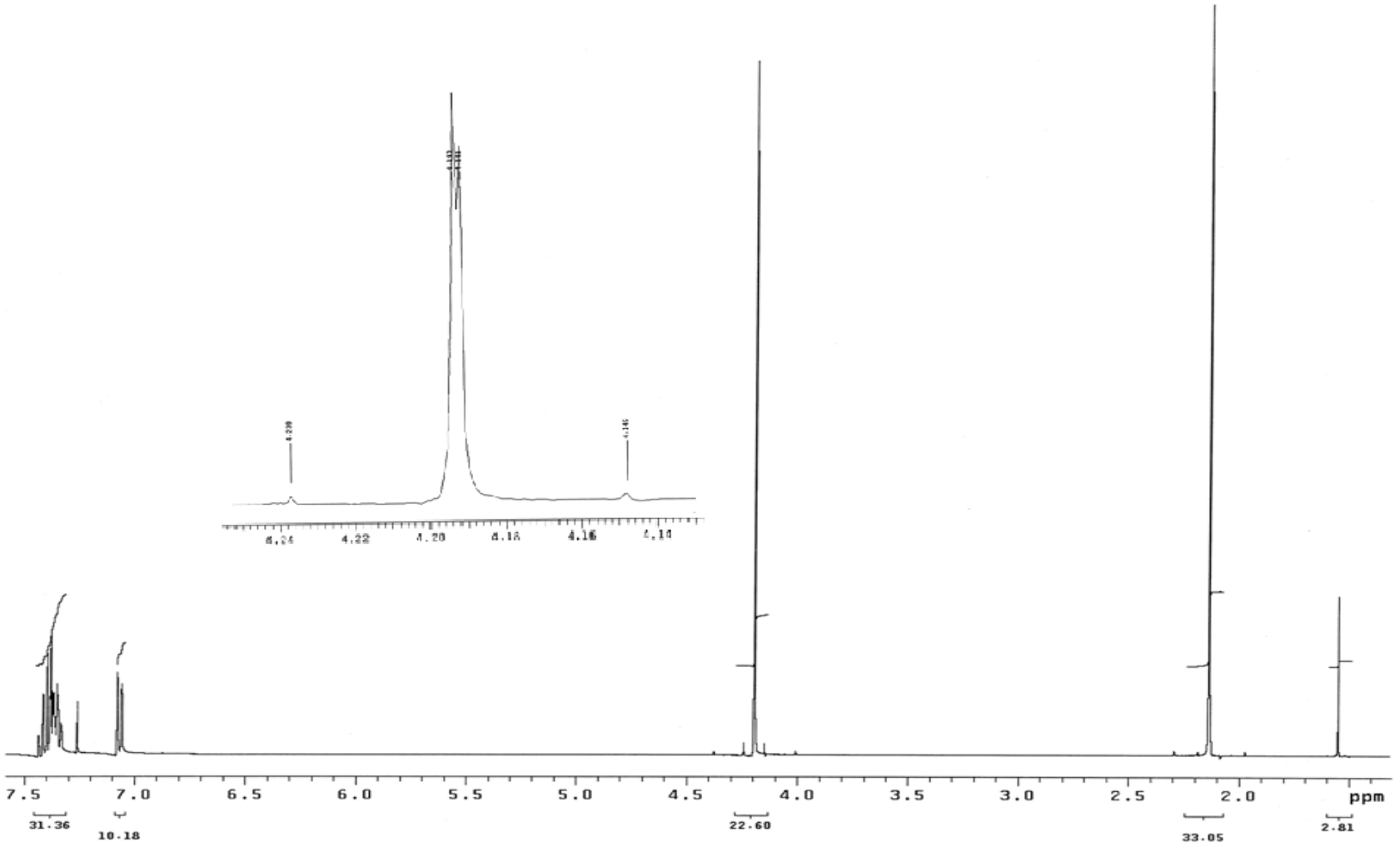

Figure 4.25. ^{1}H NMR spectrum of compound 15 in $CDCl_3$

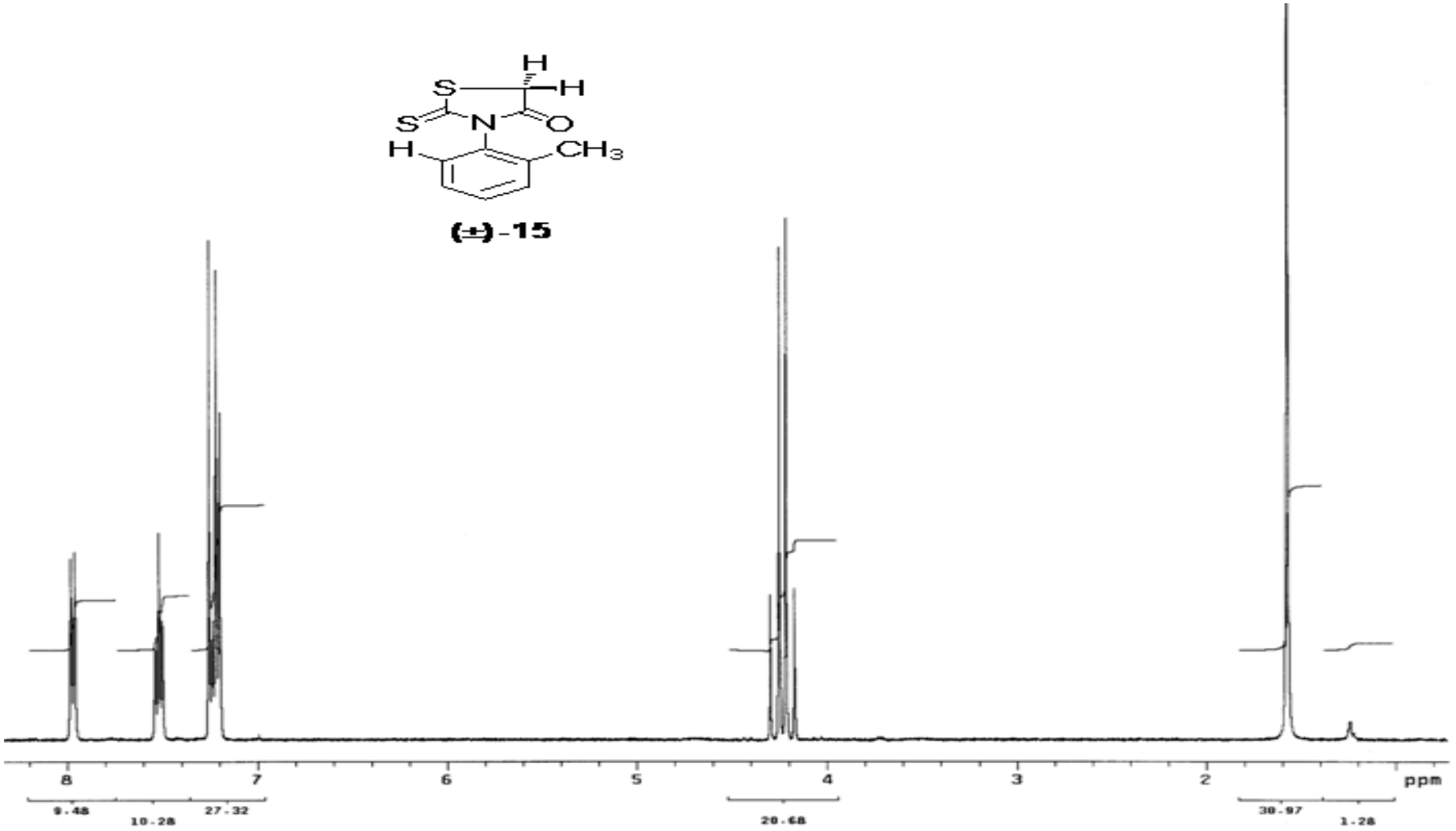

Figure 4.26. ^{1}H NMR spectrum of compound 15 in DMSO-d_6

4.2. ^{13}C NMR Spectra of the compounds

The ^{13}C NMR spectra of the compounds were studied for the identification and for further proof for the chirality of the molecules. The ^{13}C NMR results are summarized in Tables 4.3, 4.4 , and 4.5 for compounds (±)-1-5, (±)-6-10 and (±)-11-15, respectively.

Table 4.3. 100 MHz ^{13}C NMR spectral data for the 5,5-dimethyl-3-(*o*-aryl)-2-thioxo-4-oxazolidinones in $CDCl_3$ at 30 °C

Carbon[a] No	Compound (±)-1	Compound (±)-2	Compound (±)-3	Compound (±)-4	Compound (±)-5
C-2	188.0	187.8	188.0	187.4	188.3
C-4	173.6	174.8	175.5	174.6	175.5
C-5	87.5	87.4	88.0	87.6	86.7
C-6,7	22.3, 25.3	23.4, 24.1	23.2, 25.1	23.7, 24.1	23.4, 23.9
C-Aromatic	128.3-158.2	128.3-132.2	123.3-136.2	98.1-140.4	128.3-131.3
C-(*o*-CH_3)	-	-	-	-	17.3

[a]: see Figure 4.1 for numbering

Table 4.4 . 100 MHz ^{13}C NMR spectral data for the 5,5-dimethyl-3-(*o*-aryl)-2-thioxo-4-thiazolidinones in $CDCl_3$ at 30 °C

Carbon[a] No	Compound (±)-6	Compound (±)-7	Compound (±)-8	Compound (±)-9	Compound (±)-10
C-2	197.0[b]	198.4	198.5	200.2[c]	198.4[b]
C-4,5	177.3, 54.1[b]	178.8, 56.1	178.7, 56.2	179.0, 57.0[c]	178.8, 55.1[b]
C-6,7	24.8, 25.9[b]	26.9, 28.3	27.0, 28.3	26.5, 28.0[c]	26.4,27.2
C-Aromatic	123.5, 158.1[b]	128.1-133.3	123.0-134.8	100.0-140.0[c]	127.1-136.3[b]
C-(*o*-CH_3)	-	-	-	-	17.0[b]

[a]: see Figure 4.1 for numbering, [b]: Solvent is Benzene-d_6, [c]: Solvent is DMSO- d_6

Table 4.5. 100 MHz ^{13}C NMR spectral data for the 3-(*o*-aryl)-2-thioxo-4-thiazolidinones in $CDCl_3$ at 30 °C

Carbon[a] No	Compound (±)-11	Compound (±)-12	Compound (±)-13	Compound (±)-14	Compound (±)-15
C-2	200.0	198.0	199.5	197.6	200.3
C-4	173.6	172.6	171.9	172.6	173.1
C-5	37.0	36.6	35.6	36.9	36.4
C-Aromatic	117.3-160.2	128.2-133.0	135.8-128.5	98.4-140.3	128.5-134.0
C-(*o*-CH_3)	-	-	-	-	17.4

[a]: see Figure 4.2 for numbering

The ^{13}C NMR spectra of the compounds (±)-1-5, (±)-11-15 and (±)-7-8 have been taken in $CDCl_3$, (±)-6 and (±)-10 in benzene-d_6, that of (±)-9 in DMSO-d_6. The chemical shift difference of the diastereotopic carbon atoms do not seem to depend on the nature and size of the *ortho* substitutent. Two signals were observed for the diastereotopic methyl carbons on C-5 of compounds (±)-1-10. They appeared around 22 and 28 ppm. The C-5 carbons gave peaks at around 55 and 88 ppm for compounds (±)-1-10, 35 and 37 ppm for compounds (±)-11-15. The carbonyl carbons for compounds (±)-1-15 resonated at around 172 and 179 ppm. The thiocarbonyl carbons resonated at around 187 and 200 ppm. The ^{13}C NMR spectra of the compounds (±)-1-15 are shown in Figures 4.27 to 4.41.

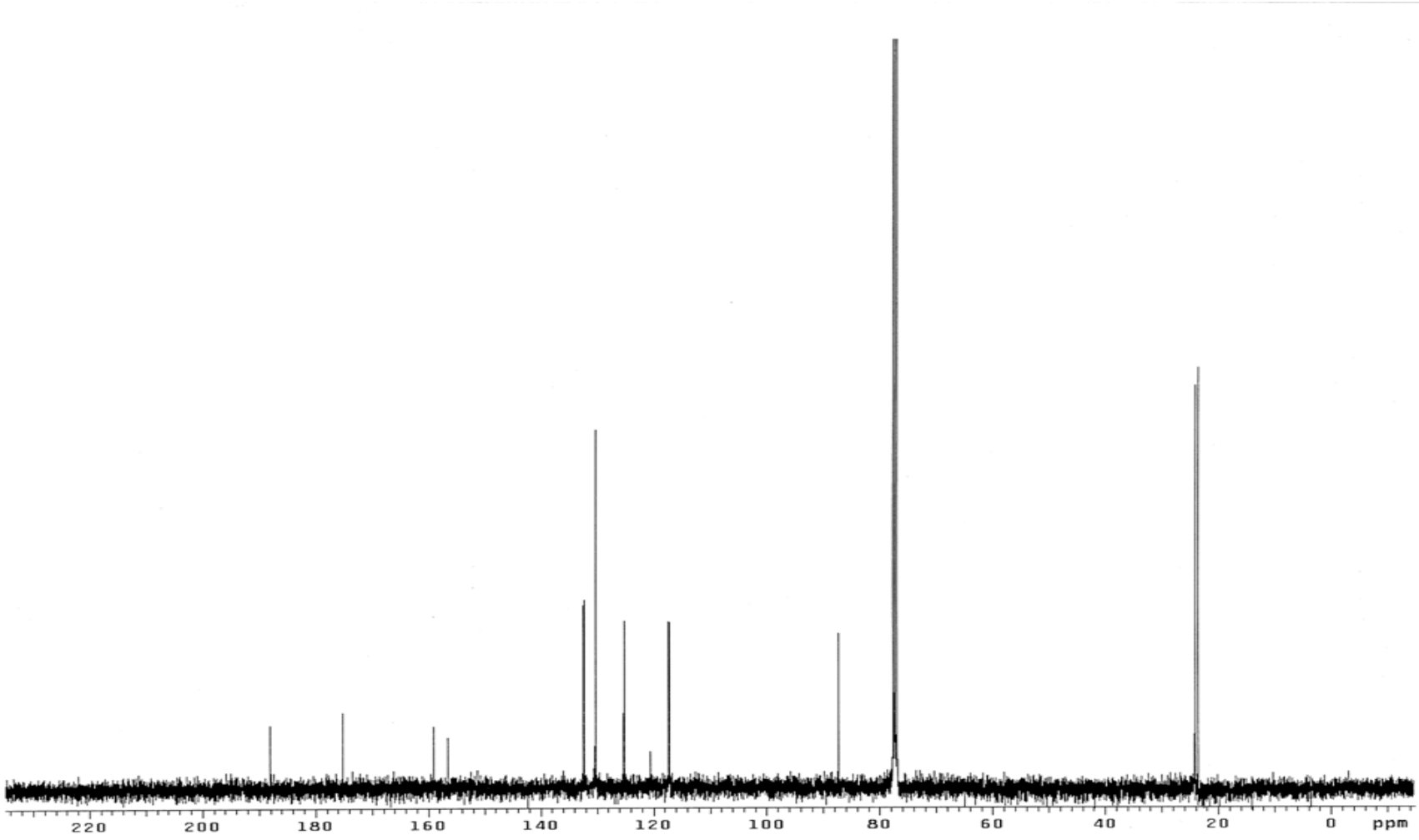

Figure 4.27. The ^{13}CNMR spectrum of compound 1 in $CDCl_3$

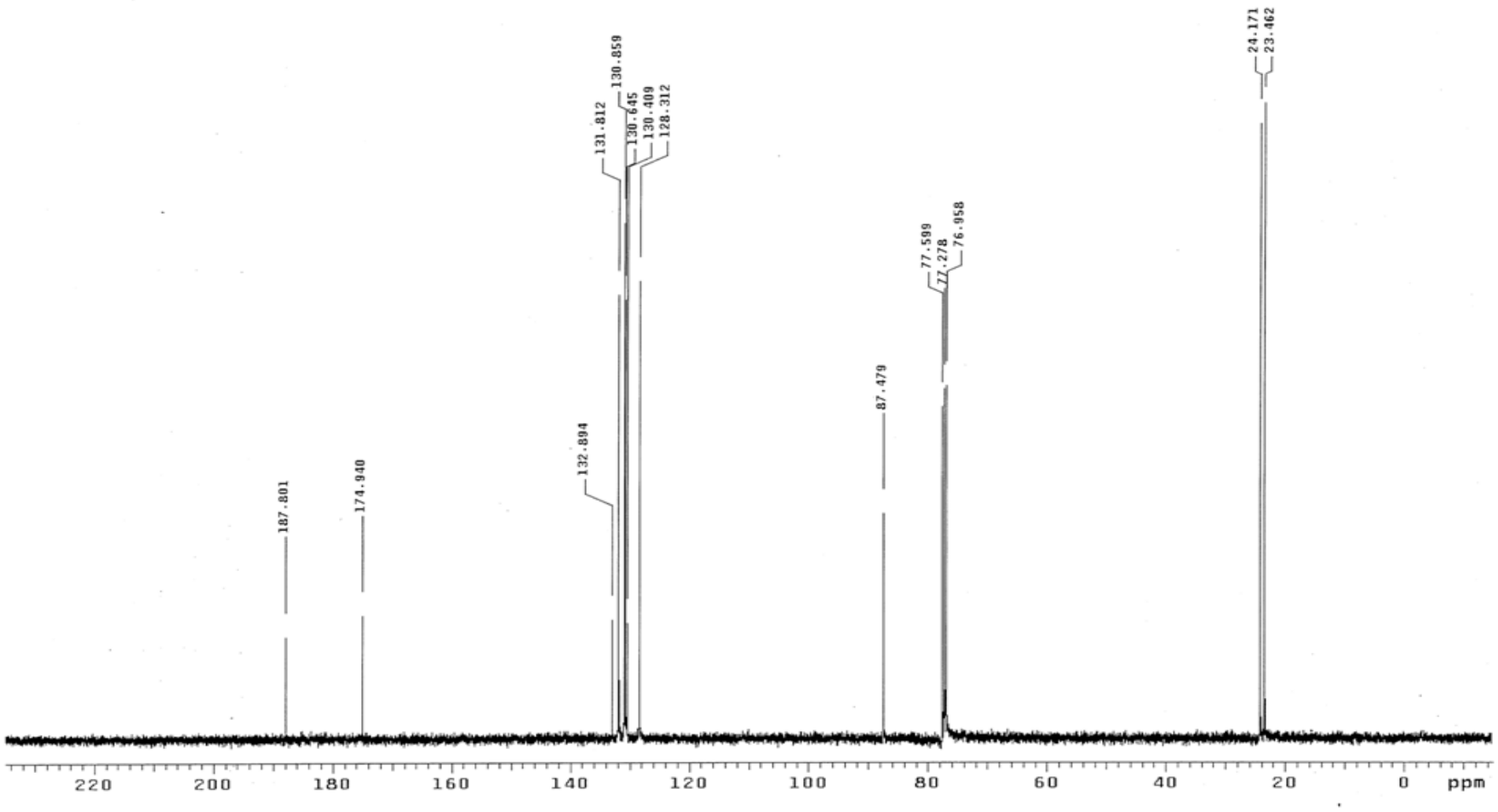

Figure 4.28. The ^{13}CNMR spectrum of compound 2 in $CDCl_3$

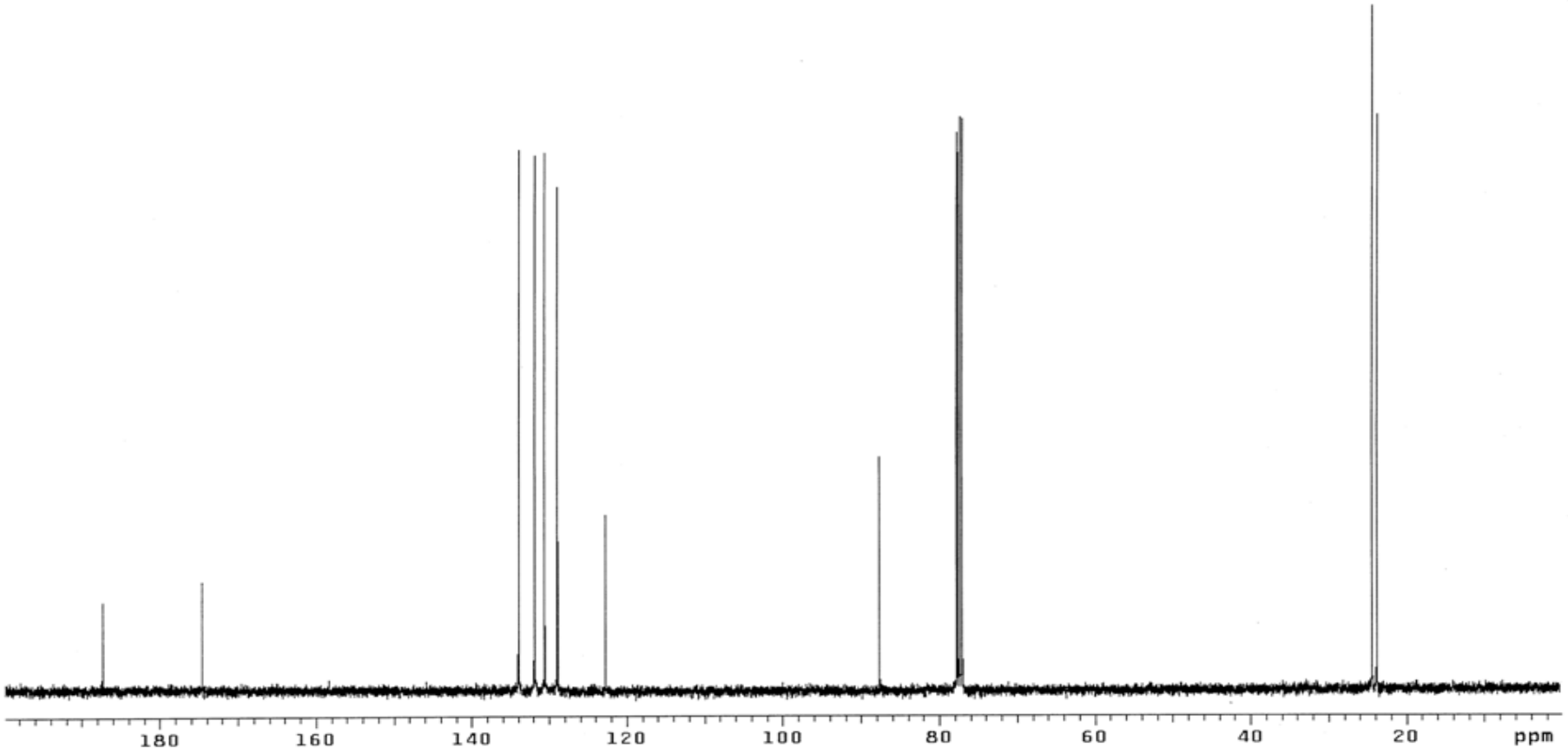

Figure 4.29. The ^{13}CNMR spectrum of compound 3 in $CDCl_3$

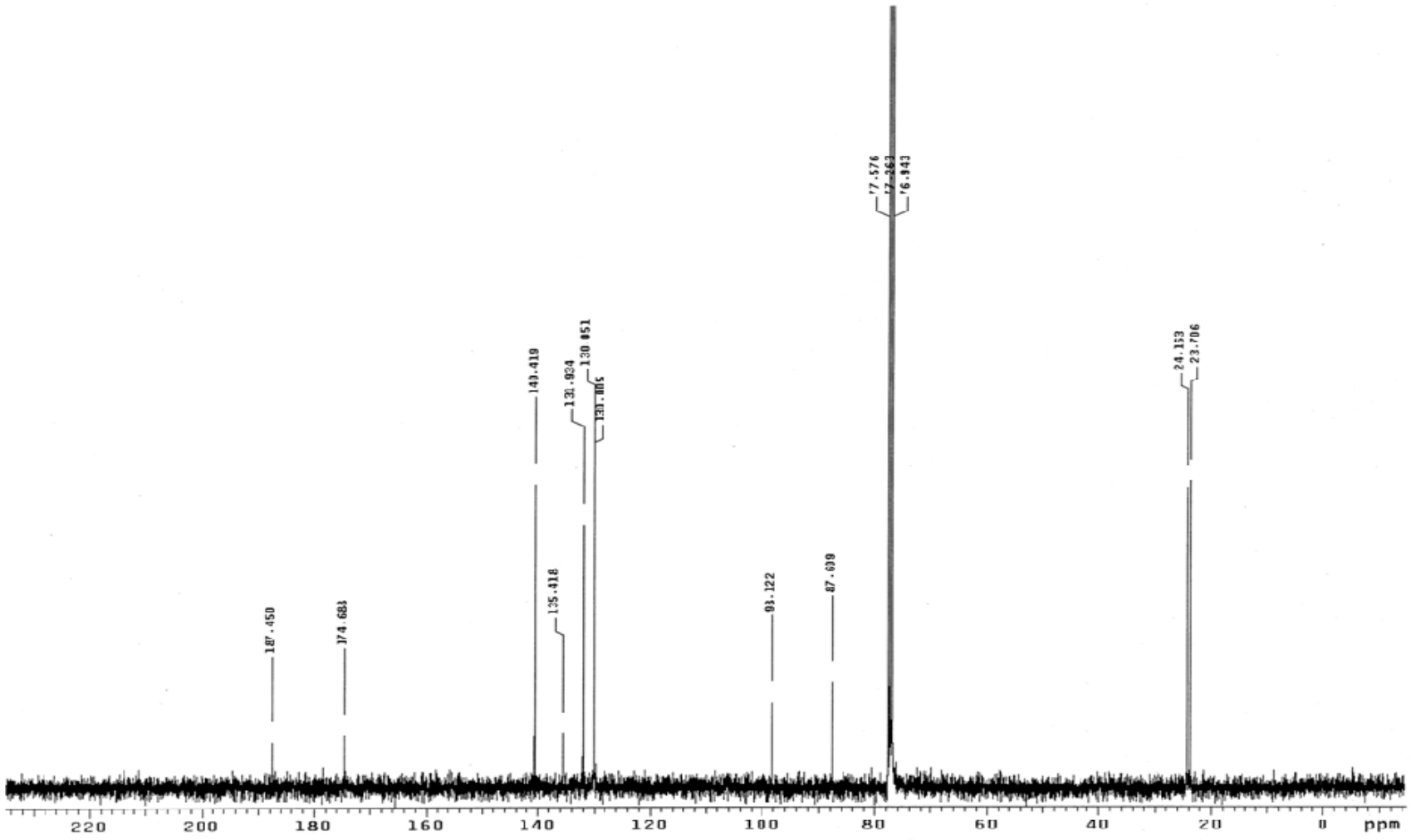

Figure 4.30. The ^{13}CNMR spectrum of compound 4 in $CDCl_3$

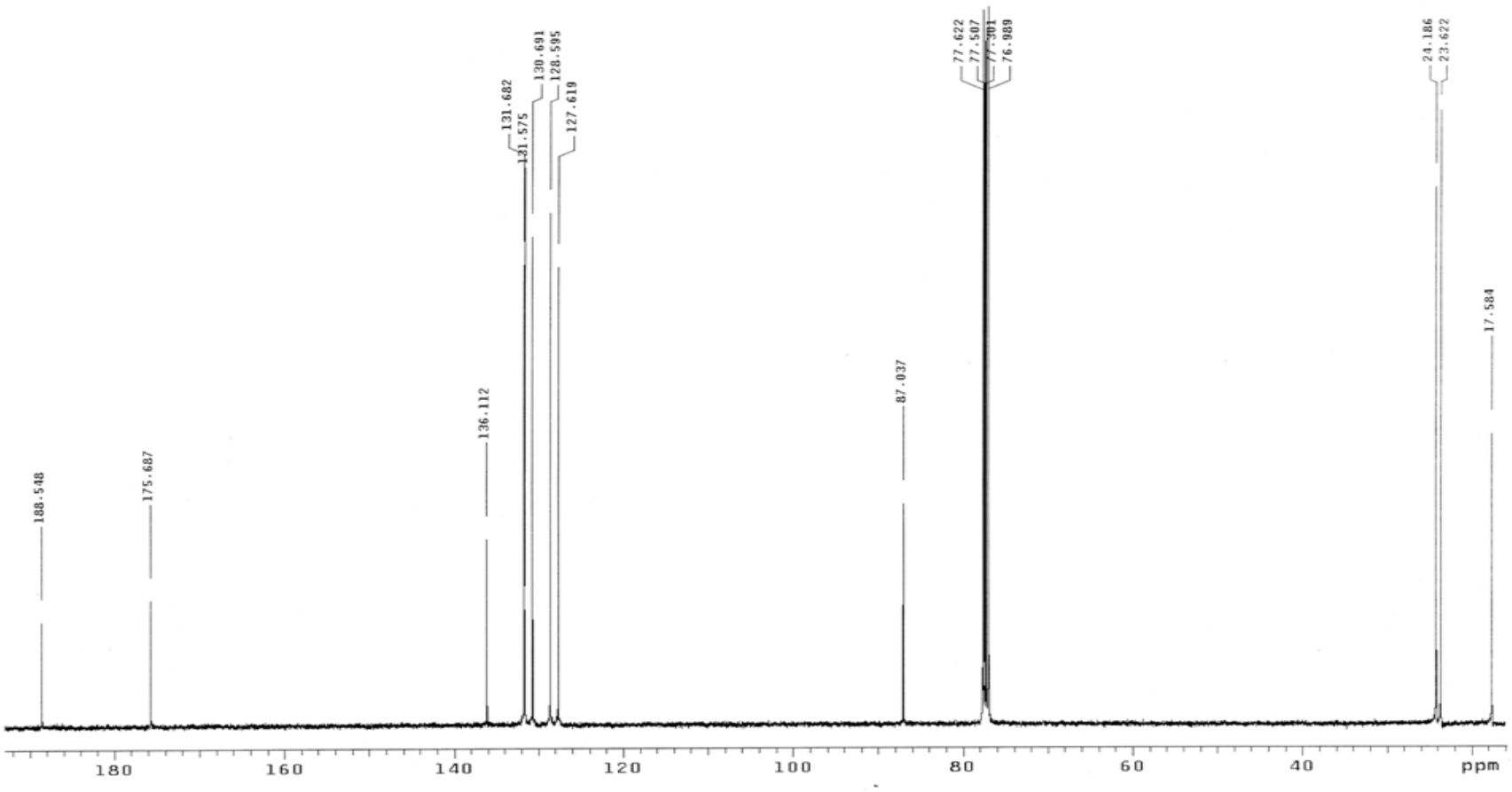

Figure 4.31. The ^{13}CNMR spectrum of compound 5 in $CDCl_3$

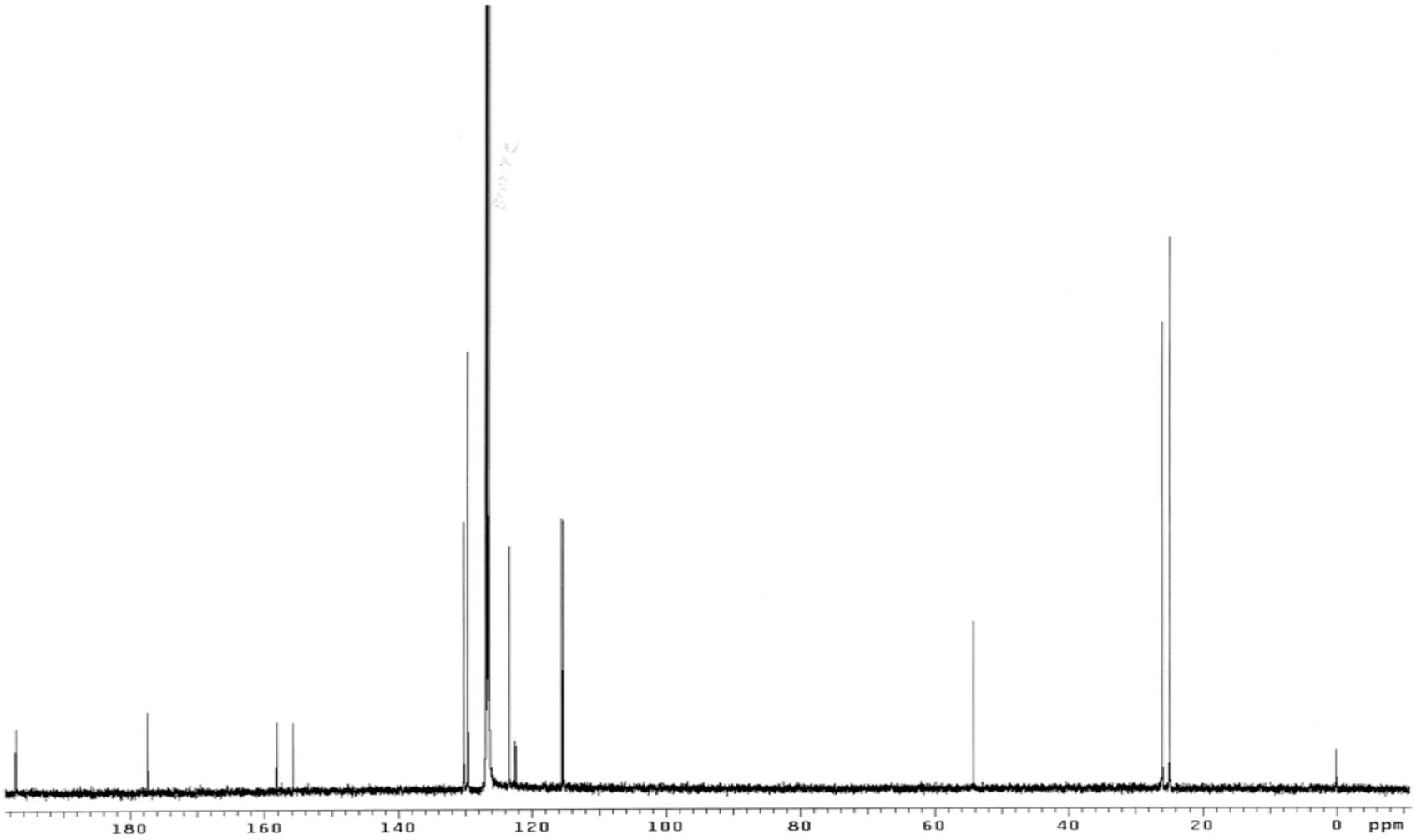

Figure 4.32. The ^{13}CNMR spectrum of compound 6 in Benzene-d_6

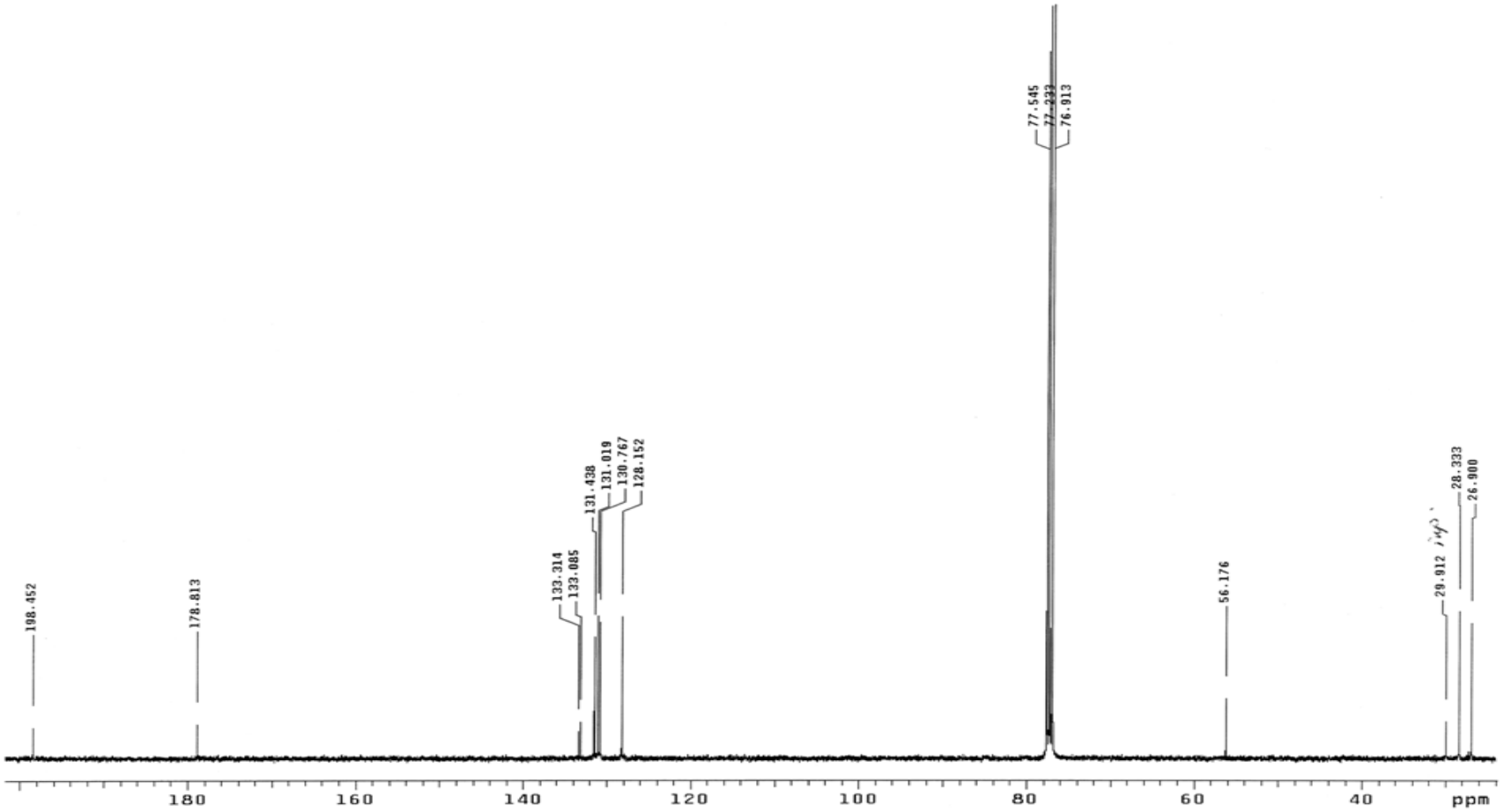

Figure 4.33. The ^{13}CNMR spectrum of compound 7 in $CDCl_3$

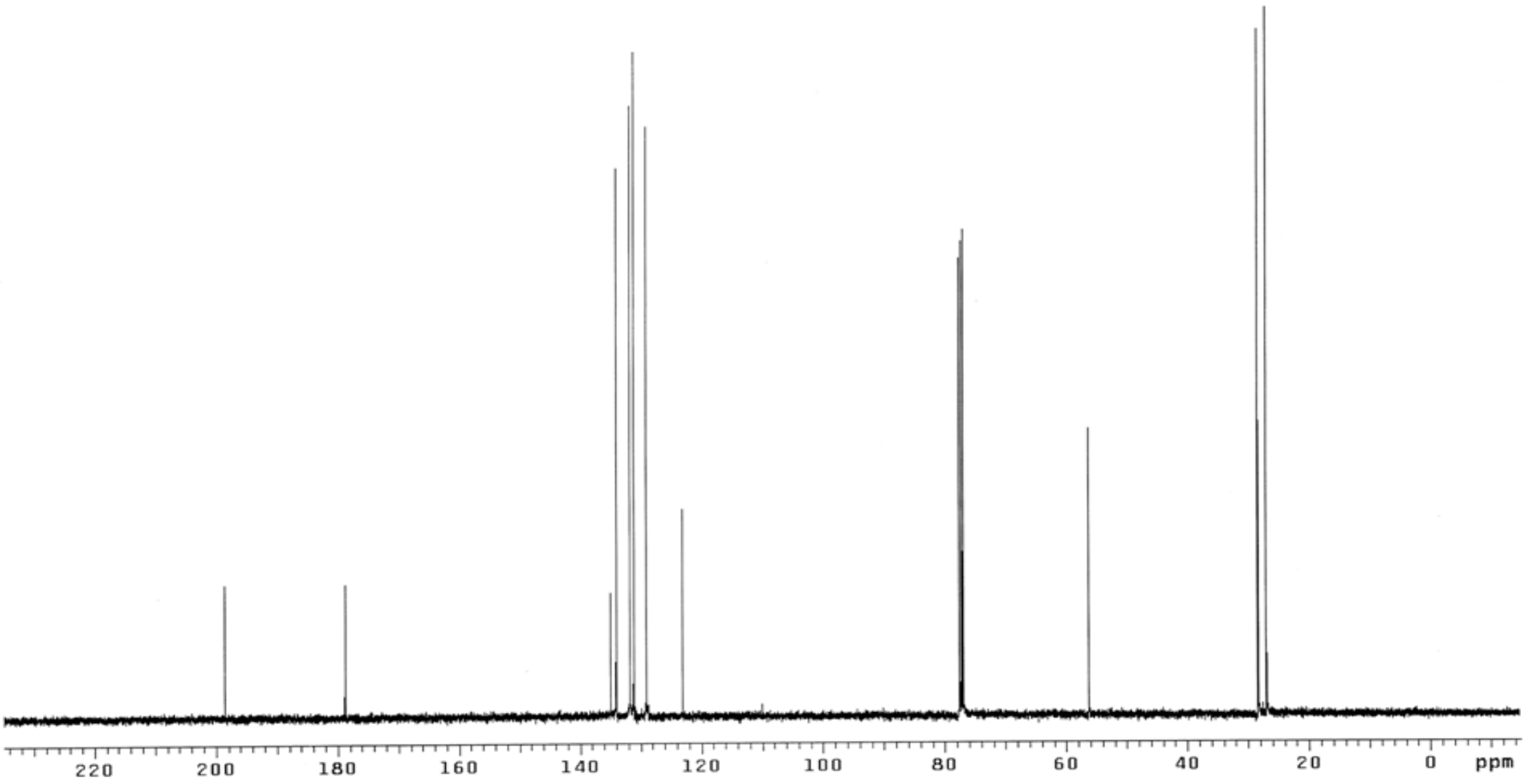

Figure 4.34. The ^{13}CNMR spectrum of compound 8 in $CDCl_3$

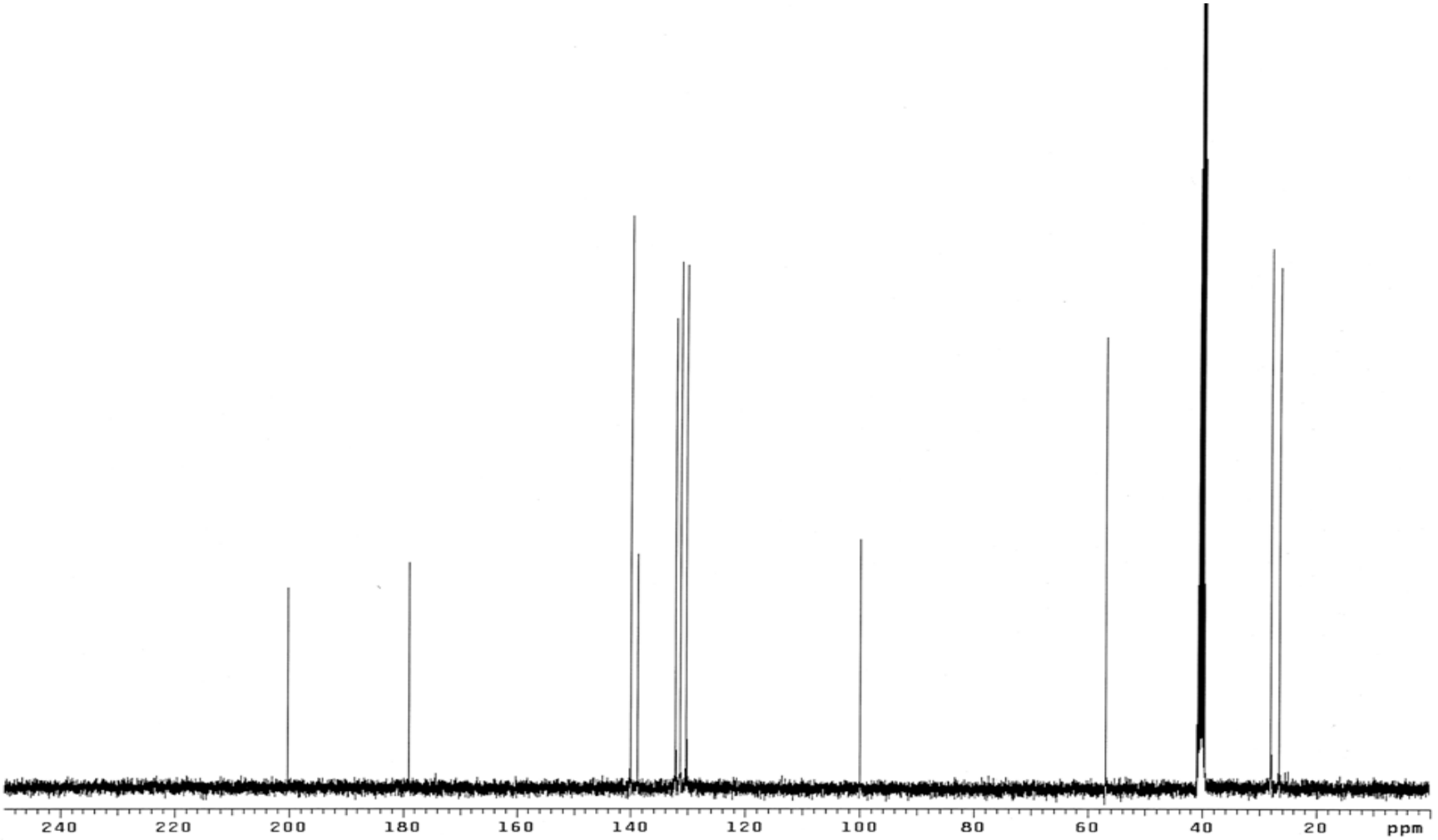

Figure 4.35. The ^{13}CNMR spectrum of compound 9 in DMSO-d_6

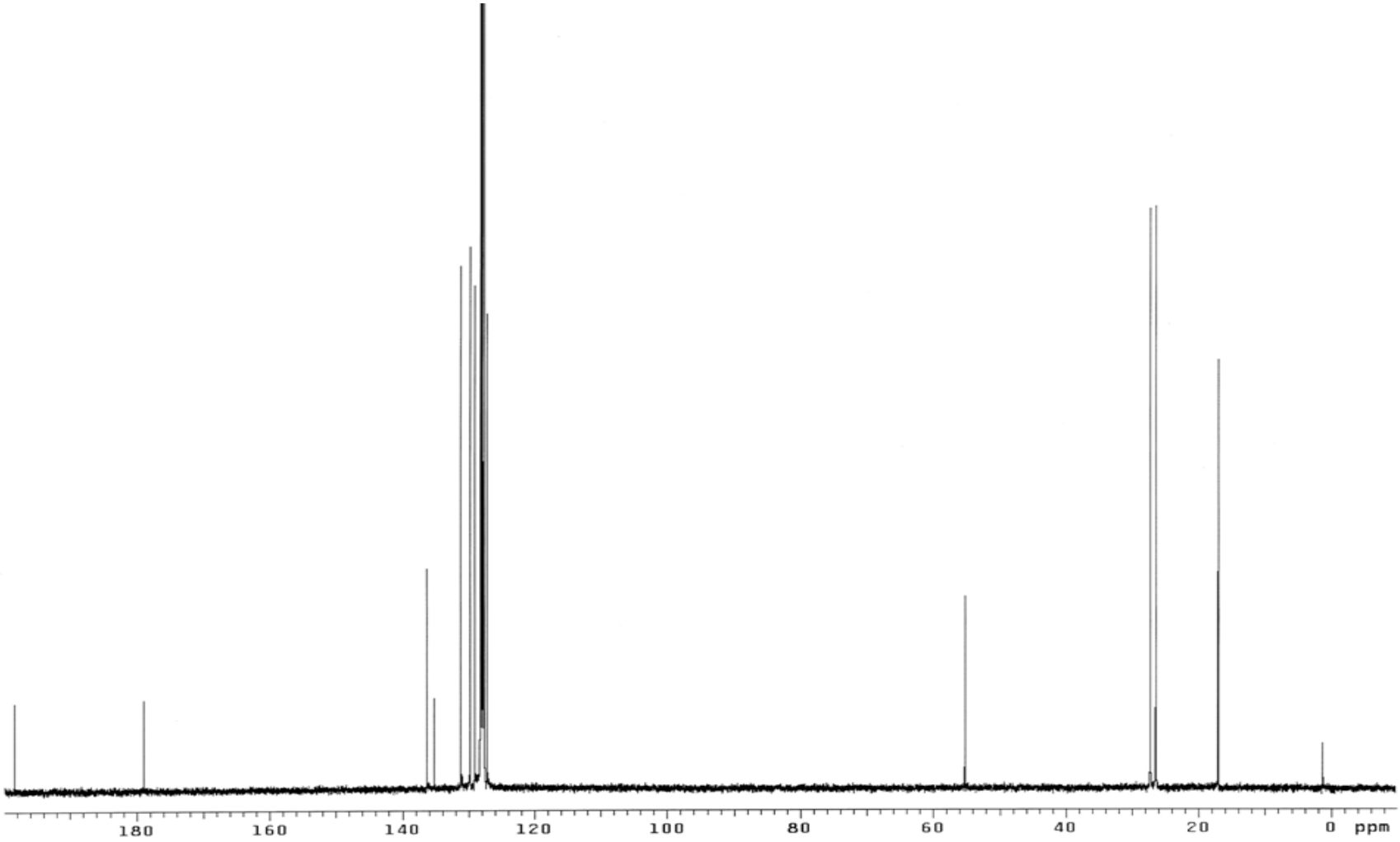

Figure 4.36. The ^{13}CNMR spectrum of compound 10 in Benzene-d_6

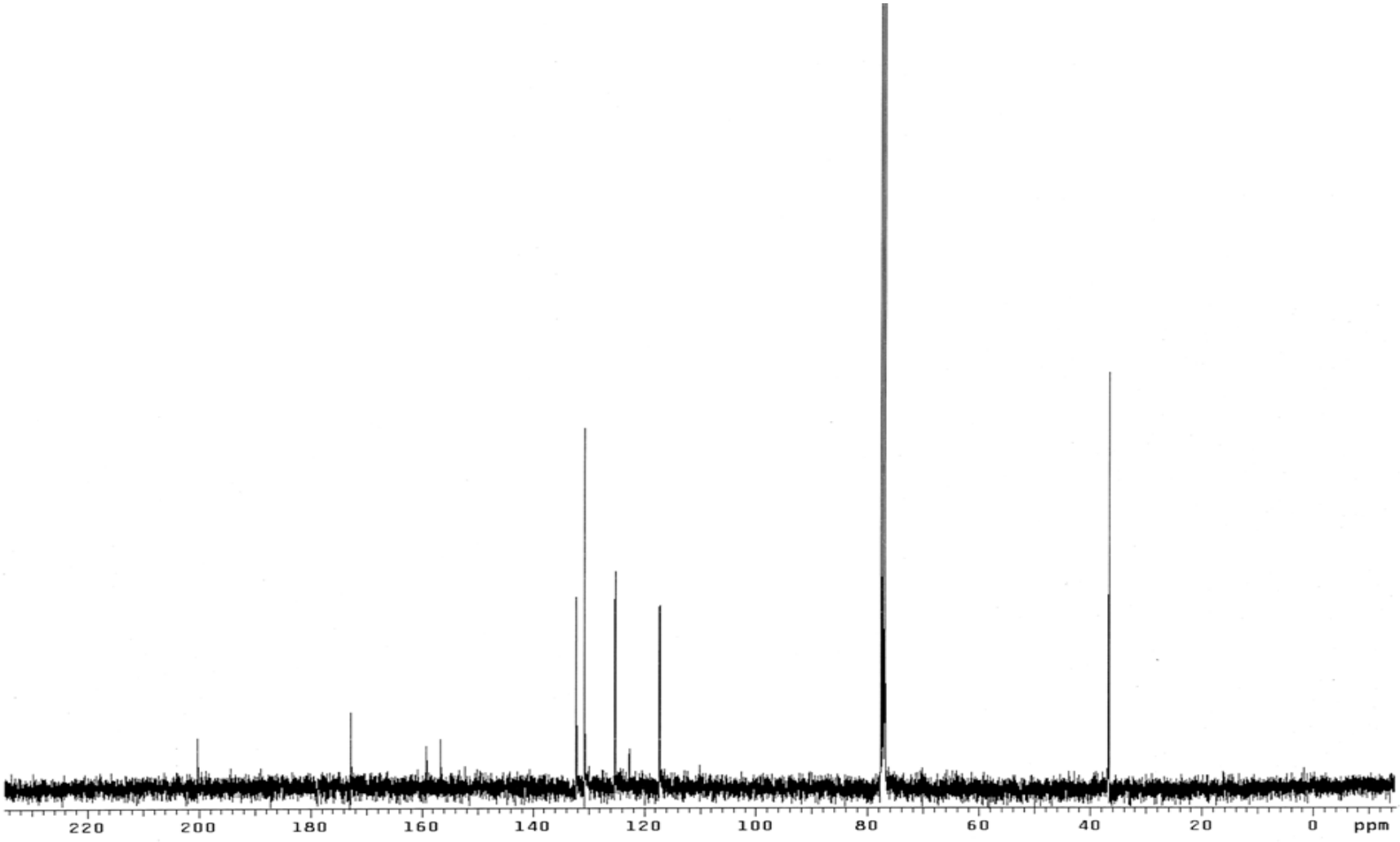

Figure 4.37. The ^{13}CNMR spectrum of compound 11 in $CDCl_3$

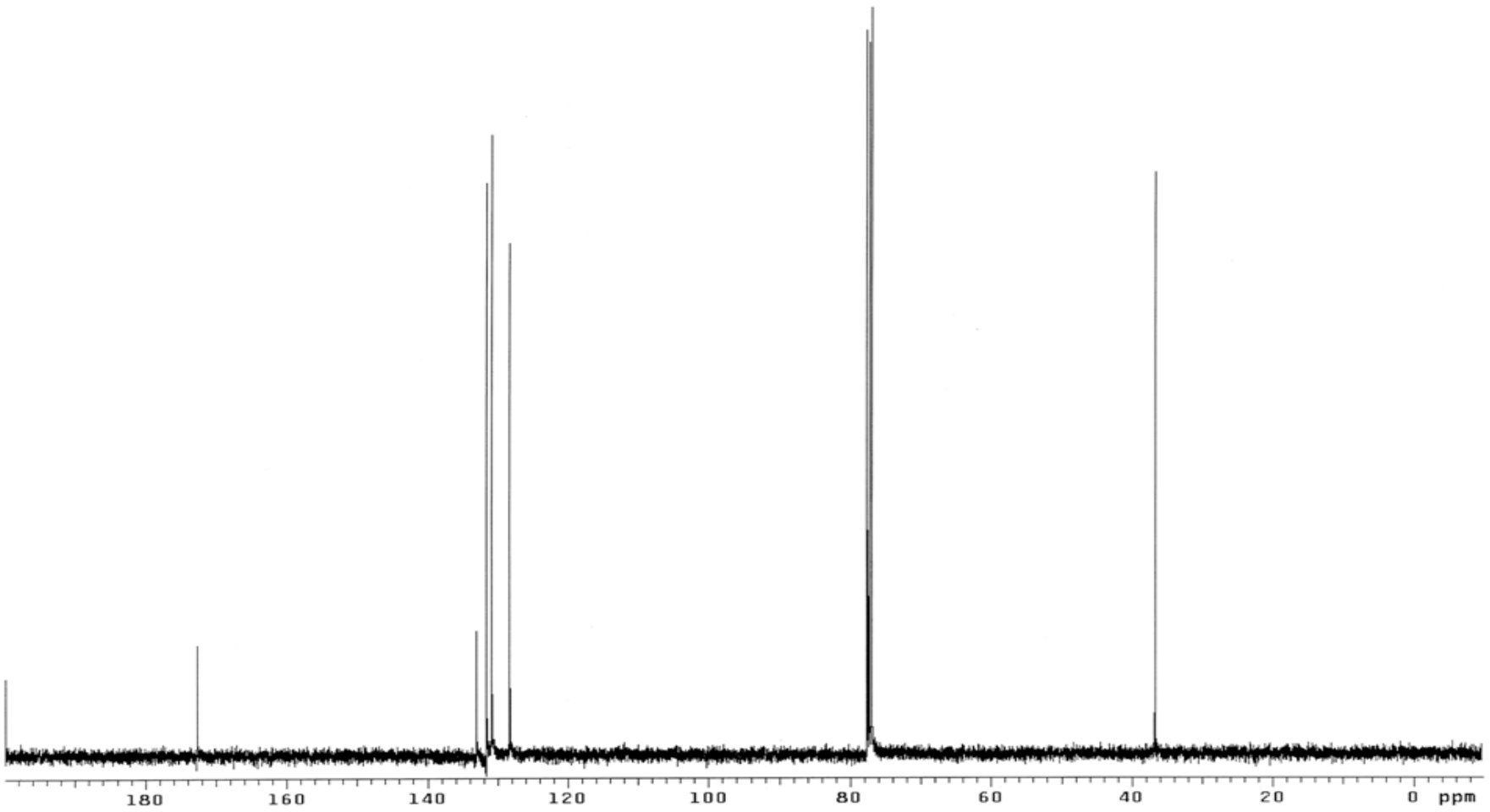

Figure 4.38. The ^{13}CNMR spectrum of compound 12 in $CDCl_3$

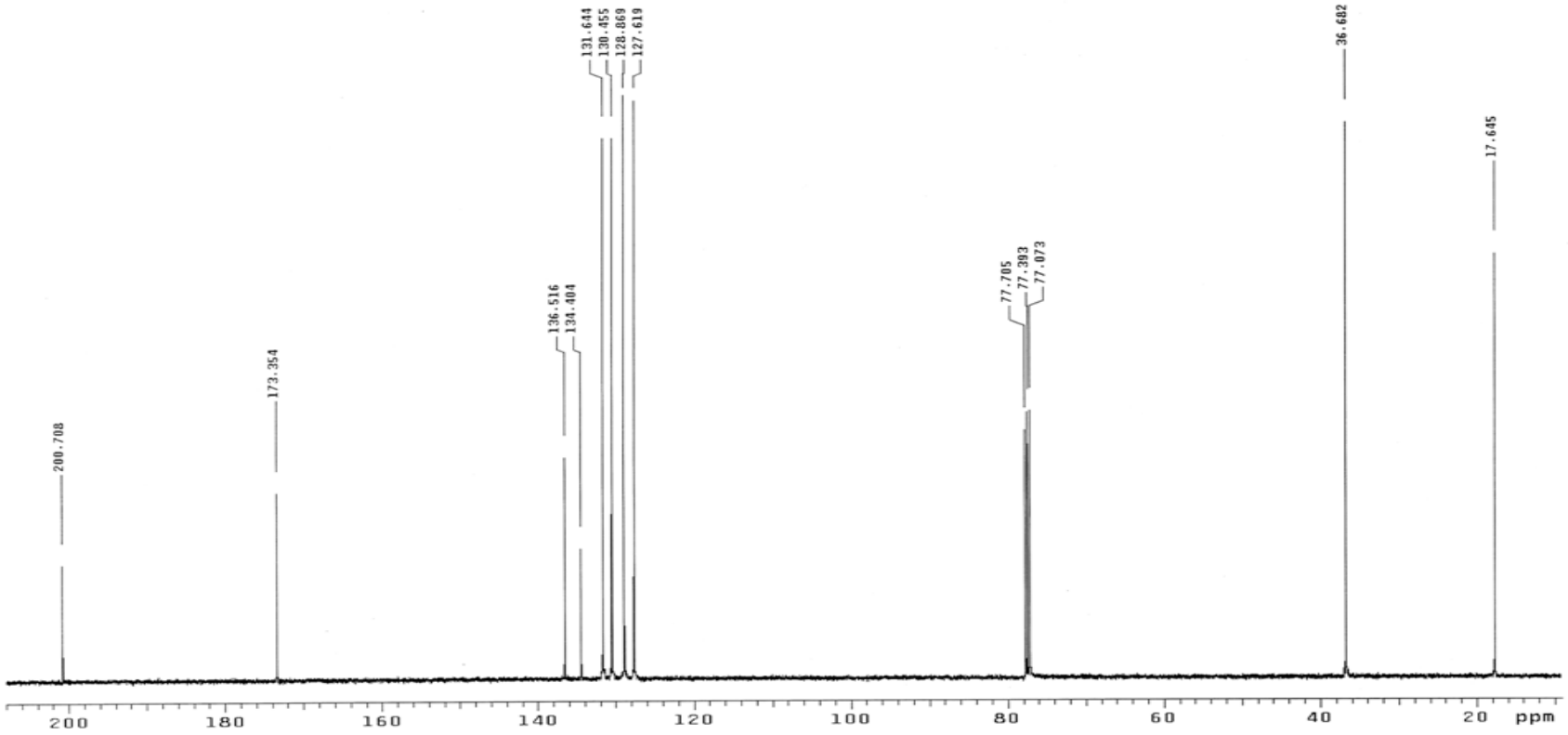

Figure 4.39. The ^{13}CNMR spectrum of compound 13 in $CDCl_3$

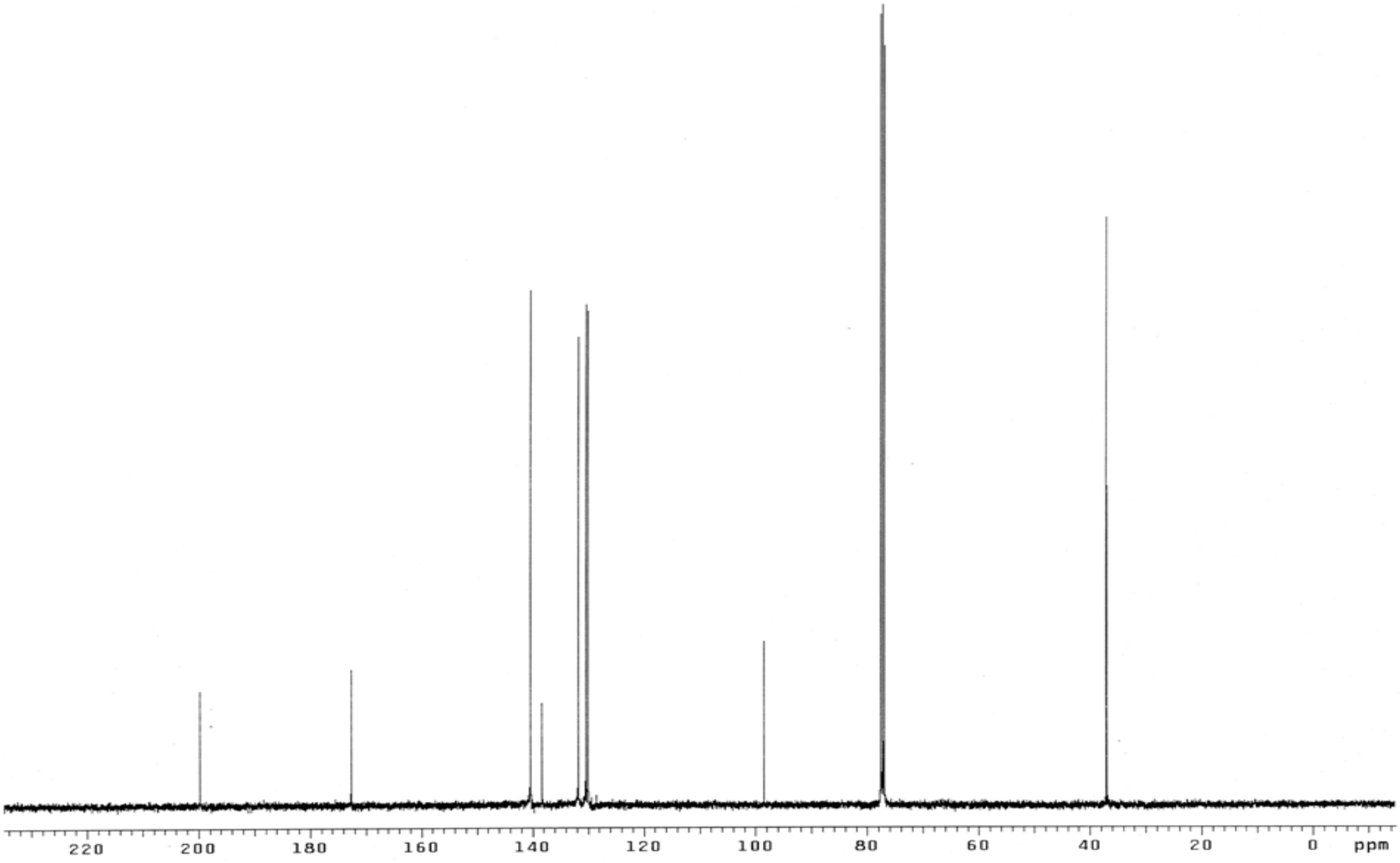

Figure 4.40. The ^{13}CNMR spectrum of compound 14 in $CDCl_3$

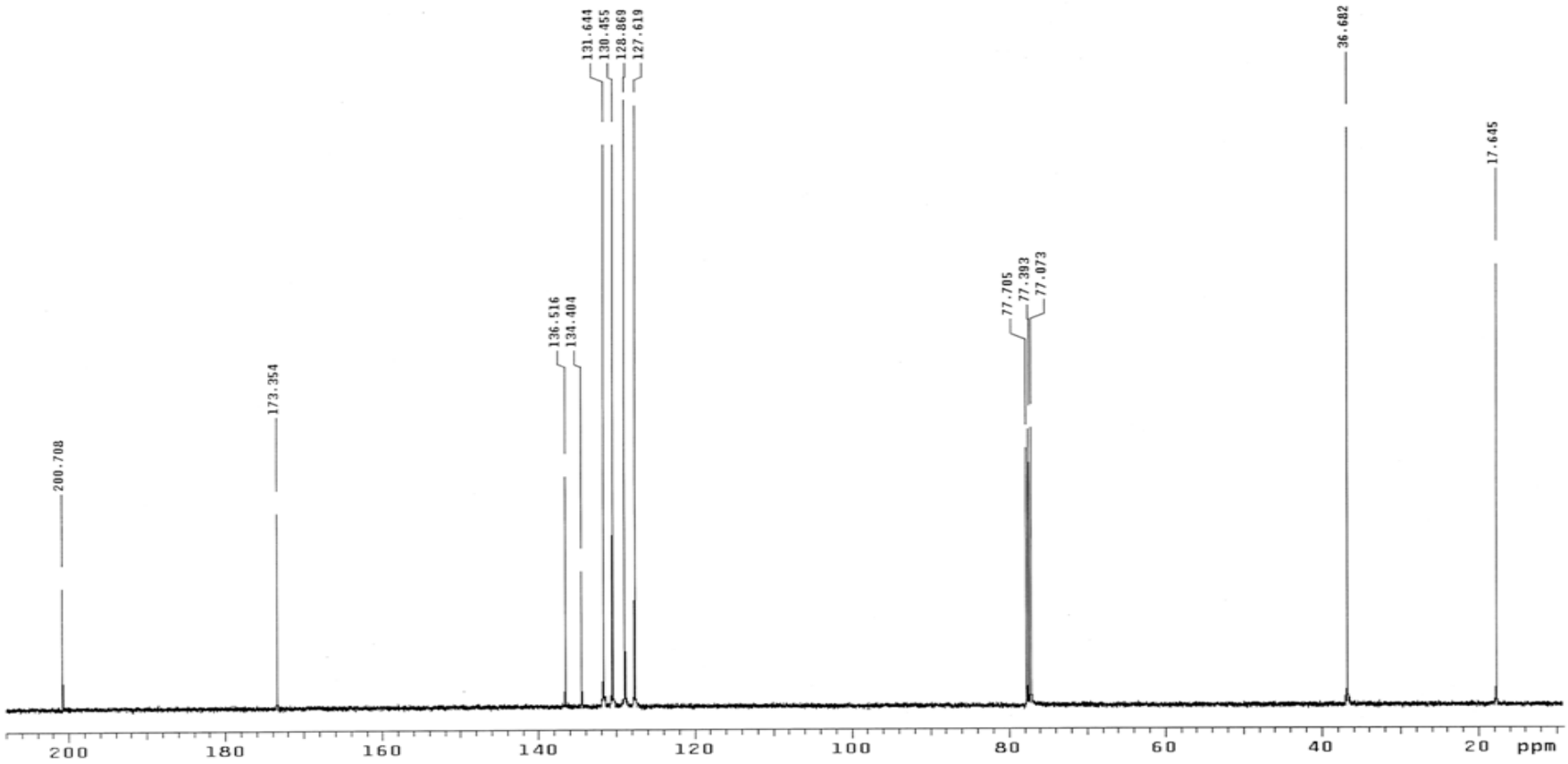

Figure 4.41. The ^{13}CNMR spectrum of compound 15 in $CDCl_3$

4.3. HPLC Analysis of the compounds

The chromatographic data belonging to experiments done on AD-H column are summarized in Table 4.6. The enantiomers of compounds (±)-2-15 were found to be atropisomeric and were either resolved or enriched micropreparatively on analytical or semipreparative Chiralpak AD-H columns using hexane-ethanol mixtures as eluent.

Table 4.6. Chromatographic data for the separation of enantiomers of (±)-2-15 on Chiralpak AD-H columns.

Compound No	Eluent(v/v) Hexane:Ethanol	Flow rate (ml/min)	k'_1	k'_2	α
(±)-2[a]	95:5	0.8	2.09	2.56	1.22
(±)-3[a]	95:5	0.8	2.12	2.47	1.16
(±)-4[a]	95:5	0.8	2.54	2.99	1.18
(±)-5[b]	95:5	2.8	0.98	1.41	1.43
(±)-6[b]	95:5	2.5	2.11	2.43	1.15
(±)-7[a]	95:5	0.6	1.65	2.77	1.67
(±)-8[b]	90:10	3.0	0.88	1.27	1.44
(±)-9[b]	90:10	3.0	1.14	1.31	1.15
(±)-10[a]	95:5	0.6	0.97	1.77	1.82
(±)-11[b]	90:10	3.5	8.16	13.5	1.65
(±)-12[b]	95:5	4.5	6.49	10.12	1.56
(±)-13[a]	50:50	0.6	3.64	4.34	1.19
(±)-14[a]	50:50	0.6	3.19	4.51	1.41
(±)-15[b]	95:5	4.5	8.63	9.62	1.11

[a]Analytical Chiralpak AD-H column was used, [b]Semi-preparative Chiralpak AD-H column was used.

The amylose based carbamate columns showed good enantioselectivities for these -in a way- N-*ortho*phenyl substituted cyclic thiocarbamate structures. The enantiomers of compound (±)-1 could not be resolved due to its fast racemization. The ^{1}H NMR of this compound however showed the diastereomeric methyl protons at C-5 which points to a "transient chirality" which is a term used by Clayden [42] to describe such axially chiral

molecules which although can not be preparatively resolved, can be differentiated on the NMR time scale. The energy barrier for this compound has therefore been determined by temperature dependent NMR.

It has been observed that the 3-(*o*-aryl)-2-thioxo-4-thiazolidinone derivatives which are unsubstituted at C-5, (±)-11-15 were better retained (Table 4.6) on chiralpak AD-H column than the corresponding 5,5-dimethyl compounds (±)-2-10, but the retention factors did not always parallel the separation factors. Enantiomers of compound (±)-15 for example, although highly retained (k_1'= 8.63, k_2'=9.62) were separated only poorly (α = 1.1) (Table 4.6). The compounds (±)-5, (±)-10, (±)-12 and (±)-15 have been semipreparatively enriched on micro crystaline triacetylcellulose [43] as well by MPLC. The enantioselectivities of the carbamate coated columns were found to be better for (±)-5, (±)-10 and (±)-12 (1.43 vs 1.3, 1.8 vs 1.1 and 1.6 vs 1.4) but slightly worse for (±)-15 (1.1 vs 1.2).

4.4. Determination of the Activation Barrier for Hindered Rotation by Thermal Racemization

After the enantiomers of (±)-2-15 were resolved by chiral chromatography, thermal racemizations were performed on single enantiomers to determine the activation energy barriers to racemization.

The thermal racemization was performed in the following way: First each enantiomer was collected separately. As soon as the enantiomer was collected, the solvent was evaporated by blowing nitrogen gas to the sample. This procedure was done until about 0.2 mg of each enantiomer was collected. Then the solid (resolved enantiomer) was dissolved in 200 µlt of solvent, and 30 µlt of the solution was injected into the HPLC column to determine the initial enantiomeric composition. The solution left was kept in a constant temperature bath, and the racemization process was followed by taking 30 µlt of the sample at regular time intervals and injecting to the column after quenching in an ice bath (Figures 4.42 to 4.55).

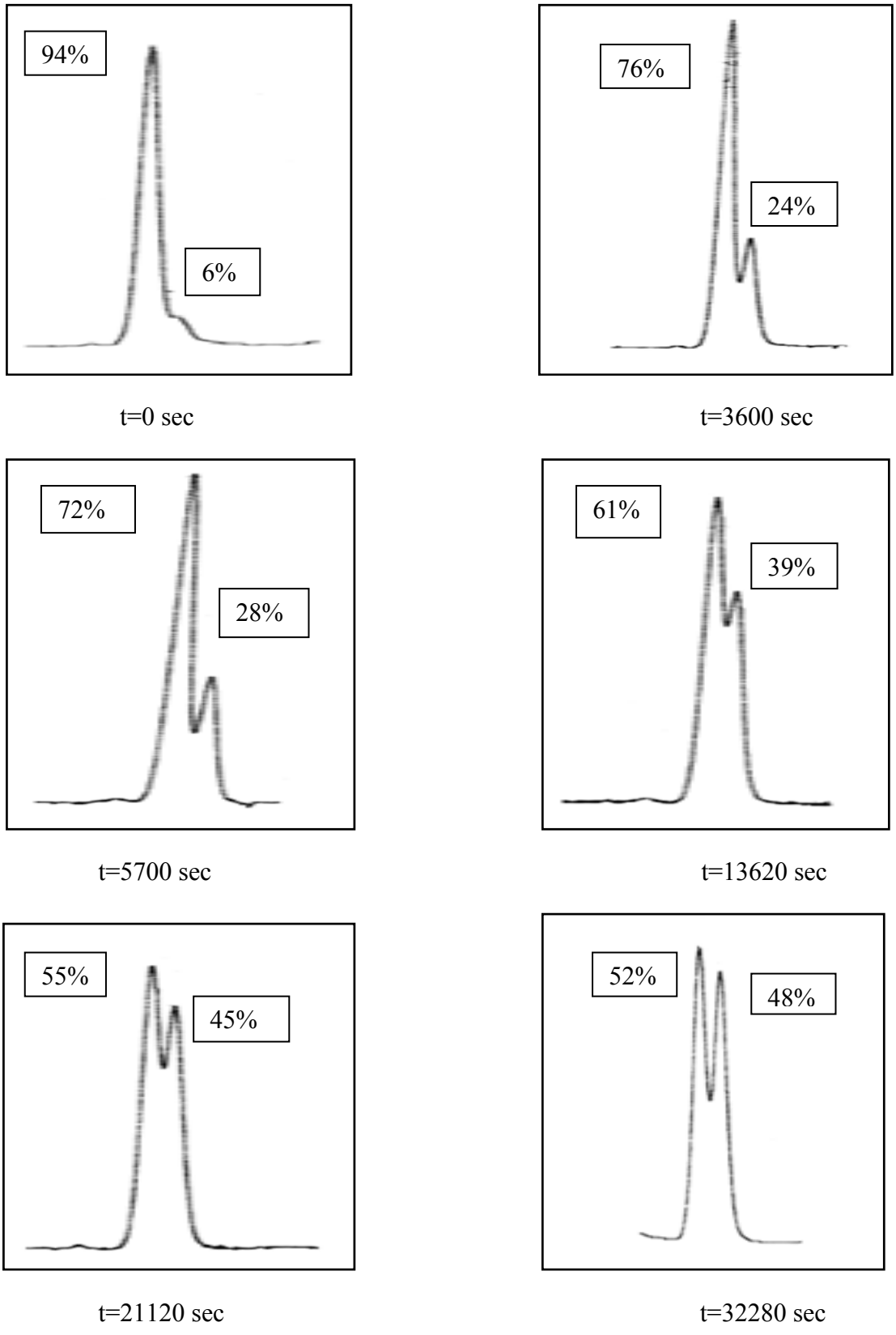

Figure 4.42. The chromatograms of first eluated enantiomer of compound 2 during thermal racemization at 343 K

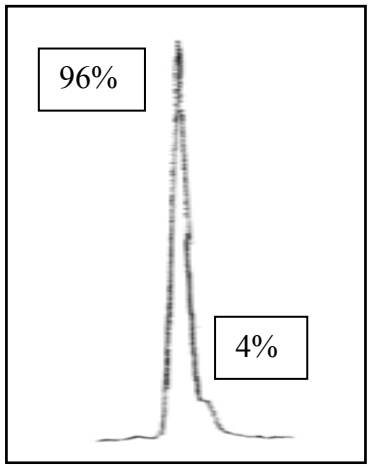

t=0 sec

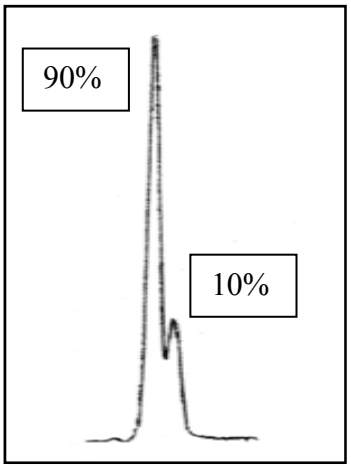

t=7800 sec

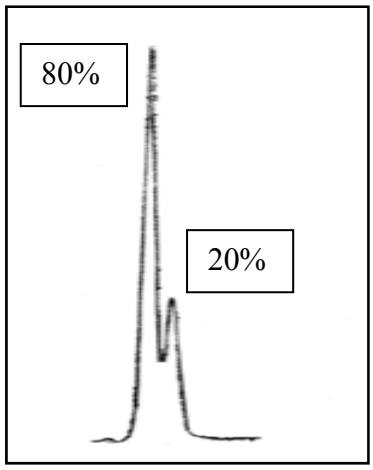

t=28100 sec

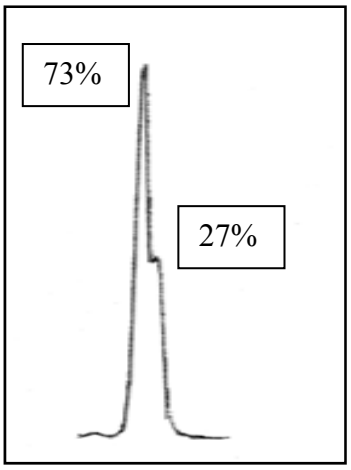

t=39300 sec

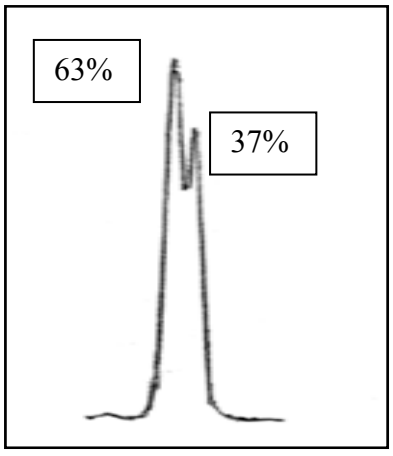

t=72900 sec

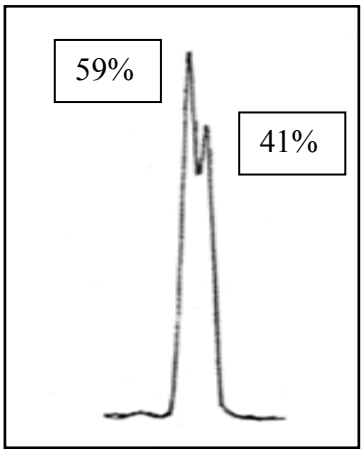

t=111600 sec

Figure 4.43. The chromatograms of first eluated enantiomer of compound 3 during thermal racemization at 343 K

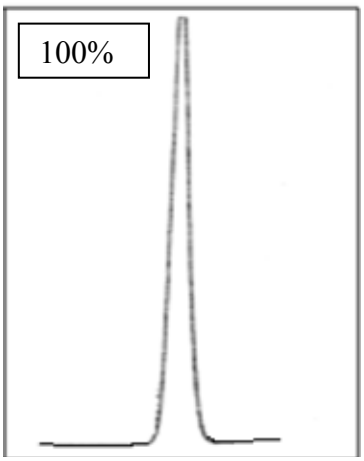

t=0 sec

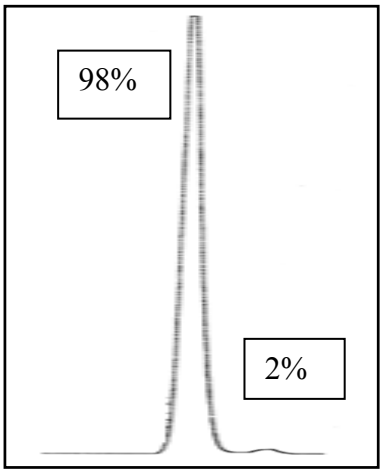

t=3600 sec

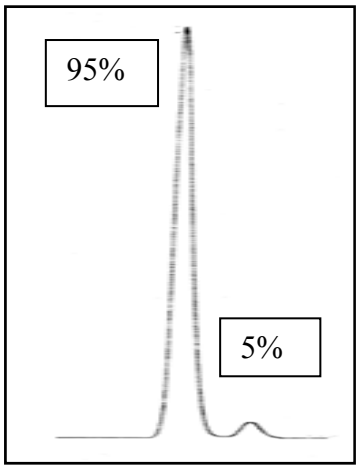

t=17400 sec

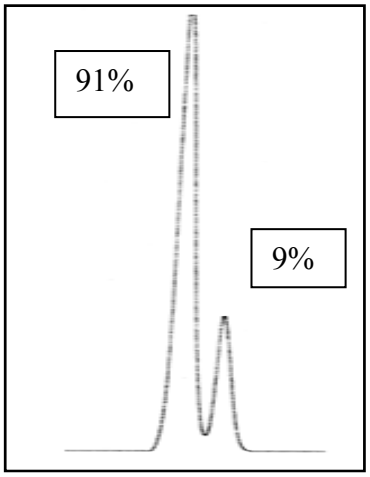

t=34200 sec

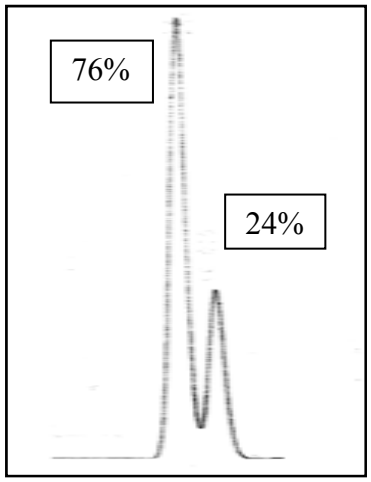

t=192900 sec

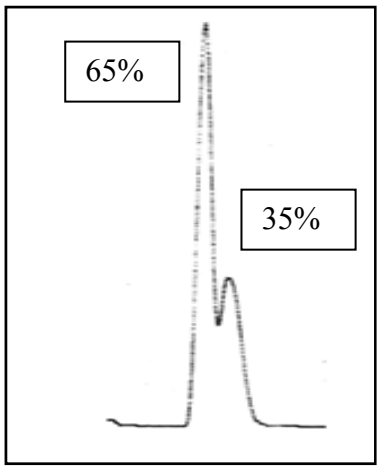

t=283700 sec

Figure 4.44. The chromatograms of first eluated enantiomer of compound 4 during thermal racemization at 348 K

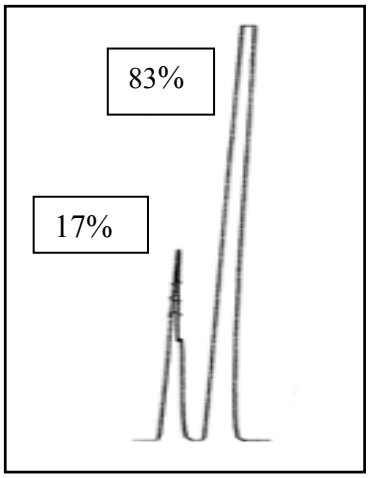

t=0 sec

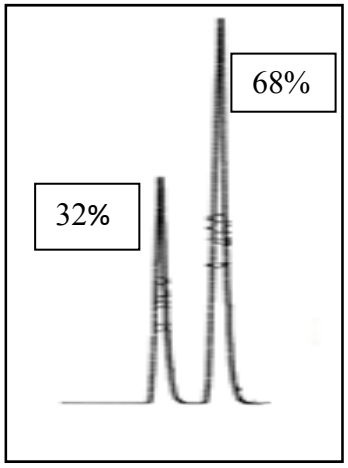

t=1800 sec

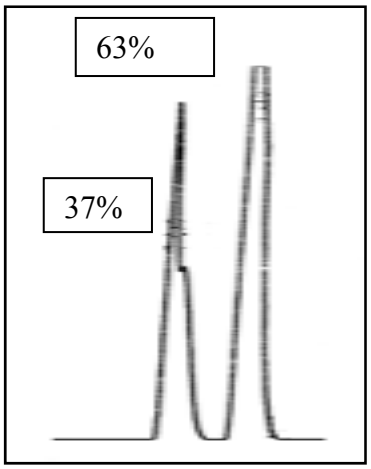

t=2700 sec

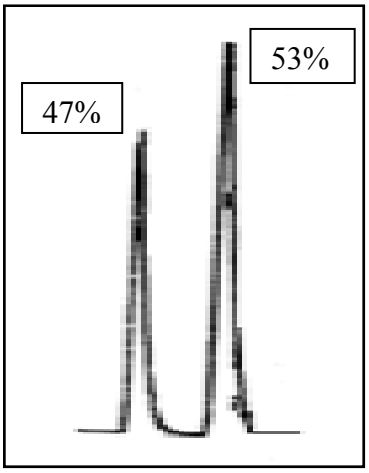

t=3600 sec

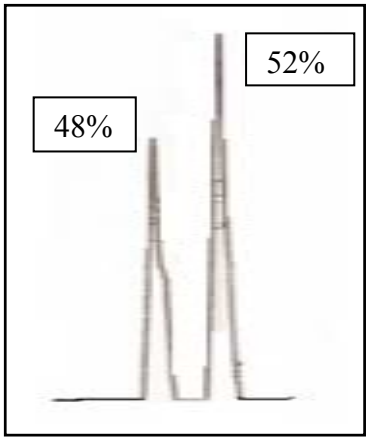

t=5400 sec

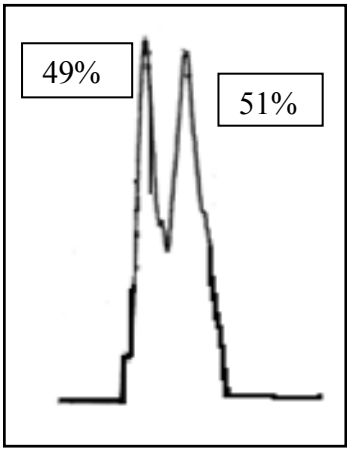

t=6300 sec

Figure 4.45. The chromatograms of secondt eluated enantiomer of compound 5 during thermal racemization at 328 K

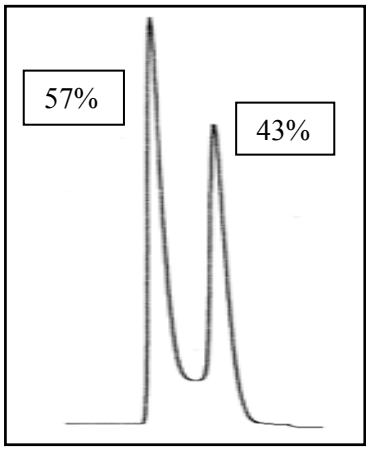

t=0 sec

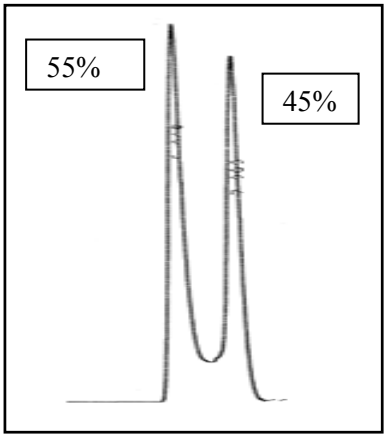

t=1440 sec

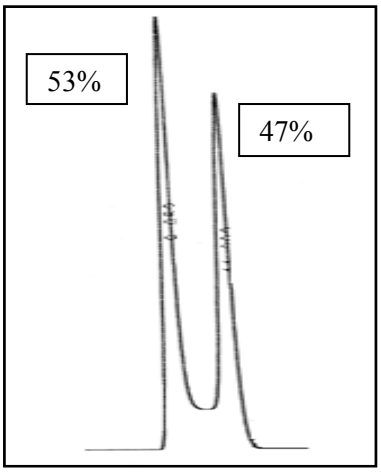

t=3600 sec

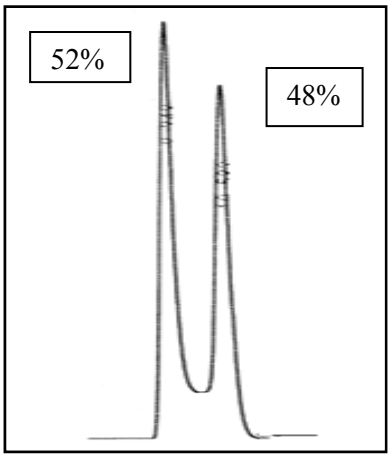

t=4920 sec

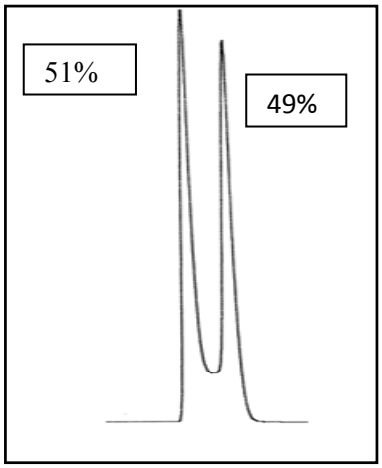

t=7920 sec

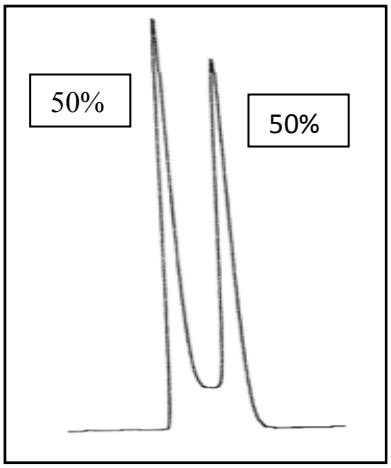

t=10020 sec

Figure 4.46. The chromatograms of first eluated enantiomer of compound 6 during thermal racemization at 280 K

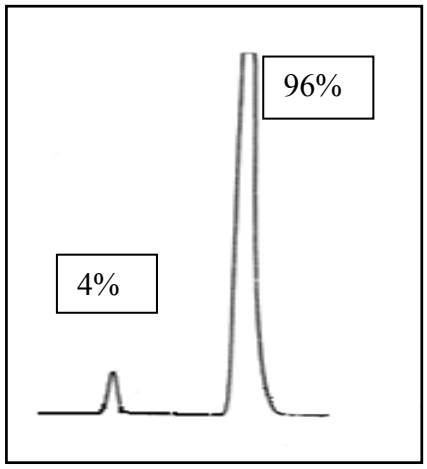

t=0 sec

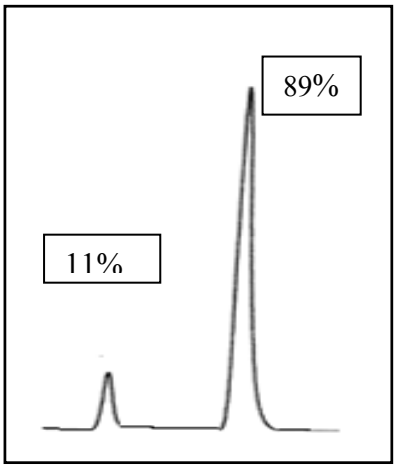

t=3600 sec

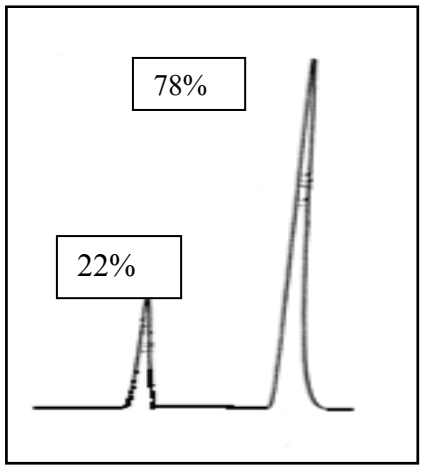

t=10800 sec

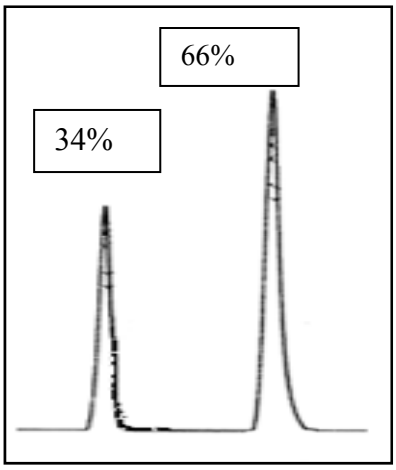

t=22500 sec

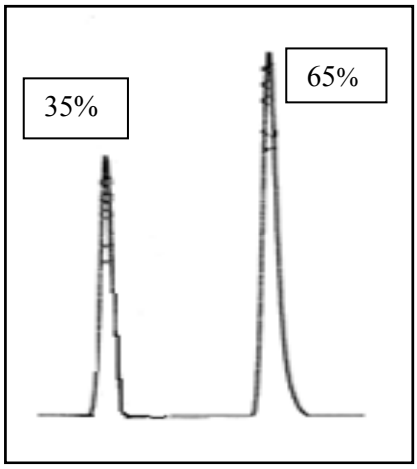

t=25200 sec

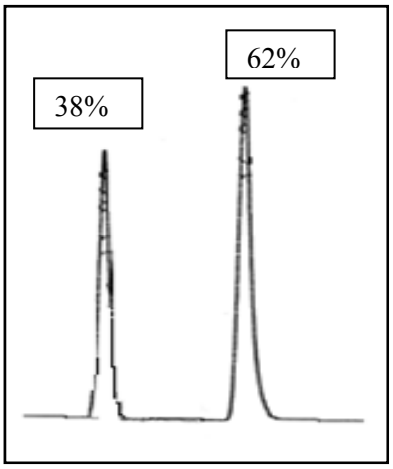

t=28800 sec

Figure 4.47. The chromatograms of first eluated enantiomer of compound 7 during thermal racemization at 348 K

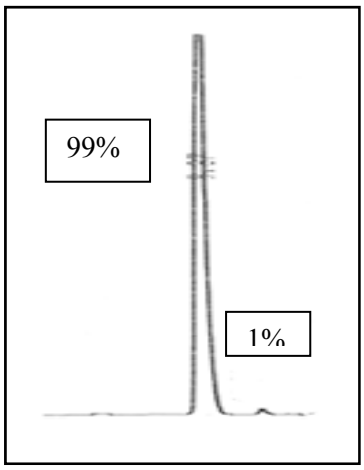

t=0 sec

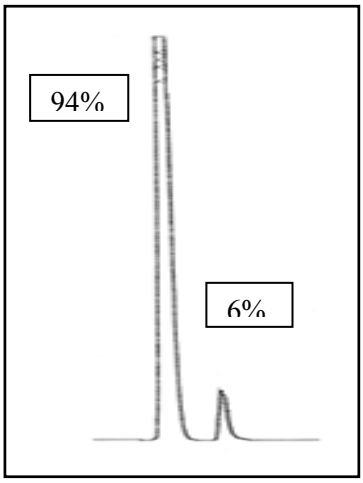

t=17700 sec

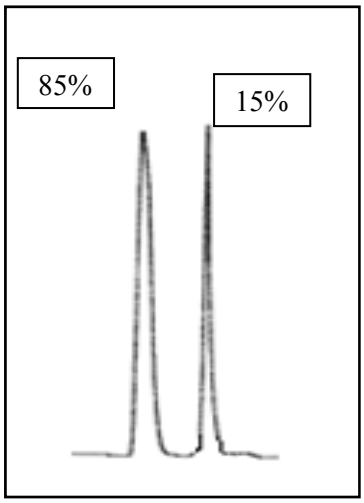

t=56700 sec

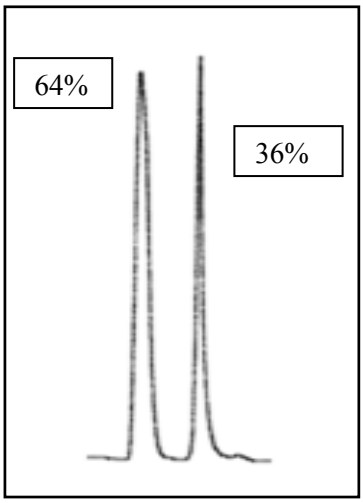

t=155700 sec

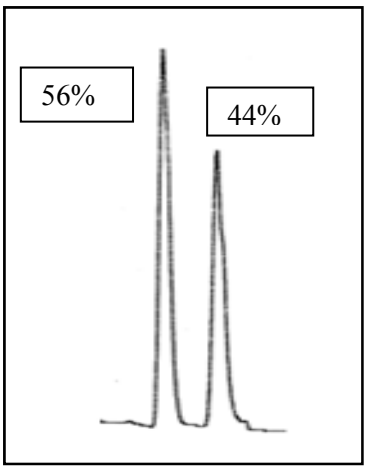

t=253800 sec

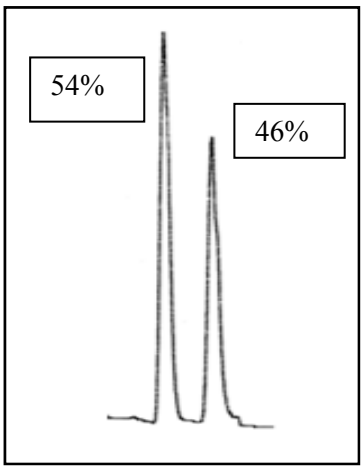

t=270900 sec

Figure 4.48. The chromatograms of first eluated enantiomer of compound 8 during thermal racemization at 348 K

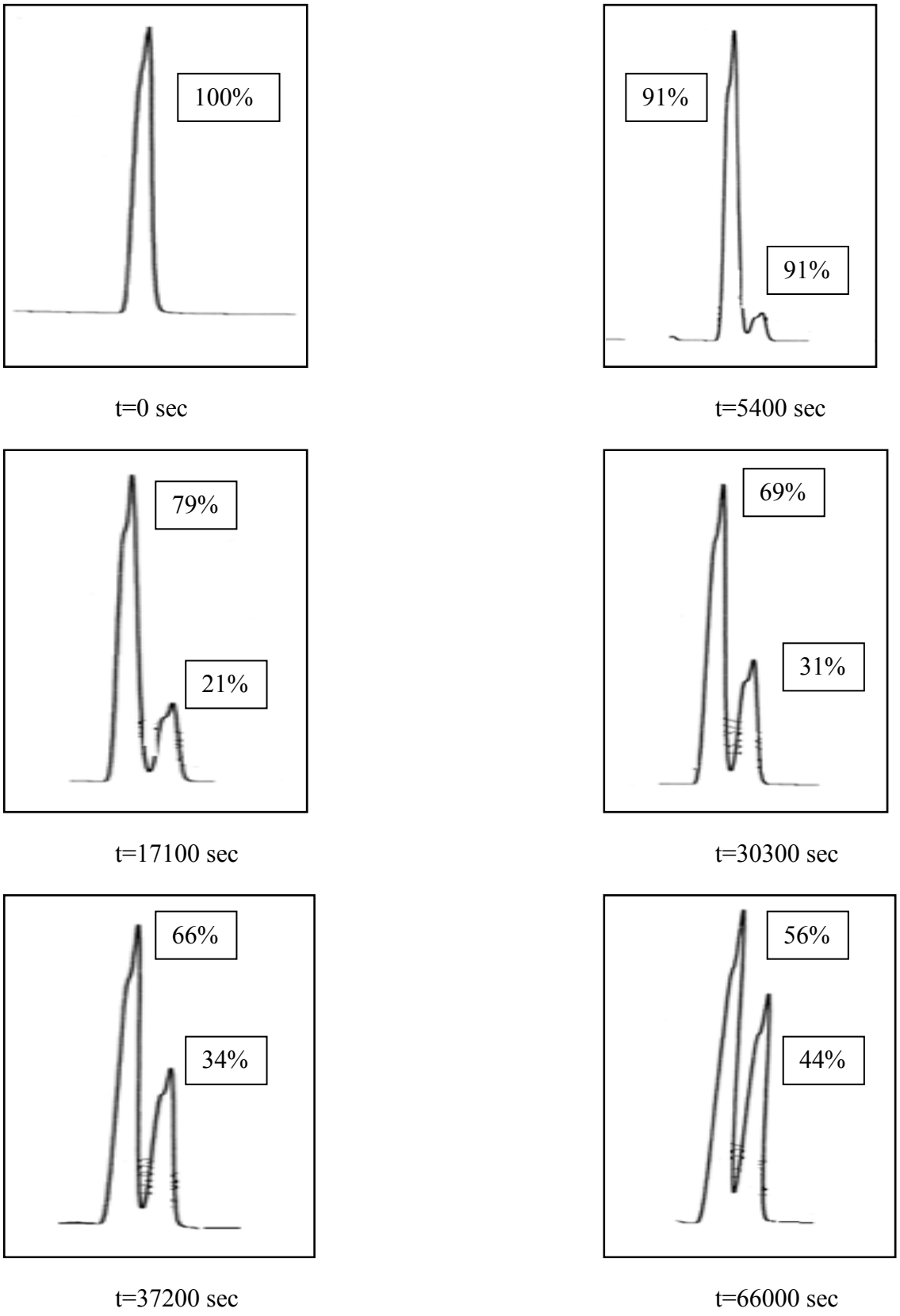

Figure 4.49. The chromatograms of first eluated enantiomer of compound 9 during thermal racemization at 378 K

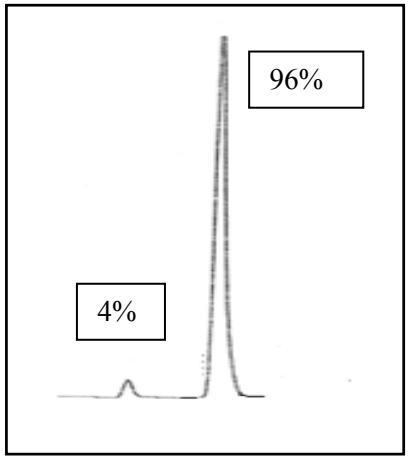

t=0 sec

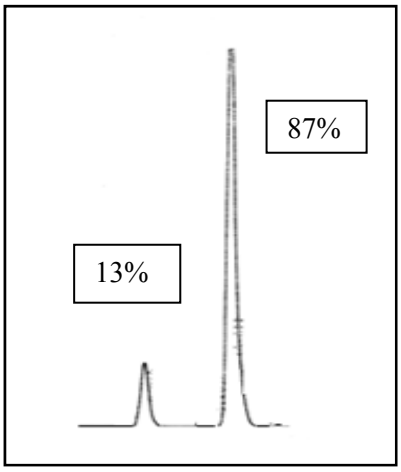

t=6300 sec

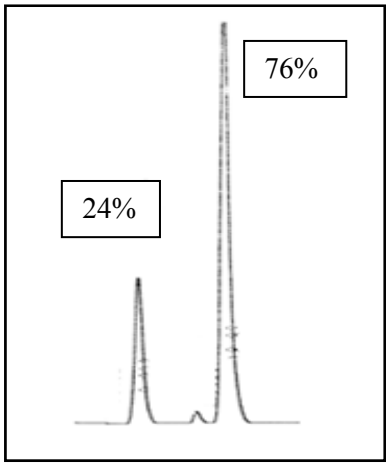

t=14400 sec

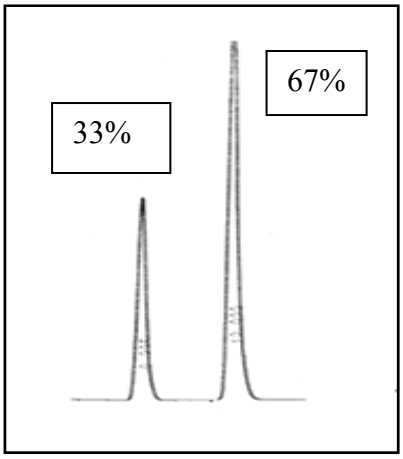

t=25200 sec

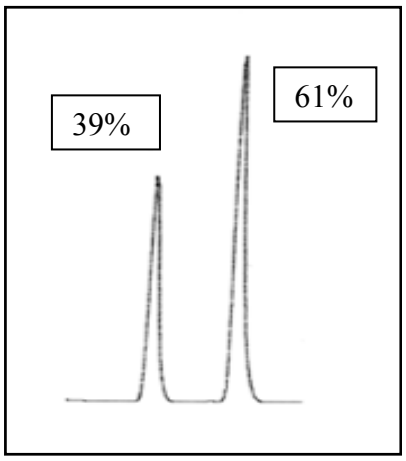

t=35100 sec

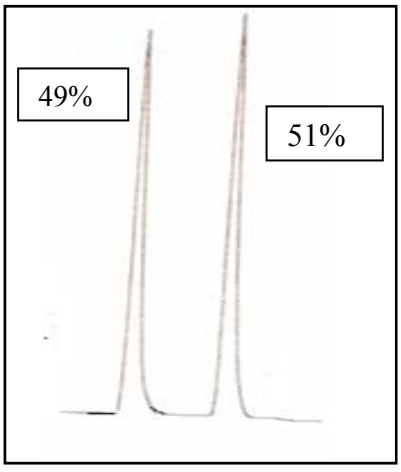

t=78300 sec

Figure 4.50. The chromatograms of first eluated enantiomer of compound 10 during thermal racemization at 333 K

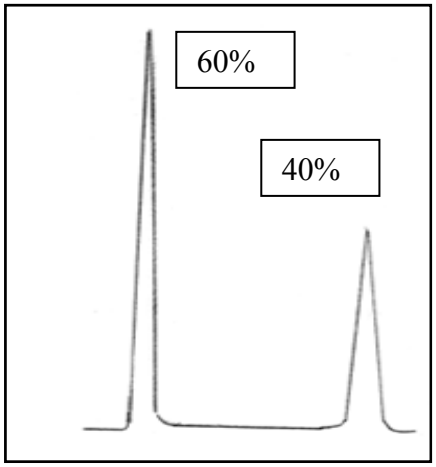

t=0 sec

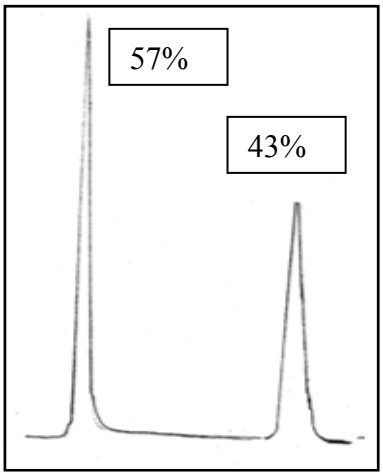

t=1800 sec

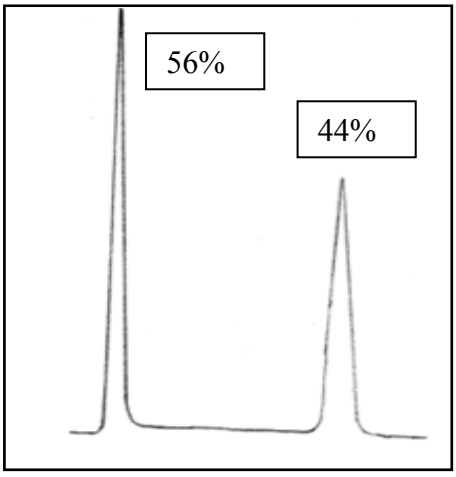

t=4500sec

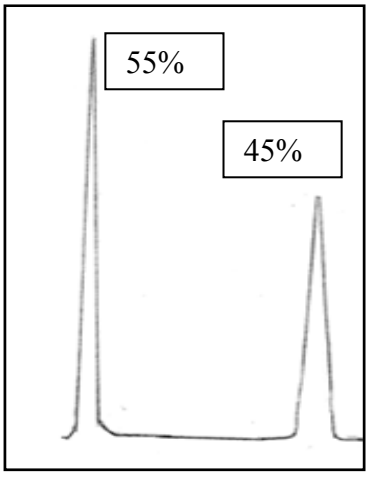

t=5100 sec

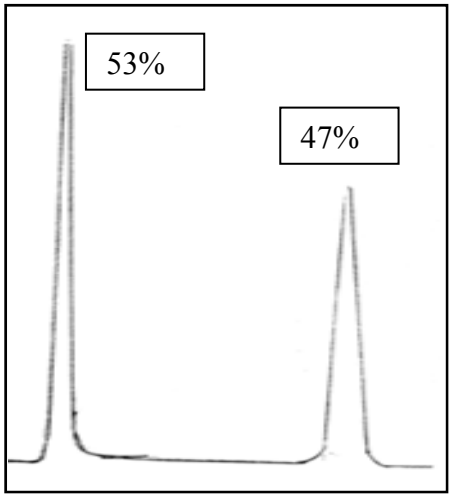

t=6600 sec

Figure 4.51. The chromatograms of first eluated enantiomer of compound 11 during thermal racemization at 280 K

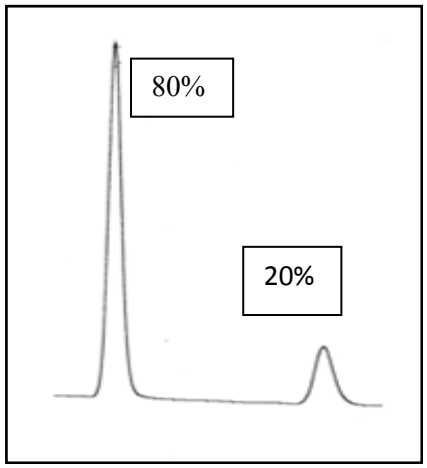

t=0 sec

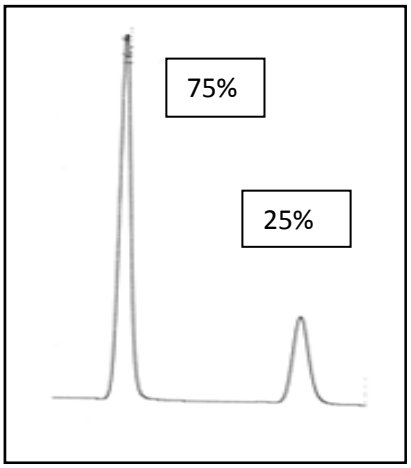

t=7200 sec

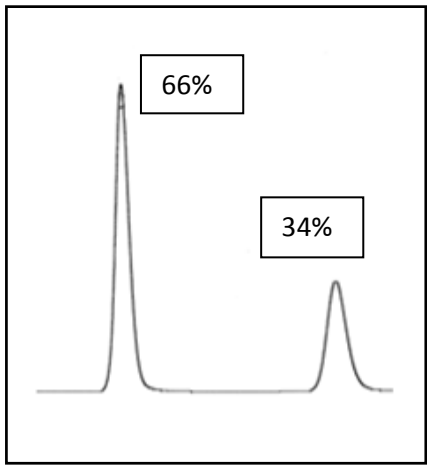

t=18000 sec

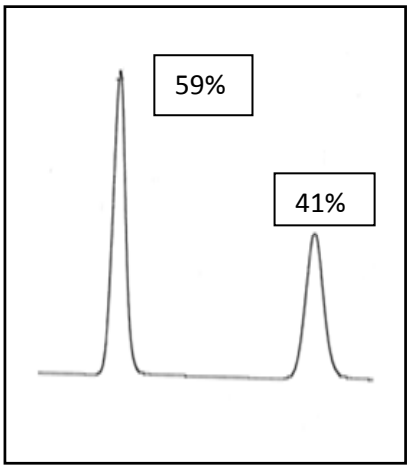

t=37800 sec

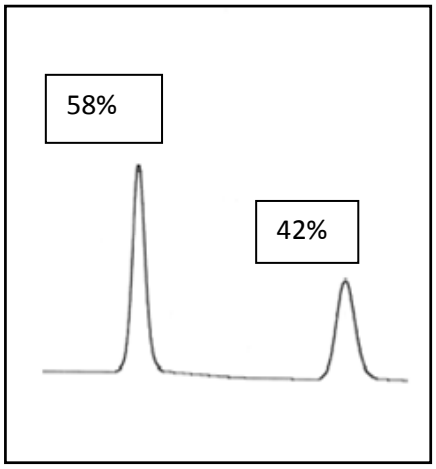

t=43200 sec

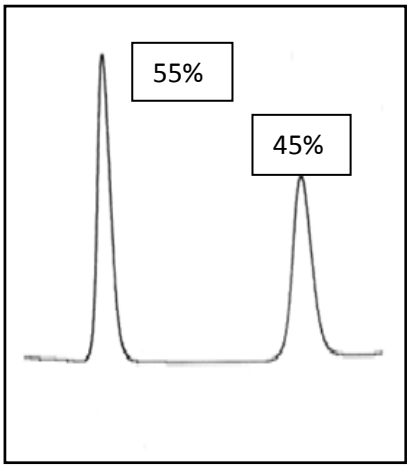

t=64800 sec

Figure 4.52. The chromatograms of first eluated enantiomer of compound 12 during thermal racemization at 353 K

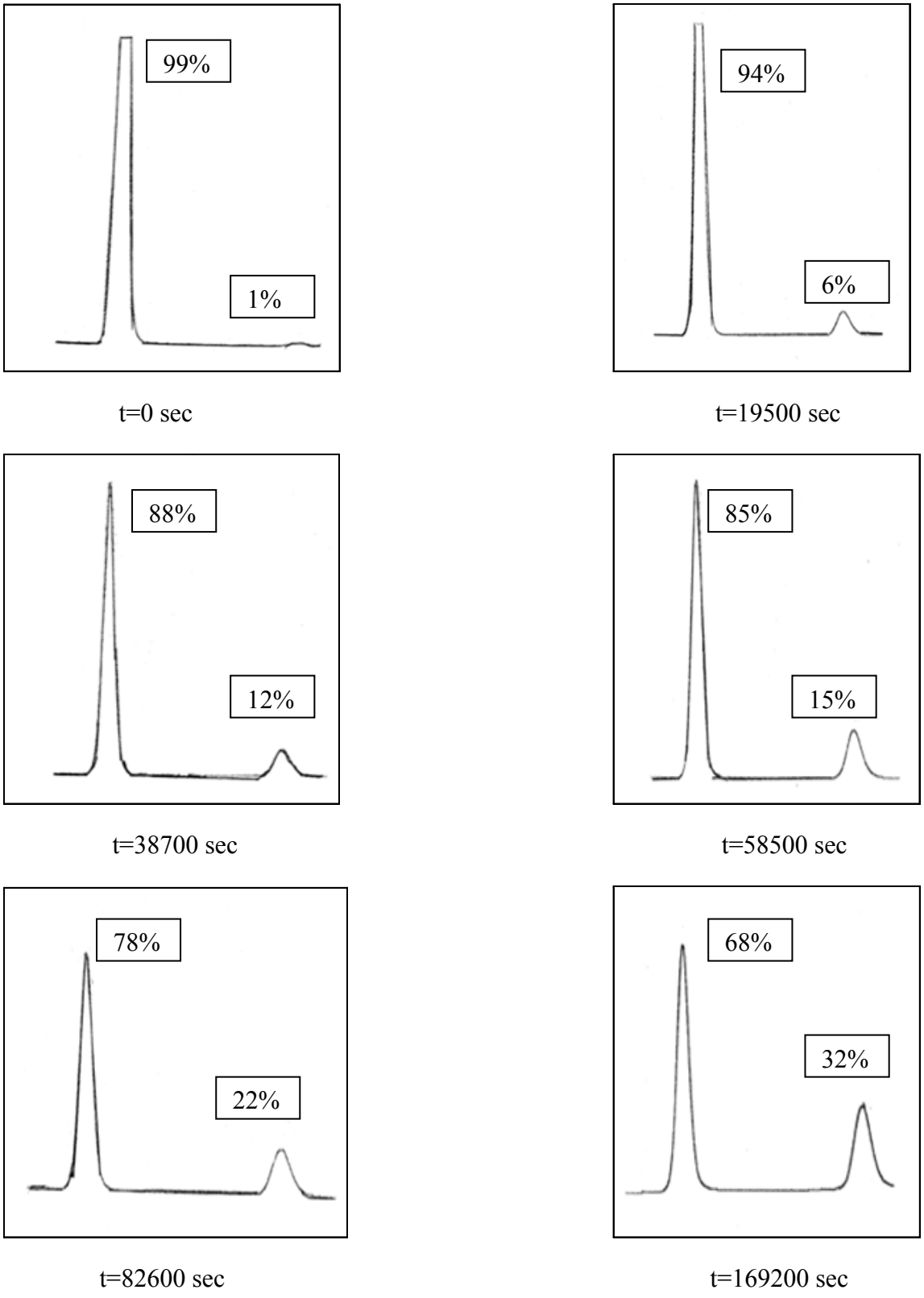

Figure 4.53. The chromatograms of first eluated enantiomer of compound 13 during thermal racemization at 351 K

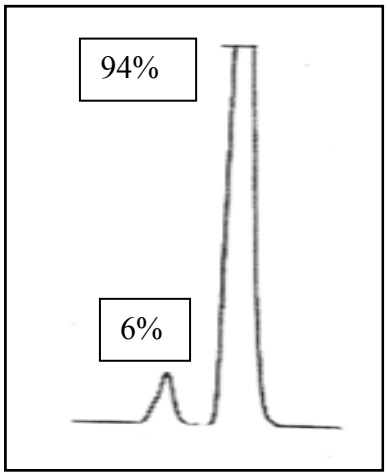

t=0 sec

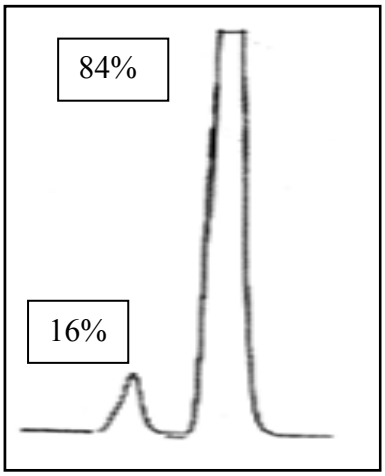

t=9000 sec

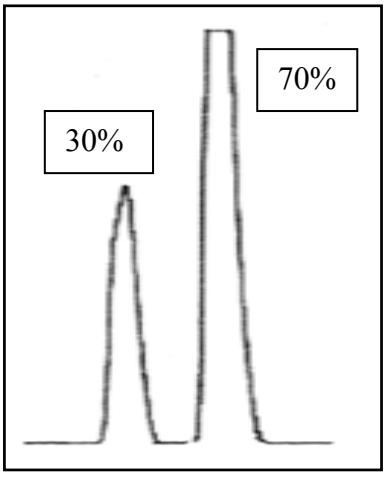

t=19800 sec

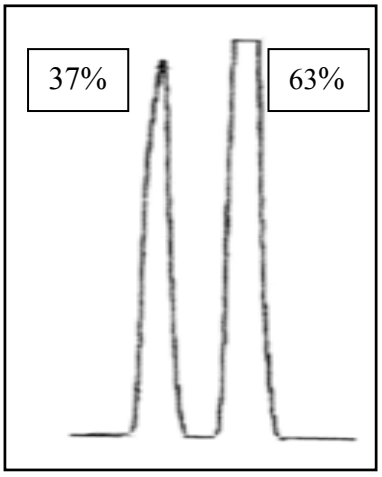

t=28500 sec

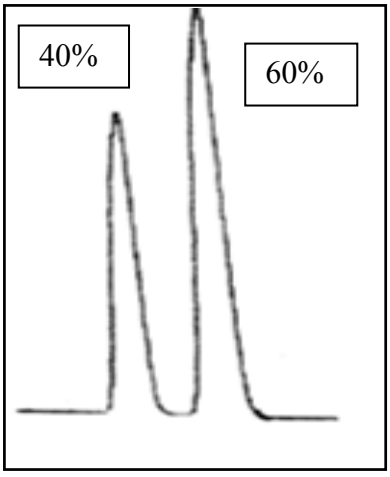

t=36900 sec

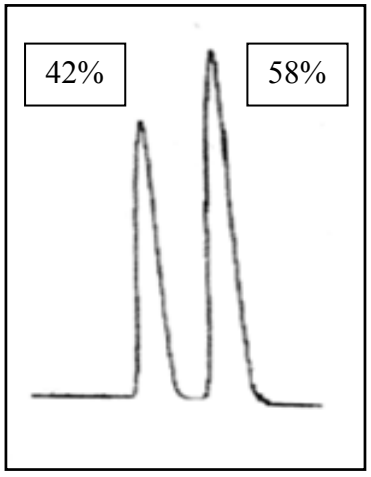

t=42000 sec

Figure 4.54. The chromatograms of first eluated enantiomer of compound 14 during thermal racemization at 383 K

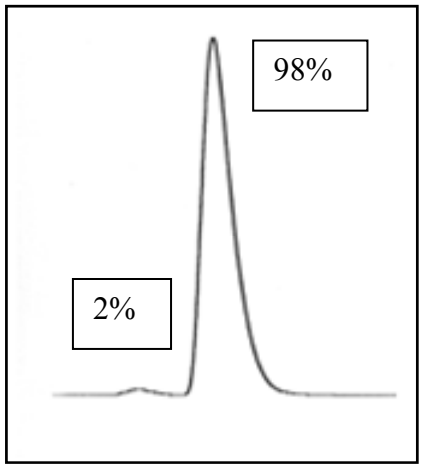

t=0 sec

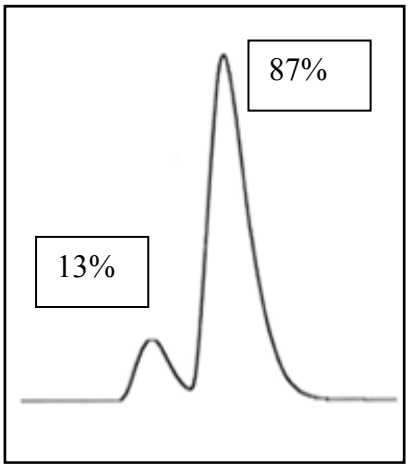

t=6000 sec

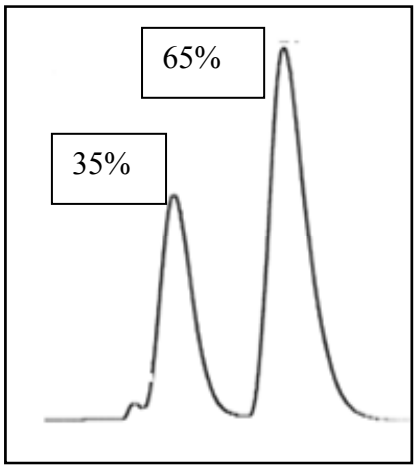

t=17100 sec

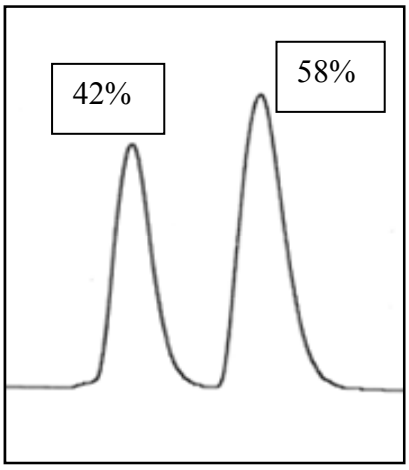

t=33900 sec

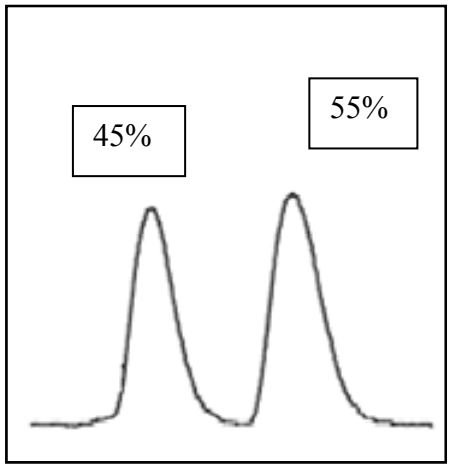

t=42900 sec

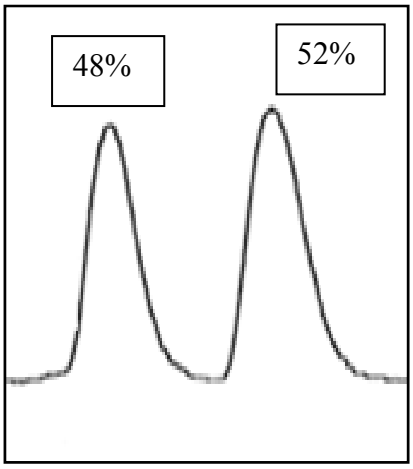

t=49200 sec

Figure.4.55. The chromatograms of first eluated enantiomer of compound **15** during thermal racemization at 348 K

After observing thermal racemization, the relative per cent composition values of the first or second eluated enantiomer, were substituted into Equation 2.12.

$$\ln ([M]-[M]_{eq}/[M]_0-[M]_{eq})=-2kt \qquad (2.12)$$

The slopes of ln $([M]-[M]_{eq}/[M]_0-[M]_{eq}$ versus time graph for compounds (±)-2-15 give the 2k values (Figures 4.56 to 4.69).

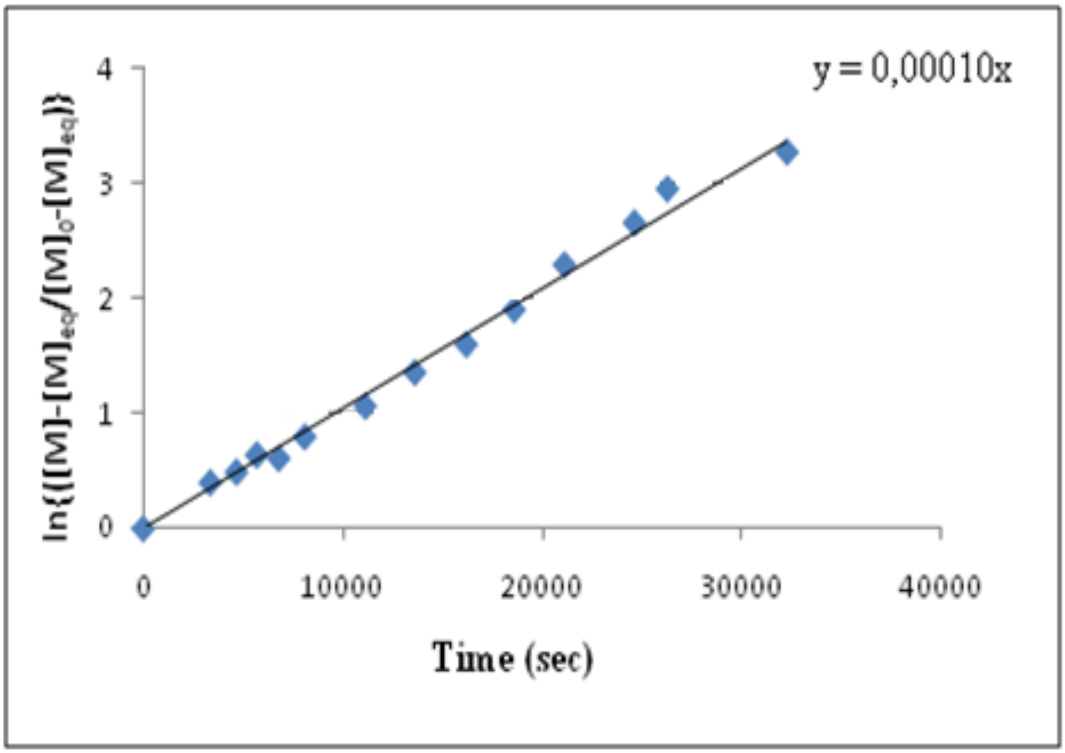

Figure 4.56. The plot of ln(($[M]_0-[M]_{eq}/[M]-[M]_{eq}$)) versus time at 343 K for 5,5-dimethyl-3-(*o*-chlorophenyl)-2-thioxo-4-oxazolidinone

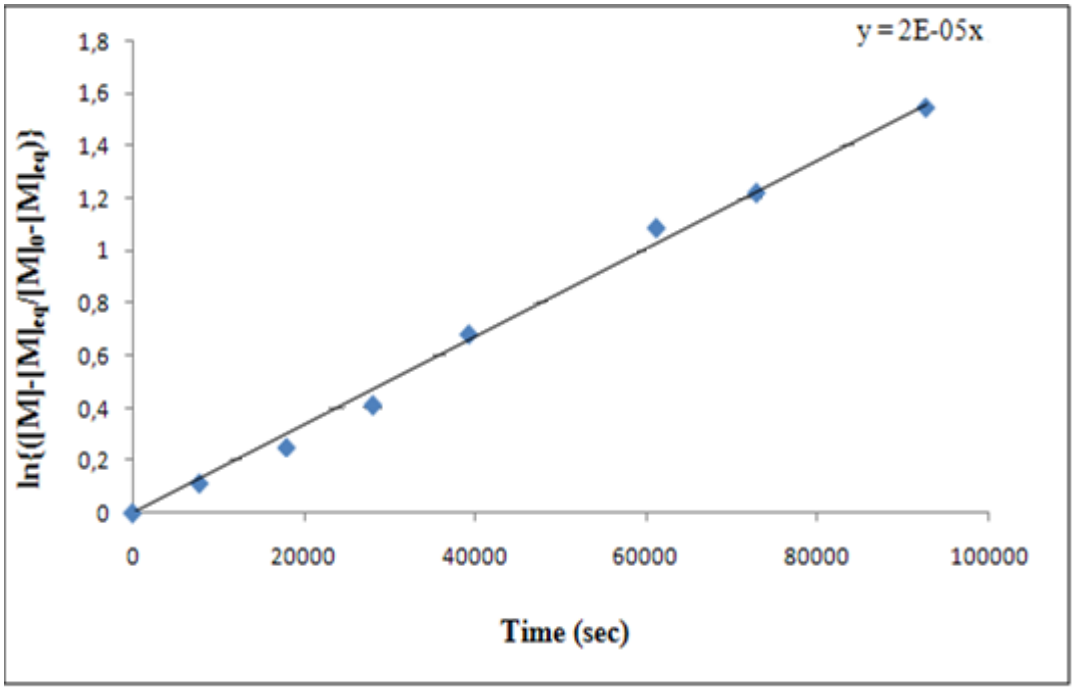

Figure 4.57. The plot of $\ln(([M]_0-[M]_{eq}/[M]-[M]_{eq}))$ versus time at 343K for 5,5-dimethyl-3-(*o*-bromophenyl)-2-thioxo-4-oxazolidinone

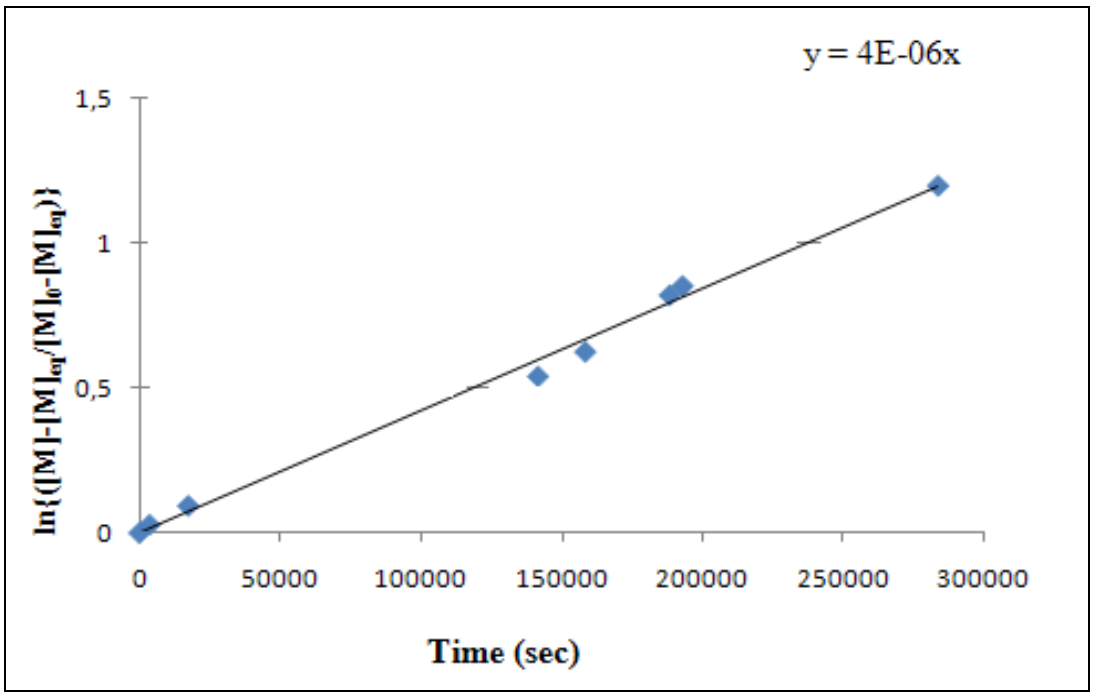

Figure 4.58. The plot of $\ln(([M]_0-[M]_{eq}/[M]-[M]_{eq}))$ versus time at 348K for 5,5-dimethyl-3-(*o*-iodophenyl)-2-thioxo-4-oxazolidinone

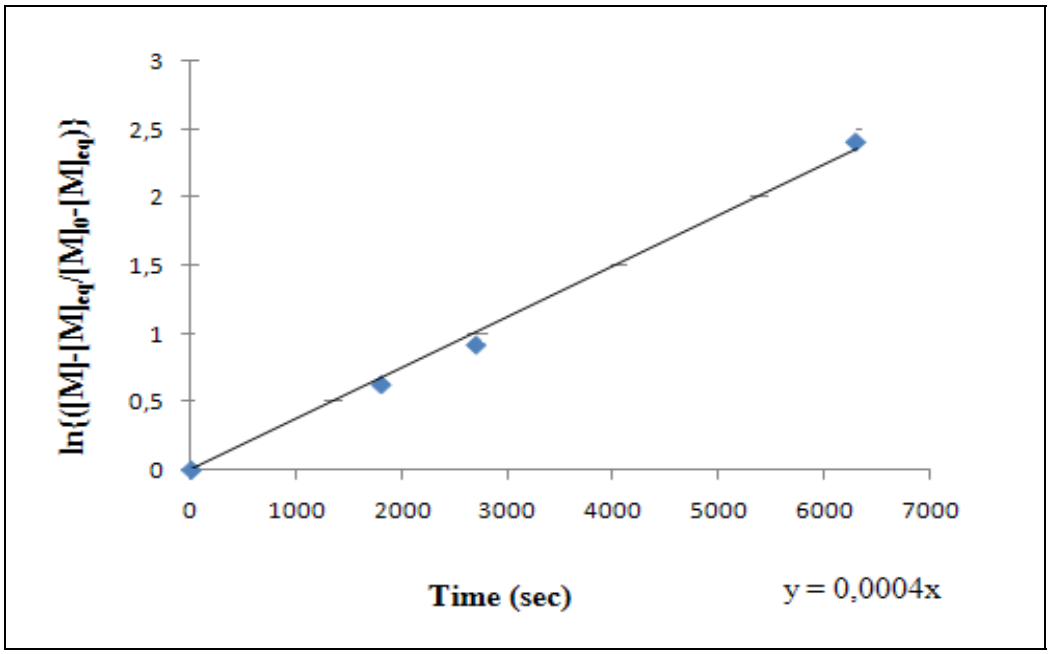

Figure 4.59. The plot of $\ln(([M]_0-[M]_{eq}/[M]-[M]_{eq}))$ versus time at 328K for 5,5-dimethyl-3-(*o*-tolyl)-2-thioxo-4-oxazolidinone

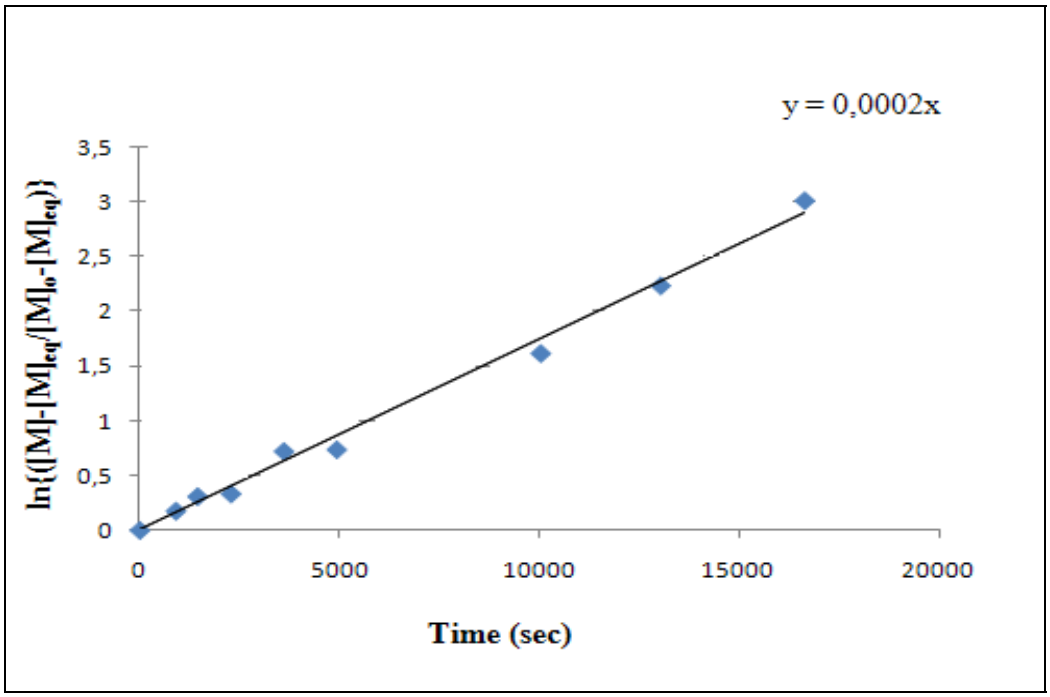

Figure 4.60. The plot of ln(([M]0-[M]eq/[M]-[M]eq)) versus time at 280K for 5,5-dimethyl-3-(o-fluorophenyl)-2-thioxo-4-thiazolidinone

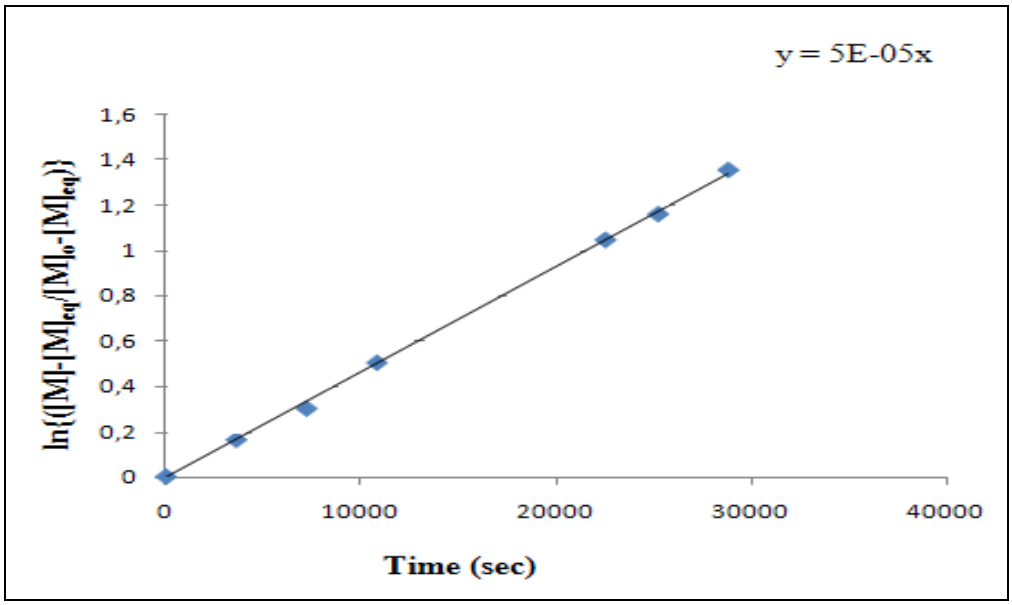

Figure 4.61. The plot of $\ln(([M]_0-[M]_{eq}/[M]-[M]_{eq}))$ versus time at 348 K for 5,5-dimethyl-3-(*o*-chlorophenyl)-2-thioxo-4-thiazolidinone

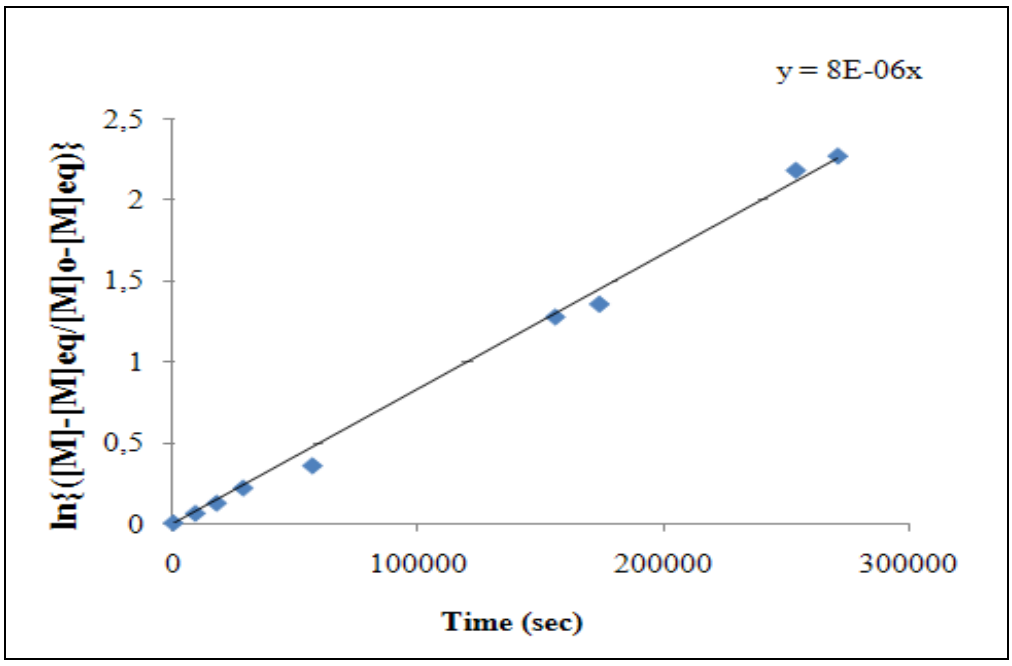

Figure 4.62. The plot of $\ln(([M]_0-[M]_{eq}/[M]-[M]_{eq}))$ versus time at 348K for 5,5-dimethyl-3-(*o*-bromophenyl)-2-thioxo-4-thiazolidinone

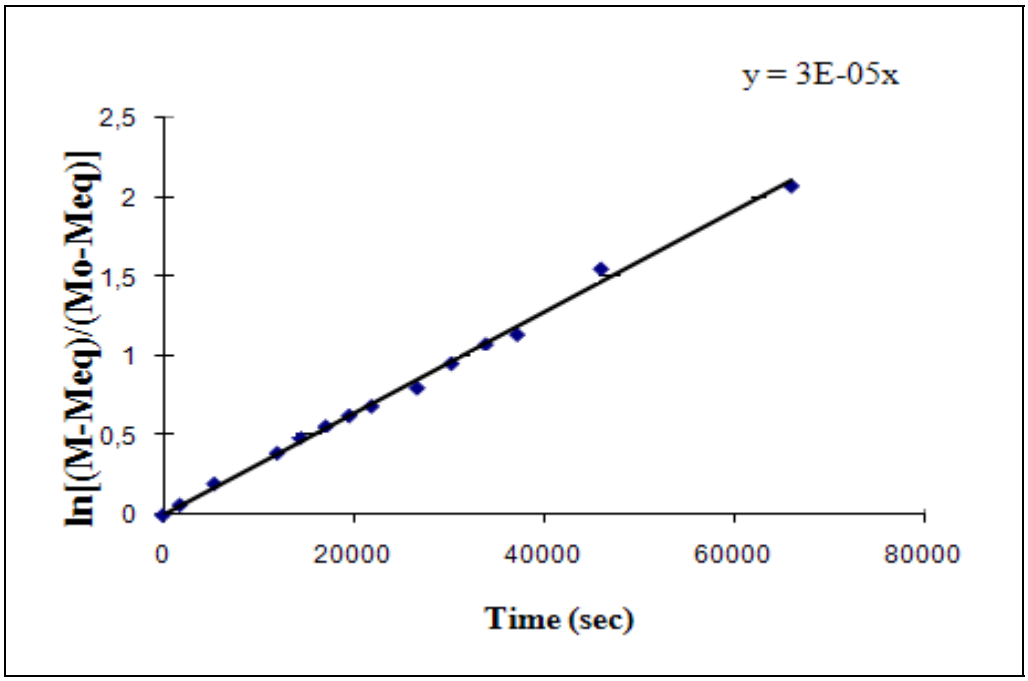

Figure 4.63. The plot of $\ln(([M]_0-[M]_{eq}/[M]-[M]_{eq}))$ versus time at 378 K for 5,5-dimethyl-3-(*o*-iodophenyl)-2-thioxo-4-thiazolidinone

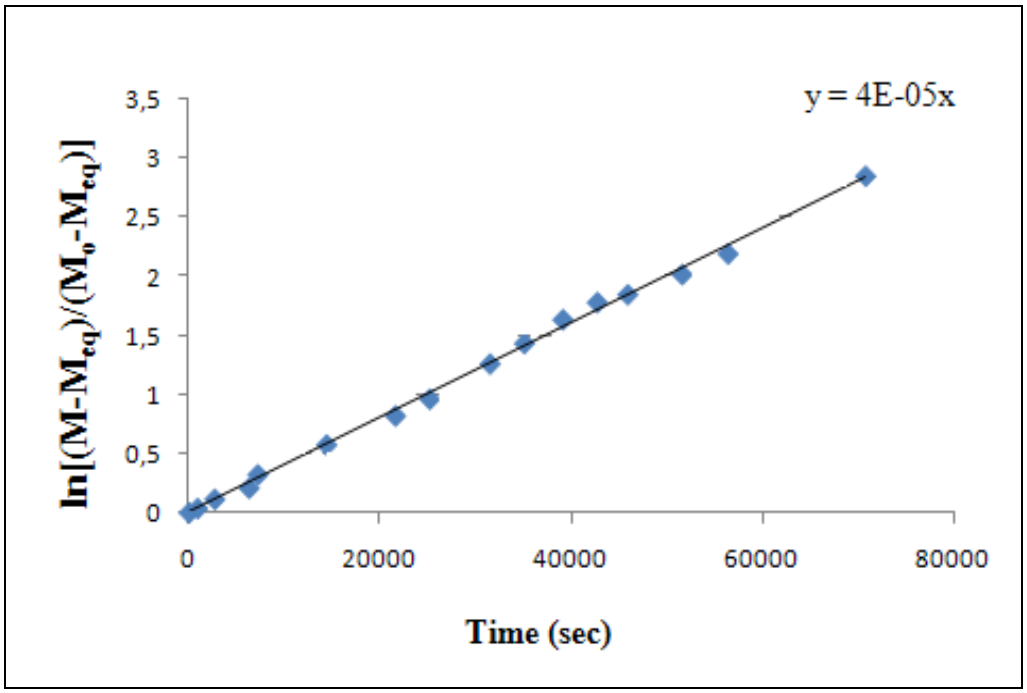

Figure 4.64. The plot of $\ln(([M]_0-[M]_{eq}/[M]-[M]_{eq}))$ versus time at 333 K for 5,5-dimethyl-3-(*o*-tolyl)-2-thioxo-4-thiazolidinone

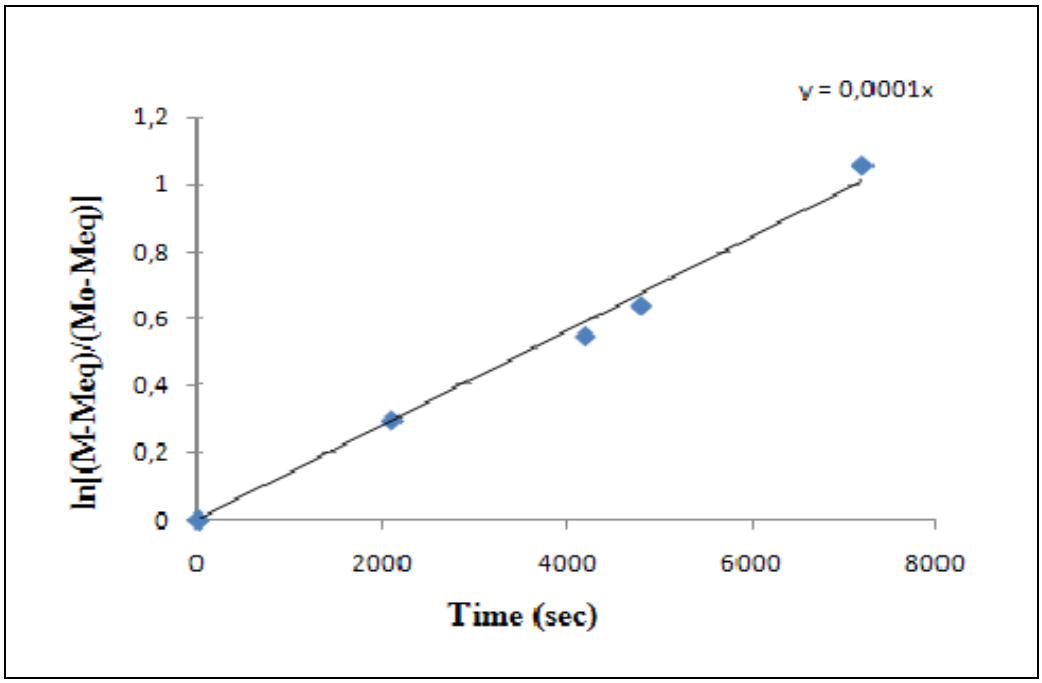

Figure 4.65. The plot of $\ln(([M]_0-[M]_{eq}/[M]-[M]_{eq}))$ versus time at 280 K for 3-(*o*-fluorophenyl)-2-thioxo-4-thiazolidinone

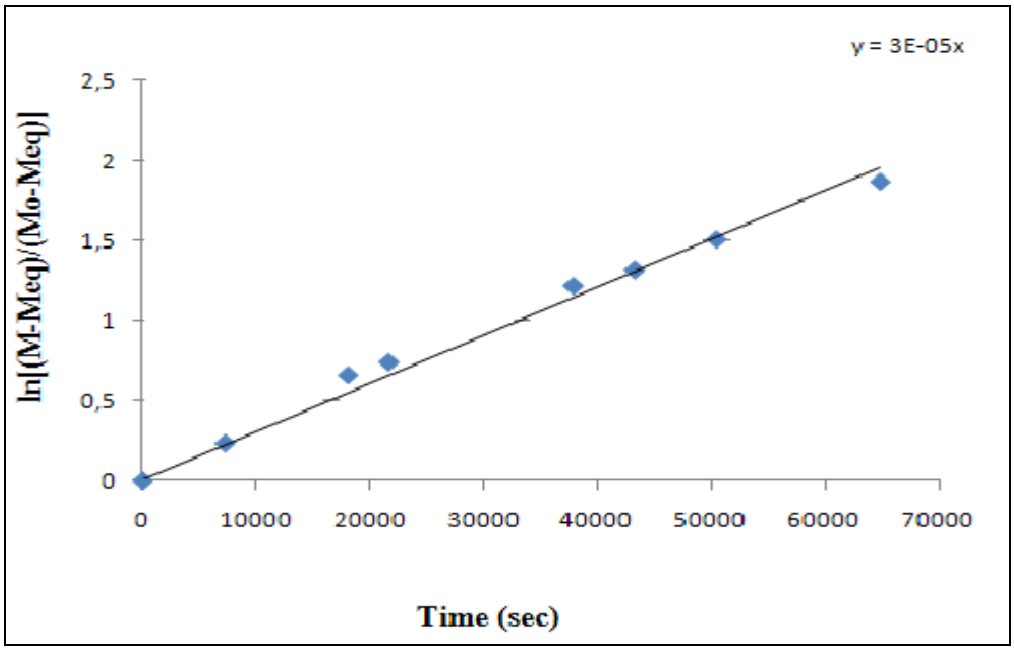

Figure 4.66. The plot of $\ln(([M]_0-[M]_{eq}/[M]-[M]_{eq}))$ versus time at 353 K for 3-(*o*-chlorophenyl)-2-thioxo-4-thiazolidinone

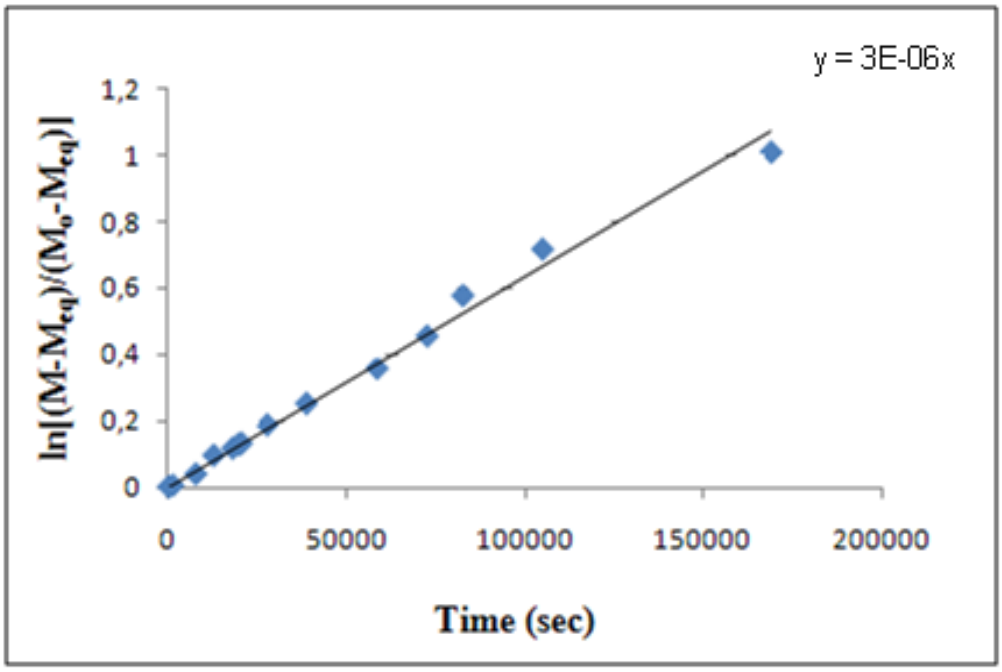

Figure 4.67. The plot of $\ln(([M]_0-[M]_{eq}/[M]-[M]_{eq}))$ versus time at 351 K for 3-(*o*-bromophenyl)-2-thioxo-4-thiazolidinone

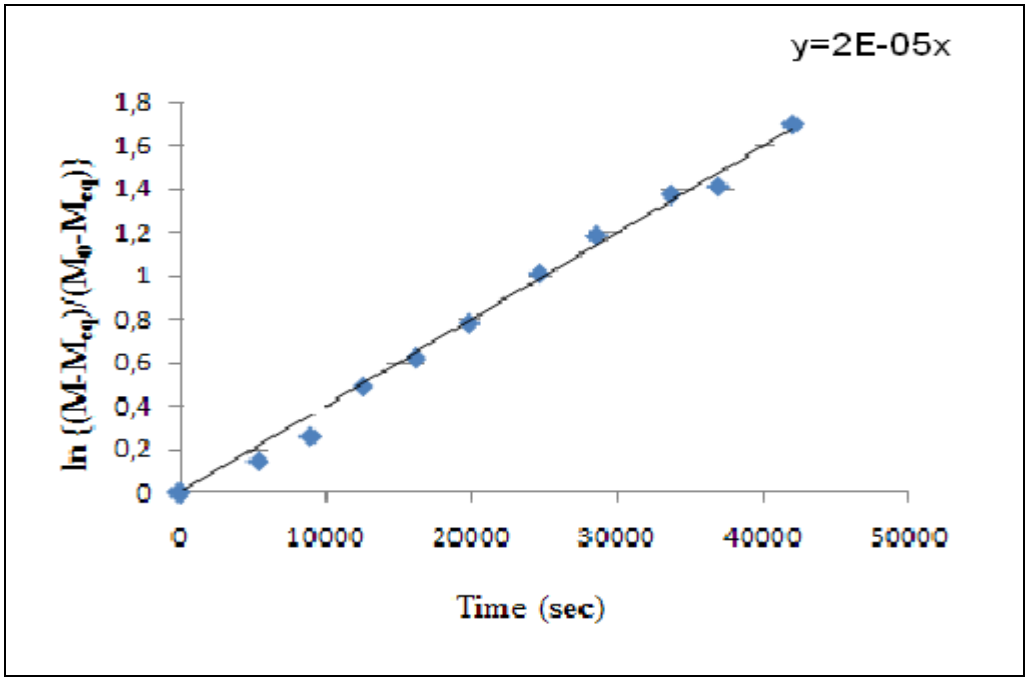

Figure 4.68. The plot of $\ln(([M]_0-[M]_{eq}/[M]-[M]_{eq}))$ versus time at 383K for 3-(*o*-iodo)-2-thioxo-4-thiazolidinone

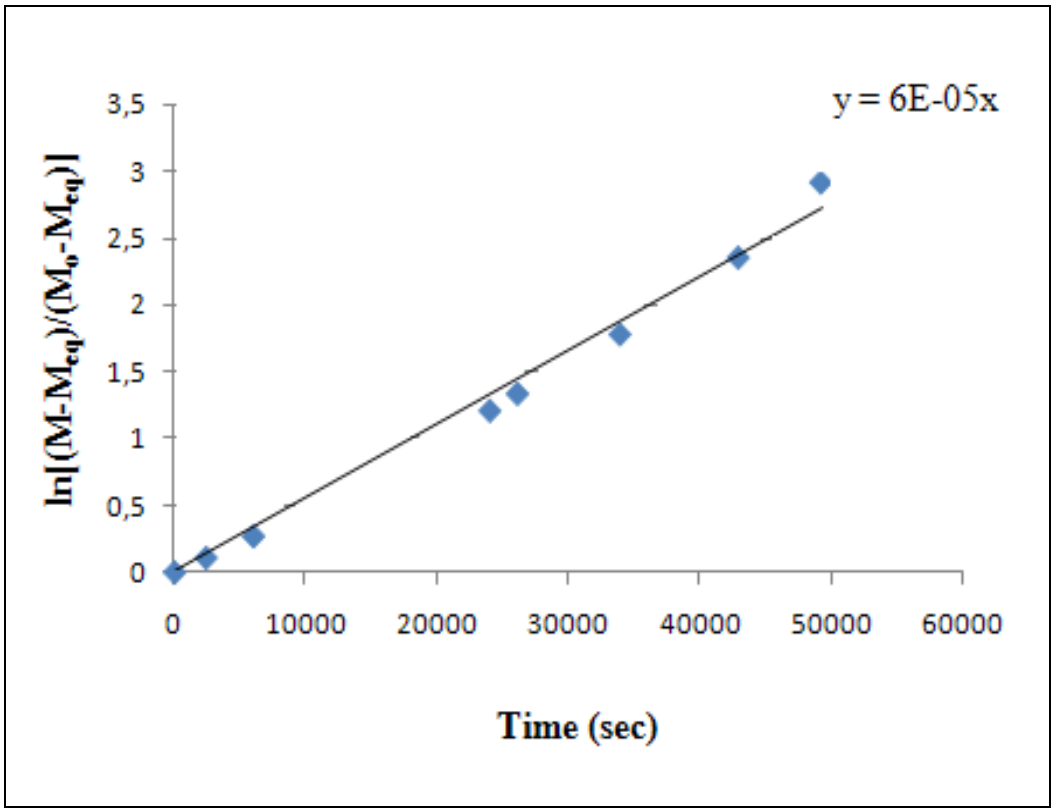

Figure 4.69. The plot of $\ln(([M]_0-[M]_{eq}/[M]-[M]_{eq}))$ versus time at 348K for 3-(*o*-tolyl)-2-thioxo-4-thiazolidinone

Having determined the rate constants for racemization k, the free energy of activations, were calculated using the Eyring Equation (2.13).

$$\Delta G^{\#}=RT\ln(k_b.T/k.h) \qquad (2.13)$$

The energy barriers for racemization for compounds (±)-2-5 are shown in Table 4.7 and for compounds (±)-6-15- in Table 4.8.

Table 4.7. Thermal racemization results of the experiments done by HPLC for compounds (±)-2-5

Compound	Solvent	Eluent	T(K)	$k(s^{-1})$	$\Delta G^{\neq}(Kj/mol^{-1})$
(±)-2	Ethanol	Ethanol:Hexane (5%:95%,v/v)	343 [a]	$5.0.10^{-5,b}$	112.6 ± 0.7^{c}
(±)-3	Ethanol	Ethanol:Hexane (5%:95%,v/v)	343 [a]	$1.0.10^{-5,b}$	117.2 ± 0.7^{c}
(±)-4	Ethanol	Ethanol:Hexane (5%:95%,v/v)	348 [a]	$2.0.10^{-6,b}$	124.0 ± 0.7^{c}
(±)-5	Diglyme Ethanol	Ethanol Ethanol:Hexane (10%:90%,v/v)	330 [a] 328 [a]	$4.6.10^{-4,b}$ $2.0.10^{-4,b}$	104.3 ± 0.2^{c} 103.8 ± 0.7^{c}

[a] The temperature at which the thermal racemization has been done, [b] The rate constant of interconversion between the enantiomers, [c] Free energy of activation determined by resolution-racemization via HPLC

The *ortho*-iodo compounds (±)-9 and (±)-14 could not be racemized at 78 ^{o}C using ethanol as a solvent. The chiralpak IB column enabled the use of toluene as solvent for the racemization of these compounds at 105 ^{o}C and 110 ^{o}C respectively for the determination of activation energies for enantiomeric interconversion. The racemization barriers for these compounds were determined as 128.2 kJ/mole and 129.0 kJ/mole respectively (Table 4.8).

Table 4.8. Thermal racemization results of the experiments done by HPLC for compounds (±)-6-15

Compound	Solvent	Eluent	T(K)	k(s^{-1})	$\Delta G^{\neq}$(kJ/mol^{-1})
(±)-6	Ethanol	Ethanol:Hexane (5%:95%,v/v)	280 [a]	$1.0.10^{-4,b}$	89.8±0.7[c]
(±)-7	Ethanol	Ethanol:Hexane (5%:95%,v/v)	348 [a]	$2.5.10^{-5,b}$	116.3±0.7[c]
(±)-8	Ethanol	Ethanol:Hexane (10%:90%,v/v)	348 [a]	$4.0.10^{-6,b}$	121.6±0.7[c]
(±)-9	Toluene	Ethanol:Hexane (10%:90%,v/v)	378 [a]	$3.0.10^{-5,b}$	128.2±0.7[c]
(±)-10	Diglyme Ethanol	Ethanol Ethanol:Hexane (5%:95%,v/v)	351 [a] 333 [a]	$2.6.10^{-4,b}$ $2.0.10^{-5,b}$	112.6±0.2[c] 111.8±0.7[c]
(±)-11	Ethanol	Ethanol:Hexane (5%:95%,v/v)	280 [a]	$5.0.10^{-5,b}$	91.0±0.7[c]
(±)-12	Diglyme Ethanol	Ethanol Ethanol:Hexane (10%:90%,v/v)	387 [a] 353 [a]	$7.4.10^{-4,b}$ $1.5.10^{-5,b}$	121.2±0.2[c] 119.5±0.7[c]
(±)-13	2-Propanol	2-Propanol:Hexane (10%:90%,v/v)	351 [a]	$3.0.10^{-6,b}$	123.6±0.7[c]
(±)-14	Toluene	Ethanol:Hexane (40%:60%,v/v)	383 [a]	$2.0.10^{-5,b}$	129.0±0.7[c]
(±)-15	Diglyme Ethanol	Ethanol Ethanol:Hexane (5%:95%,v/v)	348 [a] 348 [a]	$1.0.10^{-4,b}$ $3.0.10^{-5,b}$	114.4±0.2[c] 115.8±0.7[c]

[a] The temperature at which the thermal racemization has been done, [b] The rate constant of interconversion between the enantiomers, [c] Free energy of activation determined by resolution-racemization via HPLC

It has been found that, for the halogen series, the barriers showed a remarkable linearity with the van der Waals radii of the halogens (Figure 4.70). So it can be concluded that if the type of interactions between the *ortho* substitutent and the exocyclic groups (C=O and C=S in this case) are similar which is mainly dipolar repulsions in the planar transition state, in this case, the barrier observed is directly proportional to the size of the substitutent. This will make the barriers of the unknown derivatives predictable if two of the barriers in a series have been determined, which will help in the design of o-halo derivatives of desired barrier. The oxazolidine thiones (±)-1-5 have barriers to rotation about 4 kJ/mol lower than that of the corresponding thiazolidine thiones (±)-6-10. The decrease in the bond lenght in going from S-C to O-C should be causing this difference. Comparing the barriers of (±)-6-10 with (±)-11-15 shows that the 5,5-dimethyl subsitution decreases the barriers slightly (about 2 kJ/mol). The energy barriers for compounds (±)-5, (±)-10, (±)-12 and (±)-15 determined in ethanol were found to be 0.5-1.7 kJ/mole larger than those determined in diglyme. Van der Waals radii of several atoms and groups are shown in Table 4.9.

Table 4.9. Van der Waals radii of several atoms and groups

Atom/Group	Van der Waals radii ($^{\circ}$A)
H	1.2
F	1.47
Cl	1.75
Br	1.80
I	1.95
CH_3	2.0
O	1.4
S	1.85

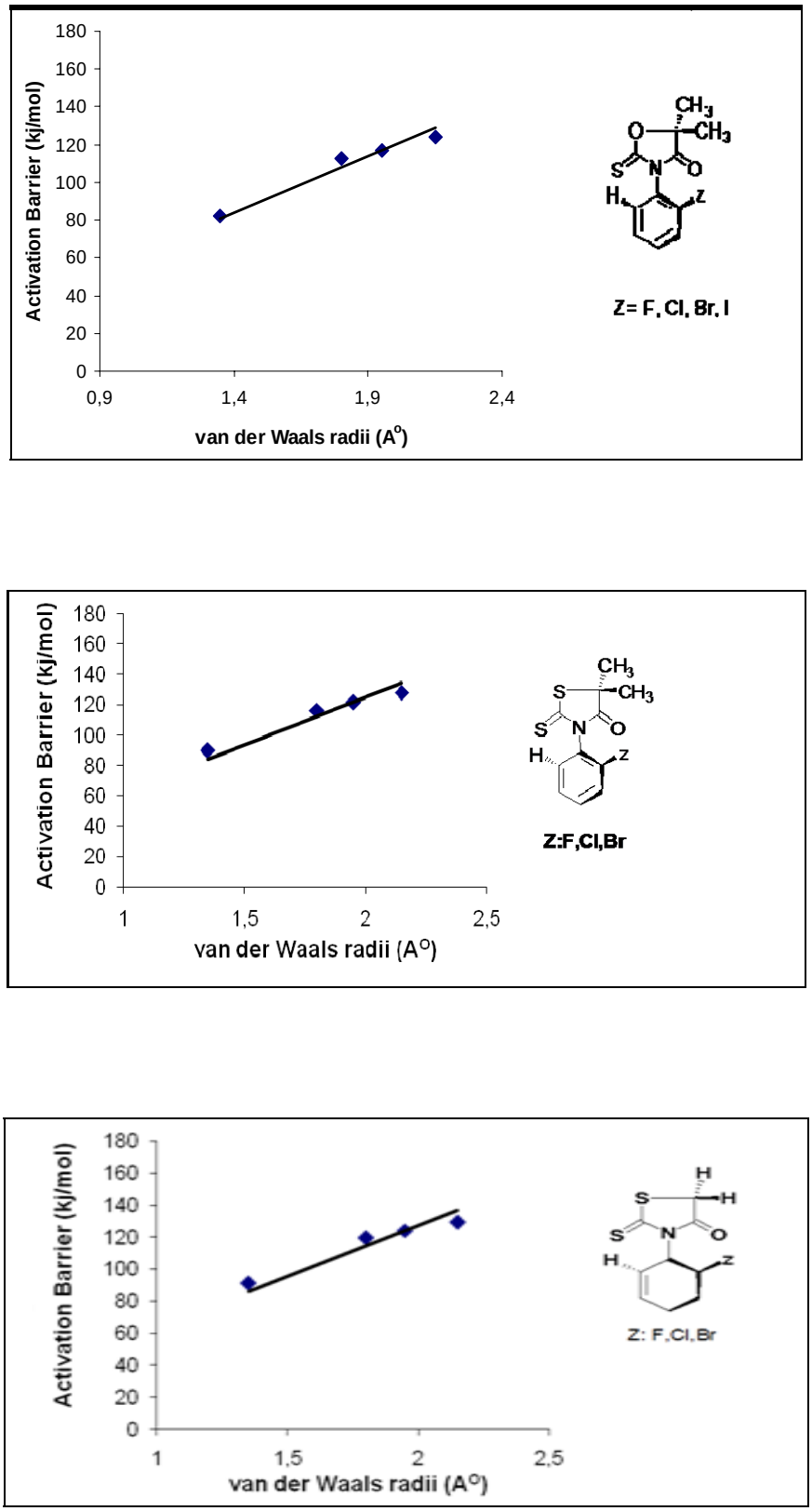

Figure 4.70. The plot of activation barriers versus van der Waals radii of the *o*-substituted halogens for the series of compounds (±)-1-4, (±)-6-9 and (±)-11-14.

The *o*-chloro derivatives were found to have 6-10 kJ/mol larger barriers than the *o*-methyl derivatives despite the smaller size of the chlorine atom with respect to methyl group. When the steric effects of a methyl and a chlorine atom are compared in different types of N-*ortho* aryl substituted heterocyclic systems such as, arylquinolones [44], and aryl 2-iminothiazolidine-4-ones [45], it had been observed that a chlorine atom exerted a greater energy barrier by about 4 kJ/mole than a methyl group in restricted internal rotation. These results were explained by the dipolar repulsions between the exocyclic oxygen of the heterocyclic ring and the chlorine atom which might increase the energy of the transition state of the compound with chlorine atom as ortho substitutent relative to that of the methyl group as *ortho* substitutent. On the other hand for N-aryl-2-(1H)quinolones and N-aryl-6(5H)-phenanthridinones [44] this difference was only 0.2 kJ/mol and for N-*ortho* aryl-2-thiobarbituric acids [46] the barriers for chloro and the methyl derivarives were about the same magnitude. Moreover, in 2,4-quinolidiones [47] the ortho-methyl derivative caused a higher barrier by 0.8 kJ/mol than the *ortho*-chloro derivative. It can be argued that the difference in the steric effects of these two groups is not always predictable because it depends on the geometries of the transition states that the two rings assume in passing one another. Thus the tetrahedral nature of the methyl substitutent may allow, depending on the geometry, a lower or a higher barrier than the spherical chlorine atom.

4.5. Determination of the Activation Barriers for Hindered Rotation by Dynamic NMR

The activation energy for racemization of compound (±)-1, the 5,5-dimethyl-3-(*o*-fluorophenyl)-2-thioxo-4-oxazolidinone, has been determined by a temperature dependent NMR experiment (Figure 4.71).

At the ordinary probe temperature (30 °C) diastereotopic 5,5-dimethyl signals were observed at 1.72 and 1.65 ppm respectively. At higher temperatures, where the rotation became faster, the two singlets slowly came to coalescence (Figure 4.71) from which the first-order rate constant for the interconversion of the M and P enantiomers has been determined and substitution of the rate constant in the Eyring equation gave the $\Delta G^{\neq}$ value [48]. The activation energy values determined by temperature dependent ^{1}H NMR in DMSO-d_6 was 3 kJ/mol higher (82 kJ/mol) than the one determined in toluene-d_8 (79

kJ/mol). The temperature dependent ^{1}H NMR spectrum of compound (±)-1 in toluene-d_8 are shown in Figure 4.72.

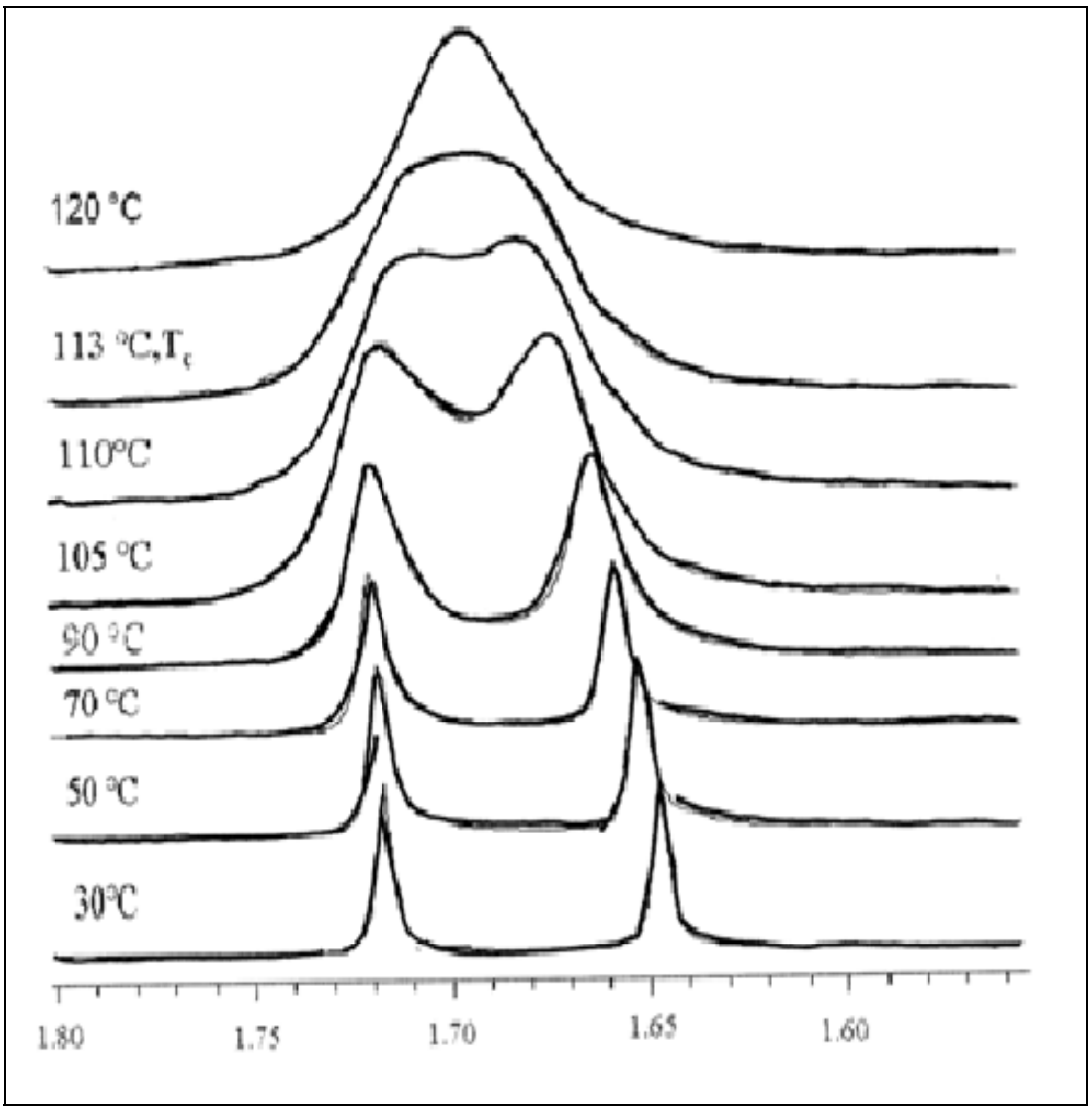

Figure 4.71. Temperature dependent ^{1}H NMR spectra of the diastereotopic C-5 methyl groups of compound (±)-1 in DMSO-d_6

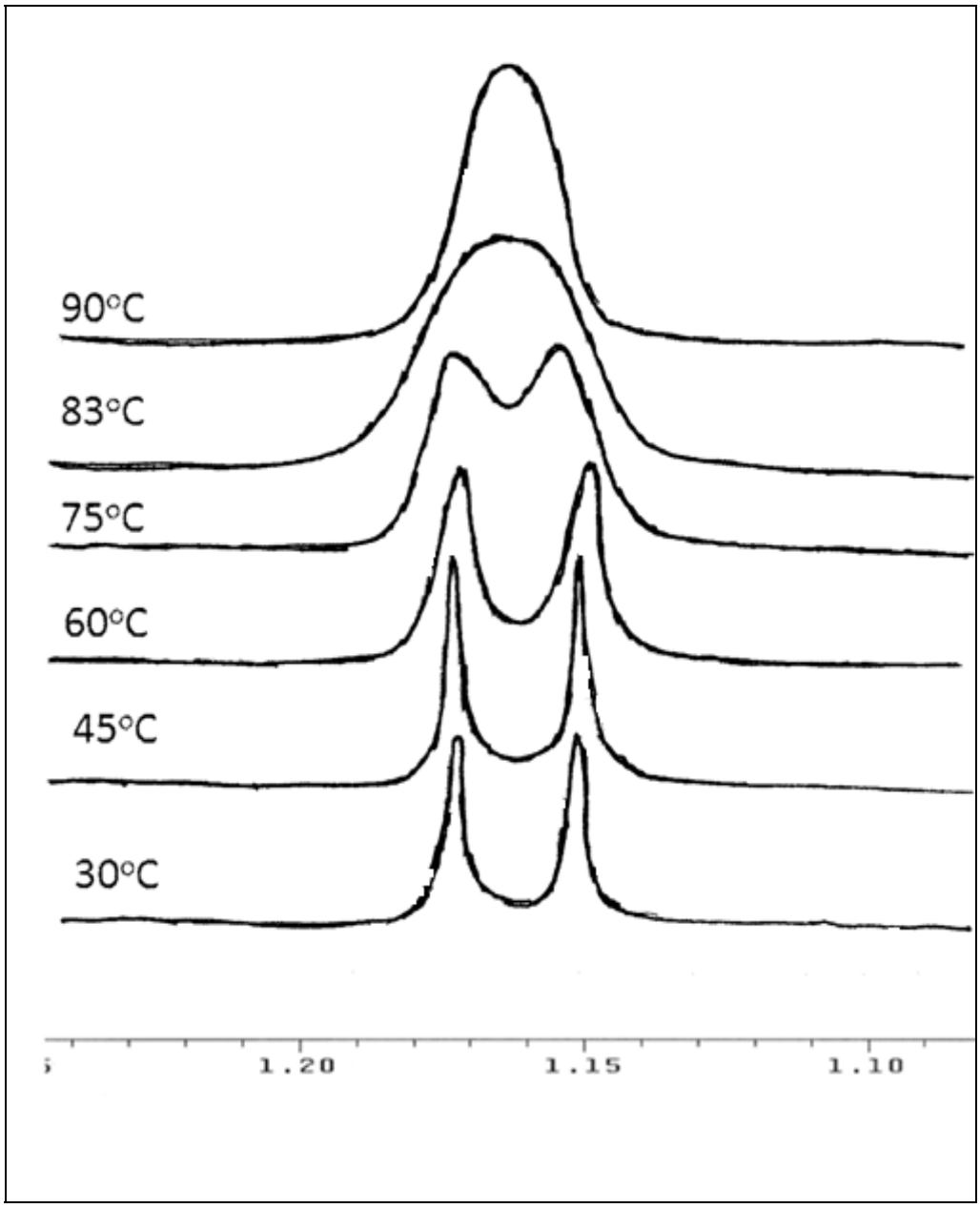

Figure 4.72. Temperature dependent ^{1}H NMR spectra of the diastereotopic C-5 methyl groups of compound (±)-1 in Toluene-d_8

4.6. Determination of the Absolute Stereochemistry of Heterocyclic compounds Bearing a Naphthyl Substitutent

4.6.1. ^{1}H and ^{13}C NMR Spectra of the compounds in the Presence of the Optically Active Auxiliary

In this study, (S)-(+)-1-(9-anthryl)-2,2,2-triflouroethanol ((S)-TFAE) was used as the chiral auxiliary compound (Figure 4.73) [49].

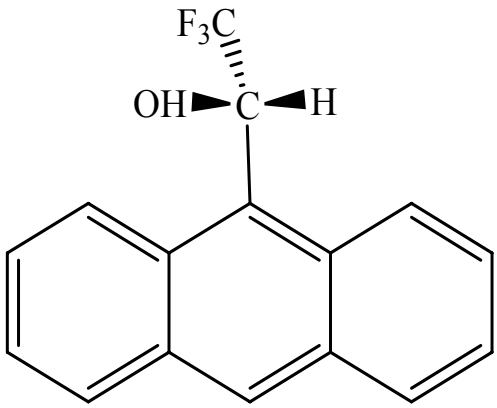

Figure 4.73. The structure of (S)-(+)-1-(9-anthryl)-2,2,2-triflouroethanol, (S)-TFAE

It was expected that in the presence of the optically active auxiliary each enantiomer of compounds (±)-16 and (±)-17 (Figure 4.74) would associate with auxiliary compound and form two diastereomeric NMR distinquisable complexes in solution.

A close contact between the solute and chiral auxiliary molecule is expected as a result of a strong intermolecular hydrogen bonding and π-π interactions between the napthyl substitutent of the compounds studied and anthryl group of chiral auxiliary.

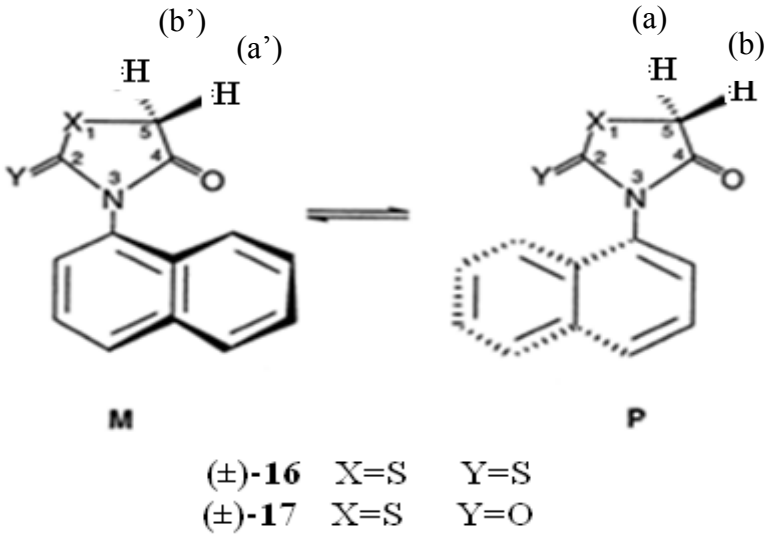

Figure 4.74. The structrure of the compounds studied

Herein, the naphthyl bearing heterocyclic compounds exist as two enantiomeric M and P atropisomers which exhibit identical NMR spectra in an achiral solvent. However, due to the hindered rotation around the C-N single bond, C-5 methylene protons of 3-(α-napthyl)-2-thioxo-4-thiazolidinone and 3-(α-napthyl)-2,4-thiazolidinedione are diastereotopically related (denoted by a, b, a', and b' in Figure 4.74) and should have unequal chemical shifts if the barrier to rotation is slow on the NMR time scale. Analysis of the ^{1}H NMR spectra of these compounds did show these magnetically non-equivalent protons (Table 4.10).

Table 4.10. ^{1}H NMR spectroscopic data for the studied compounds in the presence and absence of the optically active auxiliary, (S)-TFAE at 30 ºC

Compound No	Medium	^{1}H NMR, C-5 protons (ppm)
(±)-16	Toluene-d_8	3.04 and 2.97
	Toluene-d_8+(S)-TFAE[a]	2.88, 2.86, 2.79
(±)-17	Toluene-d_8	3.08 and 3.02
	Toluene-d_8+(S)-TFAE[a]	3.08, 3.06, 2.99, 2.98

[a] 1:6 equivalent of (S)-TFAE were used

The protons at C-5 of 3-(α-naphthyl)-2-thioxo-4-thiazolidinone and 3-(α-naphthyl)-2,4-thiazolidinedione showed AB type splittings, the chemical shift differences being equal to 0.07 ppm and 0.06 ppm, respectively.

The C-5 methylene protons of 3-(α-naphthyl)-2,4-thiazolidinedione (±)-17, were differentiated in the presence of (S)-TFAE with a chemical shift difference of 0.01 to 0.02 ppm (Figure 4.75 B). On the other hand, the upfield AB splittings of 3-(α-naphthyl)-2-thioxo-4-thiazolidinone(±)-16 could not be resolved completely (Figure 4.75 A).

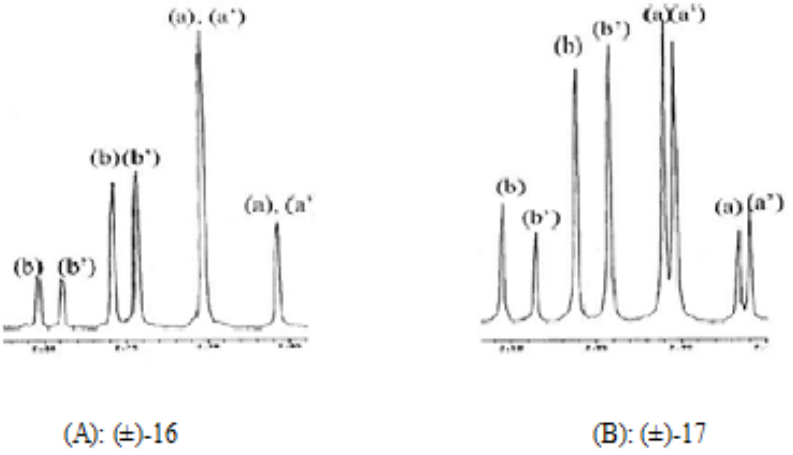

Figure 4.75. The ^{1}H NMR spectra of the compounds taken in the presence of 6 equivalent of (S)-TFAE in toluene-d_8,(A)= compound (±)-16, (B)= compound (±)-17

4.6.2. Determination of Absolute Stereochemistry

The N-*ortho*-methylphenyl substituted oxazolidinedione, thiazolidinedione and rhodanine enantiomers have been shown [50] to form association complexes with the optically active auxiliary (S)-TFAE, which led to the differentiation of the enantiomers and absolute conformation assignments. The NMR spectra of the N-naphthyl substituted derivatives in the presence of (S)-TFAE showed a strong temperature dependence which pointed to additional interactions (probably π-π interactions) with the auxiliary. Therefore the N-naphthyl substituted compounds have been studied in some more detail.

In order to obtain a solvation model for 3-(α-naphthyl)-2-thioxo-4-thiazolidinone and 3-(α-naphthyl)-2,4-thiazolidinedione, all ^{1}H NMR signals of pure (S)-TFAE and each of the racemates were compared with those of the diastereomeric association complex.

It was observed that for all of the signals of (S)-TFAE-enantiomer complexes of compounds (±)-16-17 (Figure 4.74) were shielded with respect to the corresponding pure compounds. On the other hand, a downfield shift observed for the hydroxyl proton was thought to result from hydrogen bonding with the racemates [51]. These observed upfield shifts and the downfield shift increased with decreasing temperature [52]. The upfield changes in chemical shifts observed for the aromatic naphthyl and anthryl groups may arise from ring current effects and suggest a face-to-face π stacked geometry [53-54].

The diastereomeric association complexes were thought to form in the following way: The hydroxyl group of (S)-TFAE formed a hydrogen bond with the carbonyl or thiocarbonyl groups of the enantiomers: the carbinyl hydrogen of (S)-TFAE involved in hydrogen bonding with the sulphur atom of the heterocycle ring forming a chealate-like structure and the anthryl group of (S)-TFAE formed a π-π interaction with the naphthyl substitutent of the enantiomes (Figure 4.76, model A and C).

As can be seen in Figure 4.76, during the interaction of the racemates with (S)-TFAE, two more solvation models (B and D in Figure 4.76) are possible for both conformers.

In our basic models (A and C in Figure. 4.76) (S)-TFAE forms a chelate via a hydrogen bond between the C–H proton of the (S)-TFAE and the ring sulphur atom and a hydrogen bond between the –OH group of the (S)-TFAE and the –C=S or –C=O on C-2. However, a π-π interaction would also be possible between the anthryl and the naphthyl rings, thus destroying the chelate structure without cleavage of the hydrogen bonding with the C-2 thiocarbonyl group.

In the models B and D (Figure 4.76), $anthryl_2$ can not approach the naphthyl due to the presence of $anthryl_3$ and the weak basicity of the naphthyl. Therefore, either carbinyl hydrogen bonding (A and C) or π-π interaction (B and D) should be preferred at a given

time, one being more populated than the other. The models B and D were thought to be less populated than the models A and C since they have less interactions. Compared to model D, model B would be even less populated due to the weaker π-π interaction.

Therefore, it was thought that model B may have little or no effect on the observed chemical shifts. The observed ^{1}H NMR signals should be consistent with the time-averaged populations of these solvates.

In order to assign the pairs (a–b or a'–b') (Figure 4.74) corresponding to the signals of the diastereotopic methylene protons, the second eluted enantiomers of 3-(α-napthyl)-2-thioxo-4-thiazolidinone resolved by HPLC on a Chiralpak AD-H was added into a toluene-d_8 solution containing racemic compound and (S)-TFAE. It was observed in NMR that the intensity of the signals belonging to this enantiomer, which were the more shielded of the C-5 methylene proton signals increased. Thus, the more shielded signals of the enantiomeric pair belonged to the second eluted enantiomer.

The assignments of the AB peaks observed in the presence of (S)-TFAE to the four methylene groups for compounds (±)-16-17 (Figure 4.75) as a, a', b, b' has been done in the following way: It is known from our previous work [50] that the C-5 substitutent that is syn with the N-naphthyl group appears relatively more shielded compared to the C-5 substitutent which is anti with it. Thus, protons (a) and (a') were both affected by the shielding zone of the naphthyl group, giving the signals in the upfield region compared to (b), (b'). Additionally, proton (a) of the P conformer was affected by the shielding zones of anthryl$_3$ (Figure 4.76 model D) and anthryl$_1$ (Figure 4.76, model C), whereas the proton (a') was shielded by the anthryl$_2$ (Figure 4.76, model A). Anthryl$_2$ should be closer to proton (a') than it is to proton (a) because the M conformation could form a tighter complex (two fused benzene rings interact) than the P conformer. Therefore (a') appears more shielded than (a) proton.

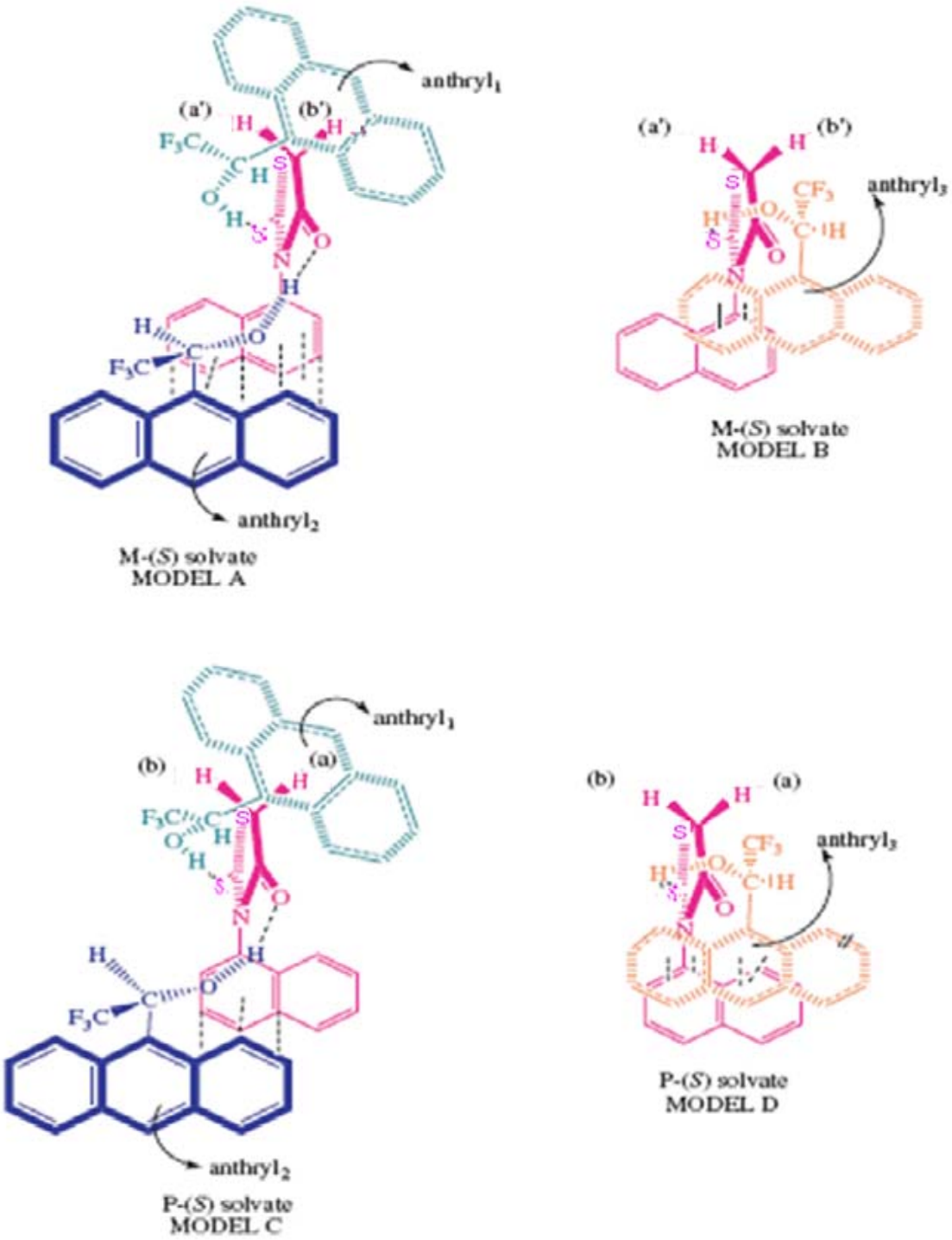

Figure 4.76. The proposed solvation models for the M and P enantiomers of studied compounds

Protons (b) and (b') were not affected by the naphthyl ring (Figure 4.76). Proton (b) is shielded by either anthryl$_2$ (Figure 4.76, model C) or by antryl$_3$ (Figure 4.76, model D),

depending upon the average lifetimes of models C and D (Figure 4.76) at a given temperature whereas the proton (b') was always affected by $anthryl_1$ (Figure 4.76, model A). Since (b') experiences a stronger shielding effect than proton (b) of the P conformer it appeared more shielded than b. Therefore it can be argued that for all the compounds studied, in the presence of (S)-TFAE the more shielded of the diastereotopic C-5 methylene protons (Figure 4.75) can be assigned to the complexed M conformer and the more deshielded to complexed P (Figure 4.75). Thus, the second eluted enantiomers of 3-(α-napthyl)-2-thioxo-4-thiazolidinone, (±)-16 and 3-(α-napthyl)-2,4-thiazolidinedione, (±)-17, have been assigned to M conformation.

Upon cooling, the signals of C-5 methylene protons of compounds 3-(α-naphthyl)-2-thioxo-4-thiazolidinone and 3-(α-naphthyl)-2,4-thiazolidinedione experienced upfield shifts, the relative magnitudes of the upfield shifts were in the following order: (b') > (a') > (a) > (b). The fact that the aromatic protons of the naphthyl and the anthryl rings were more shielded and the hydroxyl proton was more deshielded compared to the values at 30 ºC, pointed that all of the intermolecular interactions were getting stronger upon cooling. This result may be attributed to the slower rotation of the molecules at lower temperatures. The conformation might even have been frozen at -70 ºC (Figure 4.77 and Figure 4.78). For example, the aromatic groups of the enantiomers and (S)-TFAE could be positioned parallel to each other enhancing the intermolecular interactions. In compounds (±)-16 and (±)-17 as the temperature was lowered, the change in the chemical shift values of proton (b') of the M conformer was the most affected one and was strongly shielded. This is explained by the greater influence of model A at lower temperature.

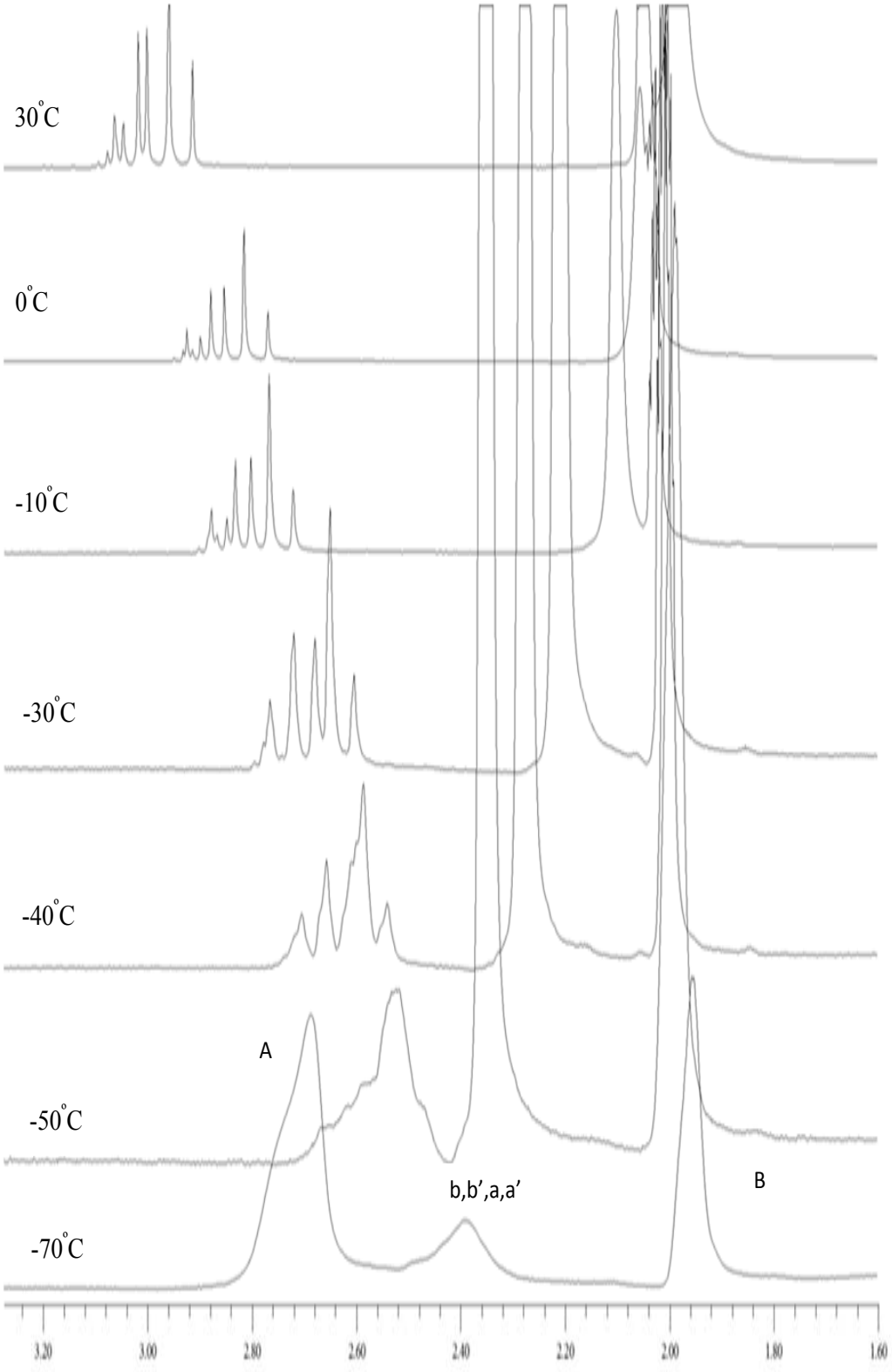

Figure.4.77. The temperature dependence of the ^{1}H NMR signals of the methylene groups on C-5 of the compound (±)-16 upon cooling from 30 to -70 ºC, A: Antryl hydroxyl hydrogen, B: Solvent

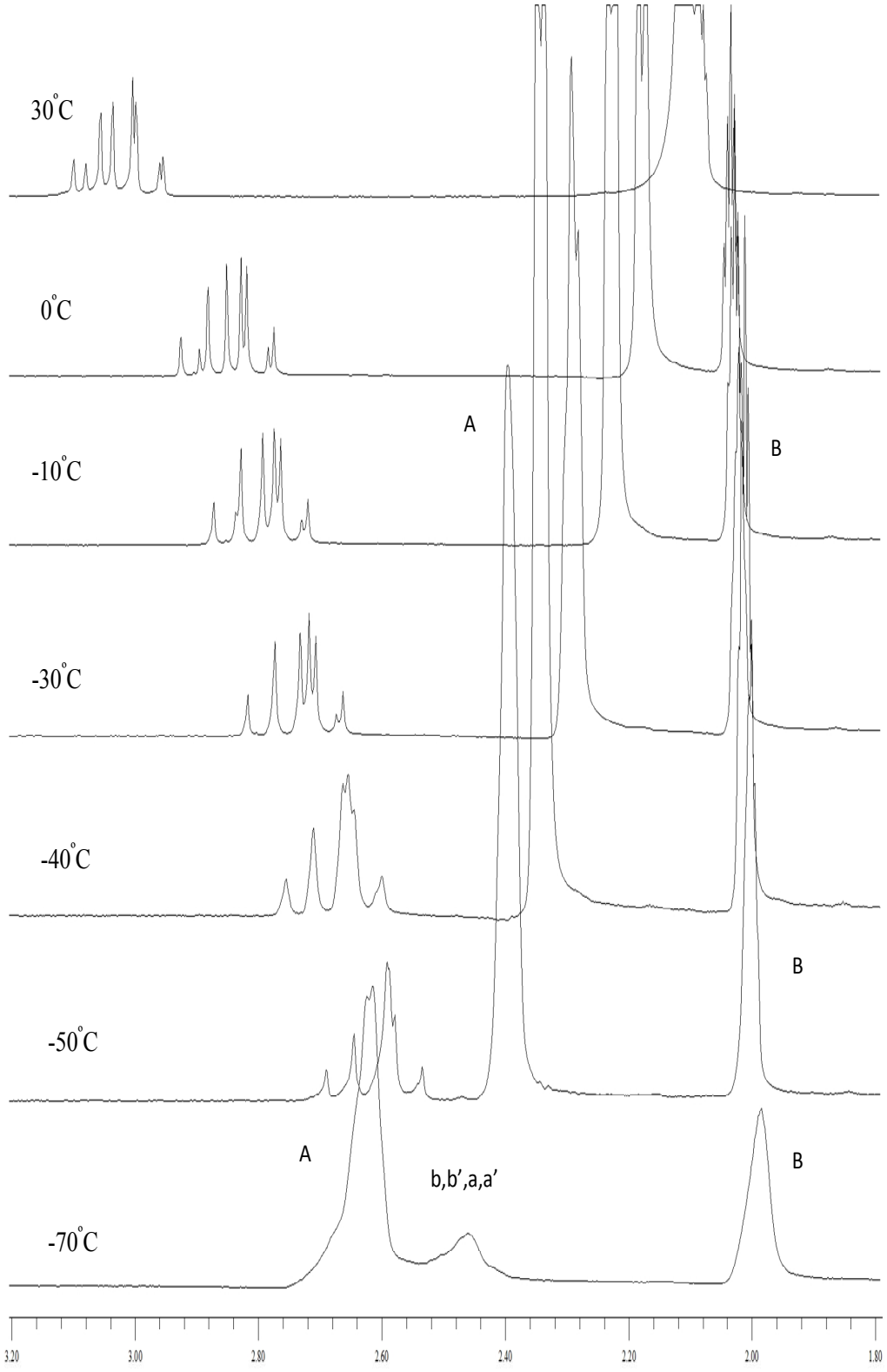

Figure.4.78. The temperature dependence of the ^{1}H NMR signals of the methylene groups on C-5 of the compound (±)-17 upon cooling from 30 to -70 ºC, A: Antryl hydroxyl hydrogen, B: Solvent

4.6.3. Determination of Activation Barriers to Hindered Rotation

Activation barriers to the hindered rotation of the compounds (±)-16-17 were determined by enantioresolution on a chiral sorbent via HPLC.

Enantioresolution of the racemic mixtures was done on Chiralpak AD-H column packed with amylose tris-(3,5-dimethyl)-carbamate as chiral stationary phase with 254 nm UV detection. To obtain a better resolution of the enantiomers, all chromatographic separations were conducted at 7 ± 2 ºC.

The activation parameters of compounds (±)-16 and (±)-17 are listed in Table 4.11. Data pertinent to the chromatographic separations of the enantiomers on Chiralpak AD-H are shown in Table 4.12.

Table 4.11. The Kinetic and Thermodynamic data for the Interconversion Process

Compound No	Solvent	T,K	k,s^{-1}	$\Delta G^{\neq}$,kJ/mol
(±)-16	Ethanol:Hexane (50%:50%,v/v)	351[a]	2.10-4[b]	111.3±0.07[c]
(±)-17	Ethanol:Hexane (70%:30%,v/v)	323[a]	5.10-5[b]	105.9±0.07[c]

[a] The temperature at which the thermal racemization has been done,
[b] The rate constant of interconversion,
[c] Free energy of activation determined by HPLC

Table 4.12. Chromatographic parameters for the separation of enantiomers by HPLC on Chiralpak AD-H at 7±2 °C

Compound No	Eluent composition	Retention times t_1,t_2,min	Capacity factors, k_1,k_2	Selectivity, $\alpha = k_1 / k_2$	Flow rate,ml/min
(±)-16	Ethanol:Hexane (50%:50%,v/v)	16.56 22.86	1.86 2.94	1.58	0.5
(±)-17	Ethanol:Hexane (70%:30%,v/v)	17.54 20.54	2.02 2.54	1.26	0.5

The barrier of compound (±)-16 was found to be higher than that of compound (±)-17. This difference was interpreted by means of the longer standart bond lenght of the C=S double bond (1.71 Å) than that of the C=O (1.22 Å) and the larger van der Waals radius of sulfur (1.85 Å) than that of the oxygen atom (1.40 Å).

In compound (±)-16 the repulsion between the thiocarbonyl sulpfur atom and the peri hydrogen of naphthyl group in the transition state serves as a steric impediment to the enantiomer interconversion and makes the passage of the peri hydrogen more difficult, which in turn, increases the barrier to hindered rotation.

Comparision of the energy barriers of compounds (±)-16 and (±)-17 with the oxazolidinone derivatives (Figure 4.79) revealed the influence of presence of sulphur atom at C-2 or at C-1 on the hindered rotation [49]. Compound (±)-16 showed a barrier greater than compounds (±)-18, (±)-19 and (±)-20 (Figure 4.79). Also, the barrier of compound (±)-17 was found to be higher than the compound (±)-20. This difference in activation barriers can be explained by considering the standart bond lenghts of C-S (1.82 Å), C-O (1.43 Å) single bond and bond lenght of C=S (1.71 Å), C=O (1.22 Å) and the larger van der Waals radius of the sulphur (1.85 Å) than the oxygen atom (1.71 Å) compared with (±)-20 [50]. Owing to the larger bond lenght of C-S, the C-2 carbonyl group of compound (±)-17 is closer to the peri hydrogen of the naphthyl substitutent in the transition state,

giving rise to an enantiomeric pair of M and P atropisomers with higher activation barriers for interconversion (106 kJ/mol vs. 104 kJ/mol).

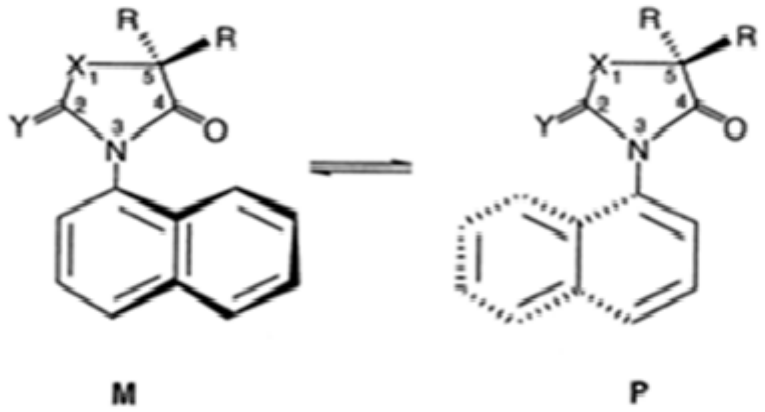

(±)-18	X=O	Y=S	R=CH_3	$\Delta G^{\neq}$=109.9 kJ/mol
(±)-19	X=O	Y=O	R=CH_3	$\Delta G^{\neq}$=85.01 kJ/mol
(±)-20	X=O	Y=O	R=H	$\Delta G^{\neq}$=103.8 kJ/mol

Figure 4.79. The general structure of the 5,5-dimethyl-3-(α-naphthyl)-2-thioxo-4-oxazolidinone, 5,5-dimethyl-3-(α-naphthyl)-2,4-oxazolidinedione and 3-(α-naphthyl)-2,4-oxazolidinedione

4.7. Enantiodifferentiation of 3-Aryl-2-Thioxo-4-Oxazolidinones and Rhodanines by Applying the Dirhodium Method

Enantiodifferentiation of 3-aryl-2-thioxo-4-oxazolidinones, compounds (±)-1-5 (Figure 4.80), and 3-aryl-2-thioxo-4-thiazolidinones, compounds (±)-11-15 (Figure 4.80), was studied by applying dirhodium method using a dirhodium tetracarboxylate complex. For this study, the enantioresolutions have been done in our labaratory by HPLC on a semipreparative Chiralpak AD-H column. The NMR spectra in the presence of the Rh^* auxiliary have been recorded in Germany [55]. It has been shown that the enantiomers of chiral soft-base ligands which are defined as large ligands having low polarizability and electronegativity, such as amides, esters, ketones, and sulfoxides, can easily be differentiated by adding an equimolar amount of the Rh_2^{II} [(R)-(1)-MTPA]4 ([Rh*], MTPA-H 5 methoxytrifluoromethylphenylacetic acid: Mosher's acid in Figure 4.80) to

their $CDCl_3$ solution and monitoring the diastereomeric dispersion $\Delta\upsilon$ of their ^{1}HNMR signals (or other nuclei) at room temperature. The ligating atom or group can be identified by a deshielding of that atom or other nuclei close-by as compared with the respective chemical shifts of the free ligand (complexation shift $\Delta\delta > 0$), particularly for ^{13}C nuclei.

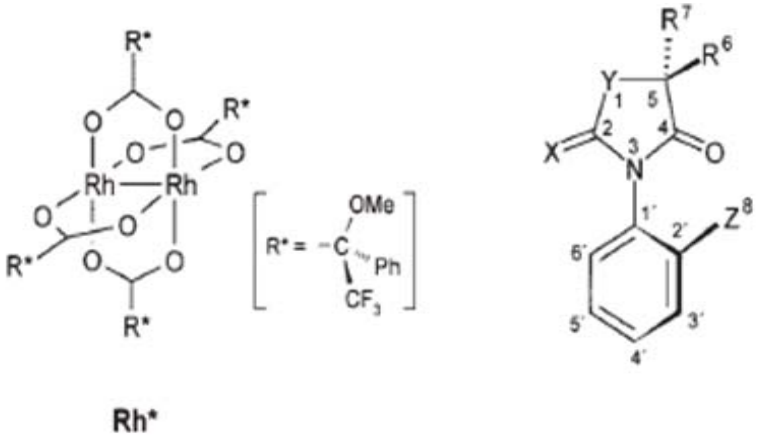

Compound No	X	Y	Z	R
(±)-1	S	O	F	CH_3
(±)-2	S	O	Cl	CH_3
(±)-3	S	O	Br	CH_3
(±)-4	S	O	I	CH_3
(±)-5	S	O	CH_3	CH_3
(±)-11	S	S	F	H
(±)-12	S	S	Cl	H
(±)-13	S	S	Br	H
(±)-14	S	S	I	H
(±)-15	S	S	CH_3	H

Figure 4.80. Structure of Rh_2^{II} [(R)-(+)-MTPA]$_4$ ([Rh* methoxytrifluoromethylphenylacetic acid : Mosher's acid) and the studied compounds

Separation of the enantiomers of compounds (±)-2-5 and compounds (±)-12, (±)-14-15 was performed by HPLC using a semipreparative Chiralpak AD-H column. Enantiomers coded by 'a' are eluted first and followed by 'b' enantiomers. The eluent was hexane:ethanol (95:5). For NMR measurements, nonracemic mixtures were prepared from enantiomerically pure samples, enantiomer a always being the major component (a:b , 2:1).

4.7.1. Complexation Shifts and Chiral Discrimination of the Compounds Studied

All compounds studied showed significant complexation shifts, $\Delta\delta$, of their ^{1}H and ^{13}C signals when the ligand molecules are mixed with an equimolar amount of Rh*; positive values indicate deshielding. Moreover, many of those signals are split, indicating diastereomeric adducts. Note that all adducts have a short life-time relative to the NMR time-scale so that NMR signals are always averaged over those in the free ligand and the adduct(s). Furthermore, none of the *ortho* aryl substituents is significantly involved in Rh* ligation in the presence of the C=S groups. An inspection of the data in Tables 4.13–4.14 reveals the following trends.

In the compounds (±)-1-5 and (±)-11-15, where the sulphur atoms act as quite strong binding sites, dispersion effects $\Delta\upsilon(^{1}H)$ and $\Delta\upsilon(^{13}C)$ of up to 28 and 13 Hz, respectively, can be observed, and enantiodifferentiation can be performed easily.

The presence or absence of the geminal methyl groups as no significant effect on $\Delta\upsilon$-magnitudes when compounds (±)-1-5 are compared with the corresponding ones of compounds (±)-11-15; the change from C-O in (±)-1-5 to C-S in (±)-11-15 seems to have no effect either. This indicates that the conformational equilibria within the adducts are similar for each *ortho* aryl substitutent in compounds studied.

Table 4.13. Complexation shifts and diastereomeric dispersions of compounds (±)-1-5 in the presence of an equimolar amount of Rh*; in ppm relative to TMS; solvent: $CDCl_3$

Atom		2	4	5	6 (*syn*)	7 (*anti*)	8	1′	2′	3′	4′	5′	6′
(±)-**1**	$\Delta\delta(^1H)$				−0.19	−0.18				+0.10	+0.10	+0.10	+0.24
	$\Delta\delta(^{13}C)$	+5.75	−0.78	+2.27	−0.62	−0.66		−0.83	+0.03	+0.35	+0.70	+0.41	0
(±)-**2**	$\Delta\nu(^1H)$				28	6				n.d.[a]	2	4	8
	$\Delta\nu(^{13}C)$	0	6	5	11	13		0	0	3	0	2	1
(±)-**3**	$\Delta\delta(^1H)$				−0.17	−0.18				+0.21	+0.09	+0.09	+0.09
	$\Delta\delta(^{13}C)$	+5.53	−0.71	+2.18	−0.64	−0.58		−0.86	+0.07	+0.04	+0.35	+0.61	+0.37
	$\Delta\nu(^1H)$				−18	+10				5[b]	5[b]	−2	2
	$\Delta\nu(^{13}C)$	0	−5	−3	−9	+7		0	+1	−1	−2	0	+2
(±)-**4**	$\Delta\delta(^1H)$				−0.15	−0.20				+0.09	+0.14	+0.10	+0.17
	$\Delta\delta(^{13}C)$	+5.60	−0.70	+2.23	−0.65	−0.56		−0.89	−0.03	+0.39	−1.25	+0.34	+1.90
	$\Delta\nu(^1H)$				−11	+12				n.d.[a]	+8	6	−5
	$\Delta\nu(^{13}C)$	0	+4	0	+7	−7		0	+2	+2	0	−1	0
(±)-**5**	$\Delta\delta(^1H)$				−0.18	−0.15				+0.09	+0.09	+0.10	+0.25
	$\Delta\delta(^{13}C)$	+5.49	−1.0	+2.0	−0.99	−0.88		−1.30	−0.56	+0.13	+0.29	+0.02	−0.21
	$\Delta\nu(^1H)$				+1	+14				+1	+4	+8	+13
	$\Delta\nu(^{13}C)$	4	−2	+3	+7	−4		+3	+4	+1	0	0	0
	$\Delta\delta(^1H)$				−0.20	−0.14	+0.11			+0.09	+0.09	+0.10	+0.23
	$\Delta\delta(^{13}C)$	+5.54	−0.68	+2.42	−0.70	−0.56	−0.09	−0.88	+0.13	+0.36	+1.43	−0.40	+0.05
	$\Delta\nu(^1H)$				−6	+9	−9			n.d.[a]	n.d.[a]	n.d.[a]	8
	$\Delta\nu(^{13}C)$	0	−2	−2	+7	−9	+2	0	+1	−2	+3	0	−3

Table 4.14. Complexation shifts and diastereomeric dispersions of compounds (±)-11-15 in the presence of an equimolar amount of Rh^{*}; in ppm relative to TMS; solvent: $CDCl_3$

Atom		2	4	5	6[a] (*syn*)	7[a] (*anti*)	8	1′	2′	3′	4′	5′	6′
(±)-1**1**	$\Delta\delta(^1H)$				−0.18	−0.16				+0.01	+0.07	+0.10	+0.09
(±)-1**2**	$\Delta\nu(^1H)$				20	15				n.d.[b]	1	n.d.[b]	n.d.[b]
	$\Delta\delta(^1H)$				−0.15	−0.14				+0.17	+0.05	+0.06	+0.05
	$\Delta\delta(^{13}C)$	+7.59	−0.01	−0.33				−0.06	−0.61	−0.10	+0.39	+0.69	+0.31
(±)-1**3**	$\Delta\nu(^1H)$				−13	−15				−10	−4	−2	0
	$\Delta\nu(^{13}C)$	+2	+5	−4				−5	−4	+3	0	+3	+2
	$\Delta\delta(^1H)$				−0.16	−0.14				+0.06	+0.08	+0.07	+0.20
	$\Delta\nu(^1H)$				9	18				0	3	4	12
(±)-1**4**	$\Delta\delta(^1H)$				−0.02	+0.05				+0.01	+0.01	+0.01	+0.03
	$\Delta\delta(^{13}C)$	+7.15	−0.25	−0.29				−0.46	−0.48	+0.33	+0.56	+0.42	−0.04
	$\Delta\nu(^1H)$				−6	+18				+2	+3	+5	+13
(±)-1**5**	$\Delta\nu(^{13}C)$	+4	−6	+7				+6	+11	−3	−1	n.d.[b]	n.d.[b]
	$\Delta\delta(^1H)$				−0.13	−0.14	+0.06			+0.04	+0.07	+0.06	+0.20
	$\Delta\delta(^{13}C)$	+7.23	+0.11	−0.14			−0.28	−0.46	−0.01	+0.24	+0.59	+0.31	−0.07
	$\Delta\nu(^1H)$				−7	−5	+12			n.d.[b]	0	n.d.[b]	n.d.[b]
	$\Delta\nu(^{13}C)$	−3	+7	−7			−7	−3	−3	0	+2	+4	+5

Assigning the stereochemical position of the geminal methyl groups in the compounds (±)-1-5 was an intriguing problem which could be solved unambiguously only for the methyl derivative (±)-5 in the presence of an equimolar amount of Rh*.

The existence of ROESY peaks (Figure 7.81) proved that the low-frequency methyl group signals correspond to the syn-position (vertical) with respect to the tolyl-methyl group (horizontal); (in M enantiomer) as shown in Figure 4.80 and Figure 4.81.

HMQC and HMBC spectroscopy (Figure 4.82) proved which of the syn- (s) and anti-methyl (a) belongs to which of the two enantiomers, arbitrarily designated A and B. First, the ^{13}C nuclei directly attached to the ^{1}H nuclei were identified by HMQC (Figure 4.82, left). Second, the HMBC cross-peaks (Figure 4.82, right) prove that the two outer methyl ^{1}H signals belong to one enantiomer (A) and, analogously the inner ones to the other (B).

Analogous experiments were conducted with the compounds (±)-1-4. The stereodifferentiation of the diastereotopic methyl groups was tentatively performed on the basis of the observation that in all cases of (±)-1-5 the sequence of their carbon atoms and their ^{13}C chemical shifts is remarkably uniform (Table 4.13 and Figure 4.83, vertical dimensions) so that, it has been assigned all *anti* and *syn* positions in analogy to the methyl derivative (±)-5. In the compounds of (±)-1-5 all enantiomers A should belong to the same absolute configuration and vice versa for B.

Once this assignment of the geminal methyl ^{13}C signals and the relative configurations of the compounds in the compounds (±)-1-5 is accepted. Figure 4.83 shows this for the halogenated derivatives in the compounds (±)-1-4; note that here the original spectra have been replaced by schematic representations for sake of clarity.

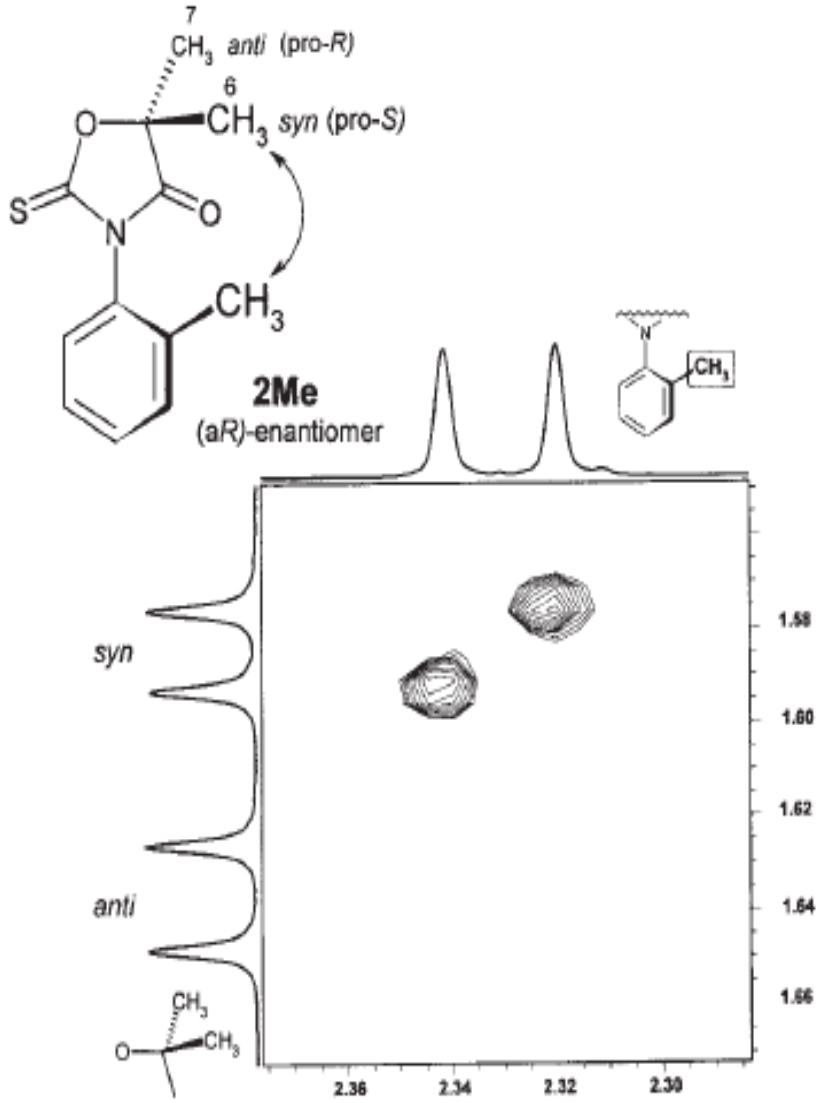

Figure 4.81. Section of the ROESY spectrum of racemic (±)-5 in the presence of an equimolar amount of Rh*

It is immediately evident that a similar signal sequence, as found for the ^{13}C nuclei, does not exist for the protons. In contrast, it can be seen that for the *syn*-CH_3 groups, which are close to the *ortho* aryl substitutent, the absolute values of the dispersion effects Δυ are strongly dependent on the nature of the halogen atoms; (±)-1: Δυ =28 Hz, (±)-2: Δυ =18 Hz, (±)-3: Δυ =11 Hz, (±)-4: Δυ =1 Hz, and (±)-5 Δυ =6 Hz (*syn*-effect), whereas such sequence does not exist for the anti-CH_3 groups situated on the back-side relative to *ortho* aryl substitutent; (±)-1: Δυ =6 Hz, (±)-2: Δυ =10 Hz, (±)-3: Δυ =12 Hz, (±)-3: Δυ =14 Hz,

and (±)-4: Δυ =9 Hz. Thus: the *ortho* aryl substitutent influences the conformational equilibria inside the Rh* ..... *ortho* aryl substitutent adducts so that the nearby *syn*-methyl protons, which are on the same side of the molecule as *ortho* aryl substitutent, experience more efficient chiral discrimination in the diastereomeric complexes exerted by the Mosher phenyl groups than the *anti*-methyl protons which are further away.

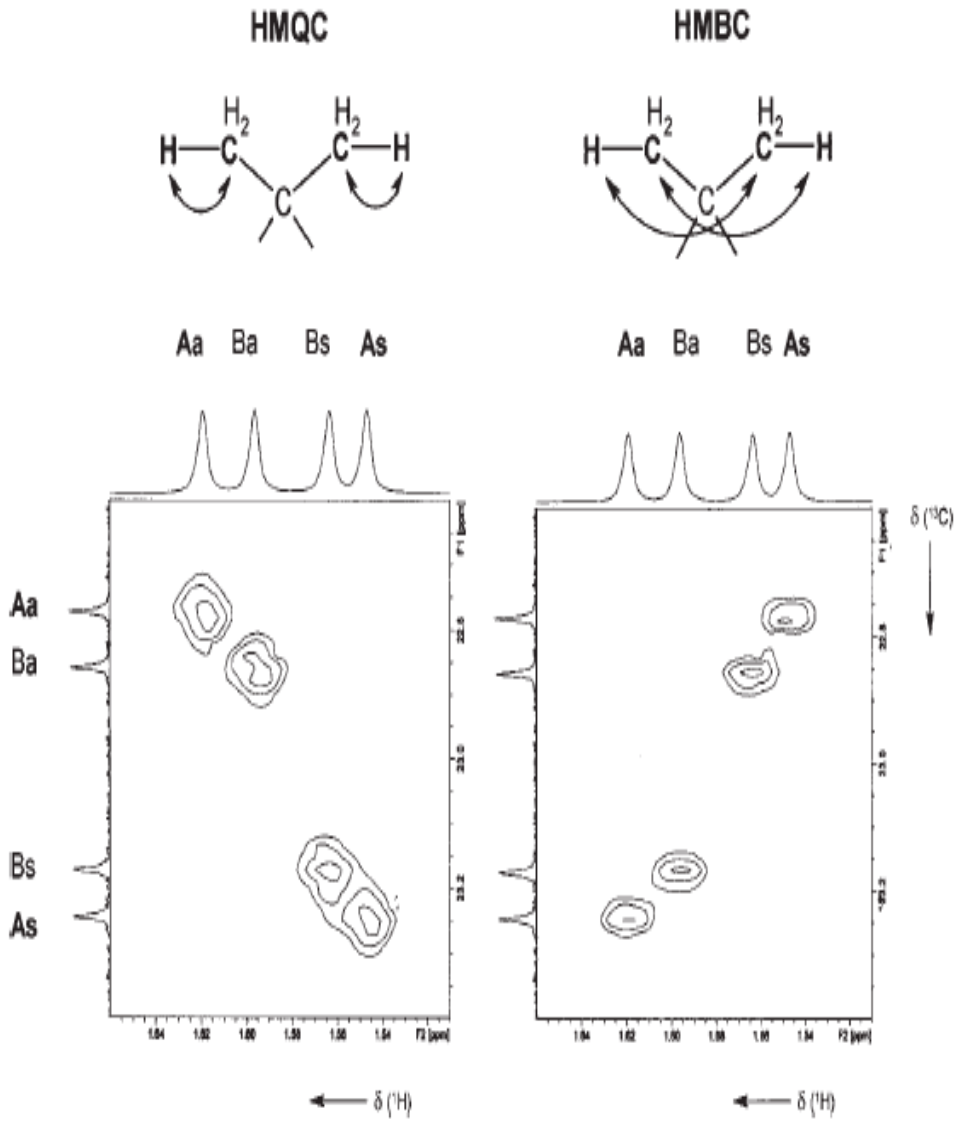

Figure 4.82. Mutual assignments of the hydrogen and carbon atoms with in the *syn*- and *anti*-methyl groups in the adducts of Rh* and the enantiomers A and B of (±)-5 by a combination of HMQC (one-bond ^{1}H, ^{13}C correlations; left) and HMBC (three-bond ^{1}H, ^{13}C correlations; right)

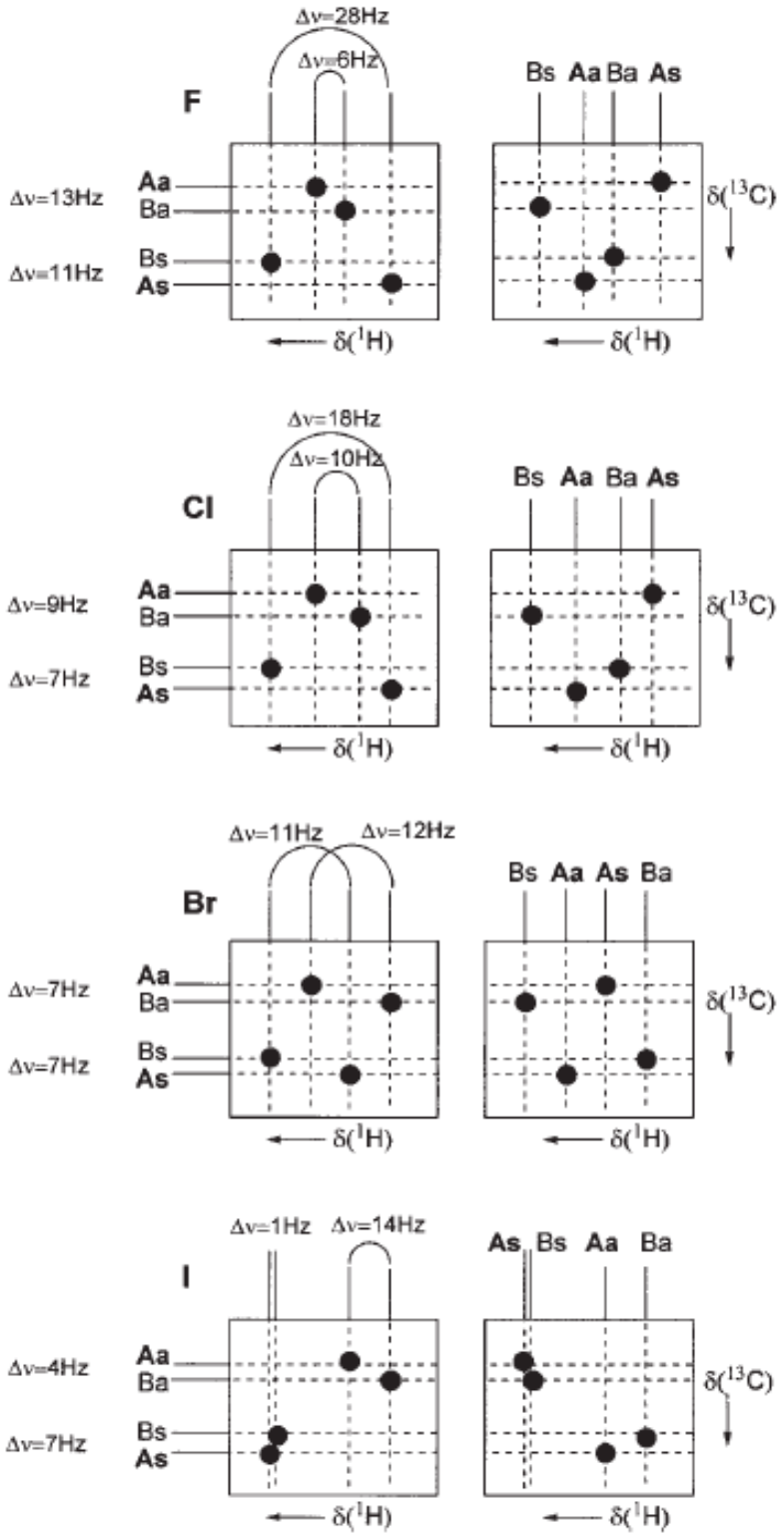

Figure 4.83. Schematic representations of the HMQC and HMBC experiments of the halogenated derivatives of compounds (±)-1-4

5. CONCLUSIONS

In this project, 5,5-dimethyl-3-(*o*-aryl)-2-thioxo-4-oxazolidinones, 5,5-dimethyl-3-(*o*-aryl)-2-thioxo-4-thiazolidinones and 3-(*o*-aryl)-2-thioxo-4-thiazolidinones have been studied. These compounds are axially chiral due to the non-planar ground states of the molecules, the C_{sp2}-N_{sp2} bond being the chiral axis and all of them exist as a pair of thermally interconvertable M and P enantiomers.

The compounds (±)-1-5 and (±)-11-15 have been synthesized as racemates by either the reaction of *o*-aryl isothiocyanates with α-hydroxyisobutyrate or by treatmentof *o*-arylisothiocyanates with the correponding thiogycolic acid ethyl ester. The compounds (±)-6-9 have been synthesized according to Modified Kaluza synthesis.

Chirality of compounds (±)-1-15 is proven by the presence of diastereotopic protons or carbon atoms detected by ^{1}H NMR or ^{13}C NMR spectroscopy. Nonequivalent protons or methyl groups present on C-5 of the heterocyclic ring which are diastereotopic owing to the stereostructures of the compounds showed different ^{1}H or ^{13}C NMR signals. Methyl groups at C-5 exhibited two distinct ^{1}H or ^{13}C NMR signals. On the other hand methylene protons at C-5 showed AB type splittings. The chemical shift differences between the diastereotopic groups can be expected to be affected by the anisotropic influence of the substitutent at the *ortho* position as well as by the dihedral angles between the two rings, which in turn will be determined largely by the size of the ortho aryl substitutent. In every series it was found to increase from 0.01 ppm for *o*-methyl and 0.02 ppm for *o*-fluoro derivatives to 0.07 ppm for the *o*-iodo compounds.

Resolution of the racemic mixtures of interconverting enantiomers was achieved on Chiralpak AD-H column, packed with amylose tris-(3,5-dimethylphenyl)carbamate as chiral stationary phase.

The barriers to partial rotation around C-N bond in compounds (±)-2-15 were determined by thermal racemization of the preparatively enriched enantiomers. The energy barrier for compound (±)-1 was determined as 78 kJ/mol in toluene-d_8 and 82 kJ/mol in

DMSO-d_6 using dynamic ^{1}H NMR spectroscopy. The thermal racemization of enriched enantiomers of compounds (±)-2-15 was followed to obtain the barriers to rotation, which were found as 103.8-124 kJ/mol for compounds (±)-2-5, 89-128.2 kJ/mol for compounds (±)-6-10 and 91-129 kJ/mol for (±)-11-15. The difference in activation barriers resulted from the longer bond lenght of the C=S double bond than that of C=O, and the larger van der Waals radius of the sulphur atom than that of the oxygen atom.

The enantiotopic protons of napthyl substituted compounds 3-(α-napthyl)-2-thioxo-4-oxazolidinone and 3-(α-napthyl)-2,4-thiazolidinedione were resolved in the presence of the chiral auxiliary (S)-TFAE. The proposed model between the compounds and the chiral auxiliary, which emphasized π-π interactions between the naphtyl and antryl groups as well as the hydrogen bonding interactions enabled the assignment of the resolved peaks to the M and P conformations. The strong temperature dependence of the spectra of the diastereomeric complexes explained was by the adoption of different solvation models at lower temperatures of the M and P conformers.

Enantiodifferentiation of 3-aryl-2-thioxo-4-oxazolidinones, compounds (±)-1-5 and 3-aryl-2-thioxo-4-thiazolidinones, compounds (±)-11-15, was also studied by applying the dirhodium method using a dirhodium tetracarboxylate complex. In compounds (±)-1-5 and (±)-11-15, where the sulphur atoms act as quite strong binding sites, the dispersion effects Δυ (^{1}H) and Δυ (^{13}C) amounted to 28 and 13 Hz, respectively. Chiral discrimination which will enable the determination of enantiomeric ratios of these thionyl compounds was possible, however determination of relative conformations of separated enantiomers could not be achieved by this method. In compounds (±)-1-5 on the other hand, a " *syn* methyl effects" was discovered which described the dependence of dispersion effects of *syn*-oriented methyl groups on the nature of the *ortho* aryl substitutent.

REFERENCES

1. Roussel, C. and N. Vanthuyne, "Atropisomerism in the 2-Arylimino-N-(2-hydroxyphenyl)thiazoline Series: Influence of Hydrogen Bonding on the Racemization Process*", J.Org. Chem*., Vol. 73, pp. 403-411, 2008.

2. Clayden, J. and M. Darbyshire, "Remote stereocontrol using rotationally restricted amides: (1,5)-asymmetric induction", *Tetrahedron Letters*, Vol. 49, pp. 8587-8590, 1997.

3. Lapierre, A. and S. Geib, "Low-Temperature Heck Reactions of Axially Chiral o-Iodoacrylanilides Occur with Chirality Transfer: Implications for Catalytic Asymmetric Heck Reactions*", J. Am. Chem. Soc.,* Vol. 129, pp.494-495, 2007.

4. Marelli, C. and C. Monti, "2-(2-Hydroxyaryl)cinnamic amides: a new class of axially chiral molecules", *Tetrahedron*, Vol. 62, pp. 8943-8951, 2006.

5. Koide, H. and T. Hata, "Asymmetric synthesis of axially chiral benzamides and anilides utilizing planar chiral arene chromium complexes", *Tetrahedron*, Vol. 60, pp. 4527, 2004.

6. Kondo, K. and T. Iida, "Further study of axial chirality due to an acyclic imide N–Ar bond: control of rotational barrier by electronic effects of acyl groups", *Tetrahedron*, Vol. 57, pp. 4115, 2001.

7. Kitagawa, O. and S. Momose, "Stereoselective synthesis of diastereomeric atropisomeric lactam with various ring sizes and their structural characterization", *Tetrahedron Letters*, Vol. 40, pp. 8827-8831, 1999.

8. Clayden, J., "Non-Biaryl Atropisomers: New Classes of Chiral Reagents, Auxiliaries, and Ligands", *J. Angew. Chem. Int. Engl*., Vol. 36, pp. 949, 1997.

9. Joshi, M. and J. Sternberg, “DPX-JE874: a broad-spectrum fungicide with a new mode of action, in Prc. 1996 Brighton Crop. Prot. Conf-Pests and Diseases”, *British Crop Protection Council*, Farnham, UK., pp. 21-26, 1996.

10. Geffken, D. and D. Rayner, “Fungicidal oxazolidinones”, US Patent, 4957933, 1990.

11. Geffken, D. and D. Rayner, “Fungicidal oxazolidinones”, US Patent, 5223523, 1993.

12. Sternberg, J. and D. Geffken,“ Synthesis and Chemistry of Agrochemicals”, pp. 216-227, *American Chemical Society,* Washington DC., 1998.

13. Raper, E., “Complexes of heterocyclic thione donors”, *Coord. Chem. Rev*., Vol. 61, pp. 115, 1985.

14. Hollenberg, A. and. J. Susulic, “Functional Antogonism between CCAAT/Enhancer Binding Protein-α and Peroxime Proliferator activated Receptor-γ on the Zeptin Promoter”, *The Journal of Biiological Chemistry*, Vol. 272, pp. 5283-5290, 1997.

15. Contello, B. and D. Eggleston, “Facile Biocatalytic Reduction of the Carbon-Carbon Double Bond of 5-Benzylidinethiazolidine-2,4-diones”, *J. Chem. Soc. Perkin Trans. 1*, Vol. 1, pp. 3319-3324, 1994.

16. Contello, B. and M. Cowhorne, “The synthesis of BRL49G53-A Novel and Potent Antihyperglycamic Agent”, *Bioorganic and Medicinal Chemistry Letters*, Vol. 4, pp. 1181-1184, 1994.

17. Hanefeld, W. and M. Schlitzer, “3-(Thiazolidine-3-aryl)rhodanines. A Novel Class of Rhodanine Derivatives”, *J. Heterocyclic Chemistry*, Vol. 31, pp. 391, 1994.

18. Contello, B. and D. Eggleston, “Synthesis of (±)-5-(4-(2-(Methyl(2-pyridiyl)amino]ethoxy)benzyl)thiazolidine-2,4-dione. (BRL49G53), its R-(+)-

Enantiomer and Analogoues", *J. Chem. Soc. Perkin Trans. 1*, Vol. 1, pp. 3319-3324, 1994.

19. Whitesitt, C. and R. Simon, "Synthesis and Structure-Activity Relationships of Benzophenones as Inhibitors of Cathepsis-D", *Bioorganic and Medicinal Chemistry Letters*, Vol. 6, pp. 2157-2162, 1996.

20. Foye, W. and P. Tovivich, "N-Glucopyranosyl-5-alklydinerhodanines: Synthesis and Antibacterial and Antiviral Activities", *J. of Pharmaceutical Sciences*, Vol. 66, pp. 1607-1611, 1977.

21. Bock, L. and R. Adams, "The Preparation and Resolution of N-2 carboxyphenyl-2.5-dimethyl-3-carboxypyrrole", *J.Am. Chem. Soc.*, Vol. 53, pp. 374-376, 1931.

22. Chang, C. and R. Adams, "Stereochemistry of N,N'-dipyrryls. Resolution of N,N',2,5,2',5'-tetramethyl-3,3'-dicarboxydipyrryl", *J.Am. Chem. Soc.,* Vol. 53, pp. 2353-2357, 1931.

23. Bock, L. and R. Adams, "Stereochemistry of Phenyl Pyrroles", *J. Am. Chem. Soc.,* Vol. 53, pp. 3519-3522, 1931.

24. Colebrook, L. and H. Giles, "High Rotational Barriers About C-N Bonds in Aryl Substituted Heterocyclic Compounds Lacking Bulky Ortho Substituents", *Tetrahedron Lett*., Vol. 18, pp. 5239-5240, 1972.

25. Colebrook, L. and H. Giles, "Hindered Internal Rotation About Aryl C-N Bonds in Aryl Substituted Heterocyclic Compounds: 3-Aryl-2-benzyl-4(3H)-quinazolinones", *Can. J. Chem.*, Vol. 53, pp. 3431, 1975.

26. Raban, M. and K. Mislow, "Determination of Optical Purity by NMR Spectroscopy", *Tetrahedron Lett.*, Vol. 26, pp. 4249-4253, 1965.

27. Vorcapic, J. and M. Mintas, “Sterically Hindered N-Aryl Pyrroles: Chromatographic Separation of Enantiomers and Barriers to Recamization”, *Journal of Chemical Society Perkin Transactions 2*, Vol. 12, pp. 713-717, 1989.

28. Doğan, İ. and A. Mannschreck, ‘‘Synthesis and NMR Studies of Chiral 4-Oxazolidinones and Rhodanines’’, *Tetrahedron*, Vol. 48, pp. 7157-7164, 1992.

29. Doğan, İ., N. Pustet and A. Mannschreck, ‘‘The Enantiomers of N-Aryl-2-thioxo-4-Oxazolidinones and N-Arylrhodanines. Investigation by Liquid Chromatography, Circular Dichroism and Thermal Racemization’’, *J. Chem. Soc. Perkin Trans. 2*, Vol. 6, pp. 1557-1560, 1993.

30. Oğuz, S. F. and İ. Doğan, ‘‘Determination of Energy Barriers and Racemization Mechanisms for Thermally Interconvertable Barbituric and Thiobarbituric acids enantiomers’’, *Tetrahedron: Asymmetry*, Vol. 14, pp. 1857-1864, 2003.

31. Vanthuyne, N. and F. Andreoli, “Synthesis, Chiral Separation, Barrier To Rotation And Absolute Configuration Of N-(O-Functionalized-Aryl)-4-Alkyl-Thiazolin-2-One And Thiazoline-2-Thione Atropisomers”, *Letters in Organic Chemistry*, Vol. 2, pp. 433-443, 2005.

32. Oki, M., “Recent advances in atropisomerism”, *Top. Stereochemistry*, Vol. 14, pp. 1, 1983.

33. Cahn, R. S. and C. Ingold, “Specification of Molecular Chirality”, *Angew. Chem. Int. Ed.*, Vol. 5, No. 4, pp. 385-415, 1966.

34. Allenmark, S., *Chromatographic Enantioseparation Methods and Applications*, 2nd Edition, Ellis Horwood, New York, 1991.

35. Loudon, G. M., *Organic Chemistry*, Addison-Wesley, Massachusetts, pp. 231-234, 1984.

36. Zief, M. and L. Crane (Editors), *Chromatographic Chiral Separations*, Marcel Dekker, New York, 1988.

37. Ernest, L. E. and H. W. Samuel, *Stereochemistry of Organic compounds*, John Wiley, New York, pp. 231-232, 1994.

38. Weisman, G. R., *Analytical Methods In Symmetric Synthesis*, Vol. 1, J. D. Morrison, Ed., Academic Press:New York, London, 1983.

39. Pomares, M. and A. Alvarez, "Preparation and Structural Study of the Enantiomers of α,α'-Bis(trifluoromethyl)-9,10-anthracenedimethanol and Its Perdeuterated Isotopomer, Highly Effective Chiral Solvating Agents", *J. Org. Chem.,* Vol. 67, pp. 753, 2002.

40. Parker, D., "NMR determination of enantiomeric purity", *Chem. Rev*., Vol. 91, pp. 1441, 1991.

41. Wenzel, T. and J. Wilcox, "Chiral reagents for the determination of enantiomeric excess and absolute configuration using NMR spectroscopy", *Chirality*, Vol. 15, pp. 256, 2003.

42. Adler, T. and J. Clayden, "Slow interconversion of enantiomeric conformers or atropisomers of anilide and urea derivatives of 2-substituted anilines", *Org. Biomol. Chem.*, Vol. 3, pp. 3173-3183, 2005

43. Isaksson, R. and R. Roschester, "Preparative and analytical enantiomer separation of some .DELTA.4-1,3-thiazoline-2-thiones on swollen microcrystalline triacetylcellulose (TAC)", *J. Org. Chem*., Vol. 50, pp. 2519, 1985.

44. Mintas, M. and A. Mannschreck, "Sterically hindered N-aryl-2(1H)-quinolones and N-aryl-6(5H)-phenanthridinones: separation of enantiomers and barriers to racemization**",** *J. Chem. Soc. Perkin Trans. 2*, Vol. 6, pp. 619, 1990.

45. Erol, Ş. and İ. Doğan, "Axially Chiral 2-Arylimino-3-aryl-thiazolidine-4-one Derivatives: Enantiomeric Separation and Determination of Racemization Barriers by Chiral HPLC", *J. Org. Chem.,* Vol. 72, pp. 2494, 2007.

46. Oğuz, S. F. and İ. Doğan, "Determination of energy barriers and racemization mechanisms for thermally interconvertable barbituric and thiobarbituric acid enantiomers", *Tetrahedron: Asymmetry*, Vol. 14, pp. 1857, 2003.

47. Sarac, A. and A. Mannschreck, "Syntheses, separation of enantiomers and barriers to racemization of some sterically hindered N-aryl-1,2,3,4-tetrahydro-3,3-dimethyl-2,4-quinolinediones and their thio analogues", *Monatshefte für Chemie,* Vol. 125, pp. 457, 1994.

48. Levine, I. N., *Physical Chemistry,* 4th Edition, Mc-Graw-Hill, New York, 1989.

49. Ordu, Ö., E. M., Yılmaz and İ. Doğan, "Determination of the absolute stereochemistry and the activation barriers of thermally interconvertible heterocyclic compounds bearing a naphthyl substituent", *Tetrahedron: Asymmetry*, Vol. 16, pp. 3752-3761, 2005.

50. Ordu, Ö. and İ. Doğan, "Determination of energy barriers to rotation and absolute conformations of thermally interconvertible 5,5-dimethyl-3-(o-aryl)-2,4-oxazolidinedione enantiomers", *Tetrahedron: Asymmetry*, Vol. 15, pp. 925-933, 2004.

51. Rotello, V. and B. Rebek, "Molecular recognition in water: new receptors for adenine derivatives", *J. Am. Chem. Soc.*, Vol. 115, pp. 797-798, 1993.

52. Hanna, G. M. and F. E. Evans, "Optimization of enantiomeric separation for quantitative determination of the chiral drug propranolol by 1H-NMR spectroscopy utilizing a chiral solvating agent", *J. Pharm. Biomed. Anal*., Vol. 24, pp. 189-196, 2000.

53. Guckian, K. M. and B. Schweitzer, "Factors Contributing to Aromatic Stacking in Water: Evaluation in the Context of DNA", *J. Am. Chem. Soc*., Vol. 122, pp. 2213-2222, 2000.

54. Muehldorf, A. And A. Hamilton, "Aromatic-aromatic interactions in molecular recognition: a family of artificial receptors for thymine that shows both face-to-face and edge-to-face orientations", *J. Am. Chem. Soc*., Vol. 110, pp. 6561-6562, 1988.

55. Gomez, E. D., İ. Doğan, E. Yılmaz, Ö. Ordu and H. Duddeck, "Atropisomeric 3-Aryl-2-Oxo-4-Oxazolidinones and Some Thione Analogues—Enantiodifferentiation and Ligand Competition in Applying the Dirhodium Method", *Chirality*, Vol. 20, pp. 344-350, 2008.